Title

The measurement of excess alkalinity in seawater media and a simple procedure to prepare a calibration buffer for pHT measurements.

Author

Paulsen, May-Linn

Publication Date

2021

Peer reviewed|Thesis/dissertation

UNIVERSITY OF CALIFORNIA SAN DIEGO

The measurement of excess alkalinity in seawater media and a simple procedure to prepare a calibration buffer for pH_T measurements.

A dissertation submitted in partial satisfaction of the requirements for the degree Doctor of Philosophy

in

Oceanography

by

May-Linn Paulsen

Committee in charge:

Professor Andrew G. Dickson, Chair
Professor Lihini Aluwihare
Professor Sarah N. Giddings
Professor Carolyn Kurle
Professor Todd Martz

2021

This Dissertation of May-Linn Paulsen is approved, and it is acceptable in the quality and form for publication on microfilm and electronically:

University of California San Diego

2021

TABLE OF CONTENTS

LIST OF FIGURES

LIST OF TABLES

ACKNOWLEDGEMENTS

I would like to acknowledge Professor Andrew Dickson for his support as the chair of my committee, and my research advisor.

I would like to acknowledge the members of the Dickson lab, and in particular thank George Anderson for his continued encouragements and insights.

I would also like to acknowledge the MCG graduate students at SIO for their helpfulness, sharing, and overall caring.

Chapter 2, in full, is a reprint of the material as it appears in Limnology and Oceanography: Methods 2020. The dissertation author was the primary investigator and author of this paper. The authors are grateful for the help of Lauren Briggs in preparing several TRIS batches, and George C. Anderson for coulometric analysis of the HCl. The authors would also like to thank Dr. Simon Clegg for his work with the Pitzer modelling of TRIS in synthetic seawater. Comments from two anonymous reviewers greatly enhanced the manuscript. This work was supported by the US National Science Foundation Grant OCE-1657799 and by a grant from the NOAA Ocean Acidification Program, NA15OAR4320071.

For Chapter 4 the author would like to thank Wiley Wolfe and Todd Martz for training on and use of their C_T measurement system. The author would further like to acknowledge the crew and student participants of the student research cruise SR1802, and especially its organizers for allowing me to participate, including Angel Ruacho, Sara Rivera, Alyssa Finlay, Lauren Manck, Kiefer Forsch, Kayleen Fulton, Margot White, and Matthew A. Pendegraft. Lastly, the author would like to acknowledge all the work carried out by Canyon Breyer on

boron measurements that ultimately did not make it into the dissertation, but that will be key moving forward with research on A_X.

Last but not least, I have to acknowledge the joy and therapeutic interactions provided by Zeph and Sir Lancelot.

VITA

2011–2013	Teaching assistant, University of Stavanger, Norway
2013	Bachelor of Science, University of Stavanger, Norway
	Chemistry and Environmental Engineering, Professor Roald Kommedal
2013–2015	Teaching assistant, University of California San Diego
2015	Master of Science, University of California San Diego
	Chemistry and Biochemistry, Professor Andreas Andersson
2015–2021	Graduate Student Researcher, University of California San Diego
2021	Doctor of Philosophy, University of California San Diego
	Oceanography, Professor Andrew Dickson

PUBLICATIONS

Paulsen, M.-L. and A. G. Dickson. 2020. Preparation of 2-amino-2-hydroxymethyk-1,3-propanediol (TRIS) pH buffers in synthetic seawater. Limnology and Oceanography: Methods, doi: https://doi.org/10.1002/lom3.10383 (2020).

Paulsen, M.-L., A.J. Andersson, L. Aluwihare, T. Cyronak, S. D'Angelo, C. Davidson, H. Elwany, S.N. Giddings, H.N. Page, M. Porrachia, and S. Schroeter. 2017. Temporal changes in seawater carbonate chemistry and carbon export from a southern California estuary. Estuaries and Coasts 41(4): 1050–1068.

Second State of the Carbon Cycle Report: A sustained assessment report · Chapter 15: Tidal wetlands and estuaries. 2018. Contributing author. U.S. Global Change Research Program.

Cavole, L.M., A.M. Demko, R.E. Diner, A. Giddings, I. Koester, C.M.L.S. Pagniello, **M.-L. Paulsen**, A. Ramirez-Valdez, S.M. Schwenck, N.K. yen, M.E. Zill, and P.J.S. Franks. 2016. Biological impacts of the 2013-2015 warm-water anomaly in the Northeast Pacific: Winners, losers, and the future. Oceanography 29(2): 273-285.

ABSTRACT OF THE DISSERTATION

The measurement of excess alkalinity in seawater media and a simple procedure to prepare a calibration buffer for pH_T measurements.

By

May-Linn Paulsen

Doctor of Philosophy in Oceanography

University of California San Diego, 2021

Professor Andrew G. Dickson, Chair

Accurately measuring the marine CO_2 system is imperative to assess the effect of oceanic uptake of anthropogenic CO_2 and the consequences for marine biogeochemical processes. CO_2 in the ocean is both a gas and an acid, so it is necessary to measure at least two parameters describing its chemistry, where two of the most commonly used parameters being pH_T and total alkalinity (A_T). While both are fairly straight forward to measure and have a long history in oceanography, they have unique challenges that can greatly reduce their quality for use in CO_2 system calculations. For pH_T measurements, especially electrometric methods involving a liquid

junction, it is crucial to calibrate the measurement using a buffer prepared in a solution similar to seawater. Chapter 2 of this dissertation describes a method to prepare 0.04 mol kg-H_2O^{-1} equimolar buffer 2-amino-2-hydroxymethyl-1,3-propanediol (TRIS)-TRIS·H^+ in synthetic seawater. Its point of success is using a simple methodology that is also reproducible, and produces a buffer with a pH_T within 0.006 of the assigned value 8.094 (at 25 °C).

The measurement of A_T and even its definition is simple, being the balance between bases and acids in seawater and measured by titration with acid. To use A_T in CO_2 system calculations, it is necessary to account for the non-carbonate alkalinity components. While most if not all inorganic bases and acids have been identified and can be accounted for, for decades there has been evidence for unidentified, likely organic, bases present at significant levels. Little advance has been made in understanding the alkalinity contribution from component "X" (A_X) due to a lack of an unambiguous measurement. Chapter 3 describes an unambiguous, open-cell titration method to measure A_X, which includes an uncertainty assessment informed both by ancillary measurements and by titration simulations using a custom chemical equilibrium model. Chapter 4 shows the success of this this titration method using a combination of well-characterized simple salt solutions and a simple seawater solution, by themselves and with the addition of one or two simple organic, proving that the system is capable of measuring A_X at 3.4 μmol kg^{-1}.

1 INTRODUCTION

1.1 A brief history of marine CO_2 research

That the ocean was slightly alkaline was noted as early as in the 18th century, when count Marsigli (1725) was experimenting with colorimetric pH indicators and different kinds of mineral water, including seawater. The alkaline nature of seawater was later also noted by others such as Bergman (1784) and von Bibra (1851) although it wasn't until the Challenger expedition that Dittmar (1880) formalized the term "alkalinity" as meaning the "potential carbonate of lime", or in modern terms, "if one added this much acid to reach a certain endpoint point, one could say that ocean had this many '$CaCO_3$ equivalents'". Naturalists and researchers were well aware that there was a link between living organisms and the carbon cycle, and in the ocean also a link to pH related properties (Lichtenberg 1811; Murray 1818). By the middle of the 19th century many oceanographic explorations included measures of alkalinity, and often an additional measure relating to pH (Göbel 1842).

Amongst these early oceanographic sampling efforts were the Challenger expedition and the lesser known Norwegian North-Atlantic expeditions, both which measured 'carbonic acid' (at the time thought of as carbon dioxide gas dissolved in water, and in modern terms similar to total dissolved inorganic carbon or C_T, see next page) and alkalinity (Dittmar 1880; Tornøe 1880). Scientific objectives for these chemical oceanographers included understanding the exchange of air and gases between the atmosphere and the oceans, and getting a sense of the overall marine chemical environment. While the tension (partial pressure in modern terms) of other gases such as oxygen and nitrogen were easily measured and understood, it was less straight forward for CO_2 since it is not present as a gas in solution, but rather the disassociated

forms of hydrated CO_2 (H_2CO_3). Following work by Arrhenius (1889) on the understanding of acids in solution, and the work of Sørensen (1909) to define pH, effort was focused on measuring the equilibrium constants of carbonic acid in aqueous solutions and understanding the relationship between the various parameters that could be measured to describe it (Johnston 1916). Provided that the alkalinity of seawater consisted purely of carbonate and hydrogen carbonate, and that these were the only buffering agents in seawater, it should be possible to calculate e.g., the tension of CO_2 (in modern terms, partial pressure of CO_2 or $p(CO_2)$) or the amount of 'carbonic acid' if pH was known, or vice versa. In other terms, if two parameters describing the CO_2 system were known in addition to the values of their equilibrium constants K_1 and K_2, the other two parameters could be calculated.

Around the turn of the century increased attention was given to CO_2 as a greenhouse gas and as a pollutant, and Arrhenius and Holden (1897) pointed to how the increasing use of coal and fossil fuels could potentially raise the temperature on earth if left uncontrolled. Revelle and Suess (1957) later noted that the ocean was likely to absorb a significant amount of CO_2 from the atmosphere. This added yet another motivation to measure and understand changes in the CO_2 system, particularly since the increase in carbonic acid from CO_2 uptake was slowly acidifying the surface oceans (Fairhall 1973; Zimen and Altenhein 1973). In the second half of the 20th century efforts were started to monitor CO_2 in the atmosphere (Keeling et al. 1976), and within a few decades, programs had been initiated that included mapping the distribution of the CO_2 system in the world's oceans. The Geochemical Ocean Sections Study (GEOSECS) was the first large-scale geochemical oceanographic mapping efforts, and also included an intercalibration station to ensure agreement between the various CO_2 related measurements and between the labs performing them (Takahashi et al. 1970).

The intercalibration station was particularly important, as it highlighted that there was often disagreement between the measured and the calculated values of the four measurable CO_2 system parameters (this will be discussed in greater detail in Chapter 3). While another global hydrography program (Word Ocean Circulation Experiment) following GEOSECS did, in the end, add CO_2 measurements (Wunsch 2006), it was not until The Global Ocean Ship-Based Hydrographic Investigations Program (GO-SHIP) that focus was explicitly given to the carbon system in a repeat hydrography program. In addition to these and other research cruises, there are now multiple long-term monitoring stations throughout the oceans (Bates et al. 2014). These large-scale international efforts often require more than one lab to measure the same parameter, and even if it doesn't, there is a strong need for their results need to be comparable across different laboratories. This has led to an increased focus on how to achieve adequate quality in measuring the CO_2 system parameters both in terms of understanding the relevant chemistry, and having access to appropriate calibration solutions.

1.2 The basis of seawater CO_2 chemistry

There are currently four measurable parameters that can be used to describe seawater CO_2 chemistry. These include C_T, A_T, pH, and $p(CO_2)$. C_T consists primarily of the disassociated species hydrogen carbonate and carbonate, and to a minor degree dissolved CO_2 gas and the un-disassociated carbonic acid (Eq. 1-1). (Species in brackets indicate the amount content, mol kg-sol^{-1} or mol kg^{-1}.)

$$C_T = [CO_2(aq)] + [H_2CO_3] + [HCO_3^-] + [CO_3^{2-}] = [CO_2^*] + [HCO_3^-] + [CO_3^{2-}]$$

Eq. 1-1

While pH can be similarly defined in terms of amount content of hydrogen ions, for seawater applications it is often defined on a total hydrogen ion scale, which includes the proportion of sulfate which is protonated (where S_T and K_S refers to the total amount content of sulfate and acid dissociation constant of hydrogen sulfate, respectively):

$$\mathrm{pH}_T = -\log_{10}\left([\mathrm{H}_F^+]\,(1 + S_T / K_S)\right)$$

Eq. 1-2

The reason for using pH_T is explained in Chapter 2, and contributes to reducing the uncertainty associated with seawater pH measurements. pH_T is easy to measure, and e.g., electrometric measurement methods are fairly easily integrated in sensor packages making it a convenient CO_2 related parameter to use for high-resolution sensing of the ocean. It should also be noted that pH_T is really a measure of the activity of the hydrogen ion, and is related to its amount content (or molality) through an activity coefficient. The activity coefficient is a function of the ionic composition and strength of the solution. Therefore, for calibrating pH_T measurements it is necessary to provide a solution composition similar to that of seawater so that the activity coefficient of H^+ can be thought largely the same as in the seawater sample and in the calibration solution.

Because of the ease of measurement, A_T is frequently used as a parameter describing marine CO_2 chemistry seeing as it is easily measured by adding strong acid to seawater and monitor the corresponding change in pH_T. Problems do however arise when interpreting a single value, or even changes to A_T because although the carbonate species (A_C) make up the majority of A_T, it is also composed of all other acid-base species present in a seawater sample (Eq. 1-3).

$$A_T = [HCO_3^-] + 2[CO_3^{2-}] + [B(OH)_4^-] + [SiO(OH)_3^-] + 2[PO_4^{3-}] + [HPO_3^{2-}] + [OH^-] + [\text{unidentified bases}] - [H^+] - [HSO_4^-] - [HF] - [H_3PO_4] - [\text{unidentified acids}]$$

Eq. 1-3

If A_T is to be used in CO_2 system calculations, it is necessary to calculate the contribution of A_C by subtracting out the other buffering species. This is usually done by estimating the total amount contents from *S* (borate, hydrogen sulfate, and hydrogen fluoride) or by additional measurements (silicate and phosphate). Relevant total amount contents, equilibrium expressions, and acid dissociation constants used to calculate the individual alkalinity contributions are shown in Figure 1-1.

Including the partial pressure of CO_2, $p(CO_2)$, a combination of two of these four described parameters can in theory be used to calculate the remaining two (Figure 1-2). However, the suitability for any given two parameters will depend not only on measurement methods available, but on the environment in which the samples or measurements will be collected. As can be eluded from Figure 1-2, not all pairs of measurable parameters are ideal in describing a third parameter, and each measurement is associated with a different relative uncertainty which will further depend on the available means of calibration (Dickson and Riley 1978; Dickson 2010).

$$[H_T^+] = [H_F^+](1 + S_T / K_S)$$

$$[OH^-] = K_W / [H_T^+]$$

$$[CO_2^*] = [H_2CO_3(aq)] + [CO_2(aq)]$$

$$[HCO_3^-] = \frac{C_T K_1 [H_T^+]}{[H_T^+]^2 + K_1[H_T^+] + K_1 K_2}$$

$$[CO_3^{2-}] = \frac{C_T K_1 K_2}{[H_T^+]^2 + K_1[H_T^+] + K_1 K_2}$$

$$[B(OH)_4^-] = \frac{B_T}{1 + [H_T^+] / K_B}$$

$$[SiO(OH)_3^-] = \frac{Si_T}{1 + [H_T^+] / K_{Si}}$$

$$[H_3PO_4] = \frac{P_T [H_T^+]^3}{[H_T^+]^3 + K_{1P}[H_T^+]^2 + K_{1P}K_{2P}[H_T^+] + K_{1P}K_{2P}K_{3P}}$$

$$[H_2PO_4^-] = \frac{P_T K_{1P} [H_T^+]^2}{[H_T^+]^3 + K_{1P}[H_T^+]^2 + K_{1P}K_{2P}[H_T^+] + K_{1P}K_{2P}K_{3P}}$$

$$[HPO_4^{2-}] = \frac{P_T K_{1P} K_{2P} [H_T^+]}{[H_T^+]^3 + K_{1P}[H_T^+]^2 + K_{1P}K_{2P}[H_T^+] + K_{1P}K_{2P}K_{3P}}$$

$$[PO_4^{3-}] = \frac{P_T K_{1P} K_{2P} K_{3P}}{[H_T^+]^3 + K_{1P}[H_T^+]^2 + K_{1P}K_{2P}[H_T^+] + K_{1P}K_{2P}K_{3P}}$$

$$Z = 1 + S_T / K_S$$

$$[HSO_4^-] = \frac{S_T}{1 + K_S / [H_F^+]}$$

$$[HF] = \frac{F_T}{1 + K_F / [H_T^+]}$$

$$k^\circ = 1 \text{ mol kg}^{-1}$$

$$\left(\frac{I}{m^\circ}\right) = \frac{19.924 \cdot S}{1000 - 1.005 \cdot S}$$

Figure 1-1 Equilibrium equations and expressions for relevant (identified) alkalinity species. All expressions and constants (and their references) are found in Dickson et al. (2007). (Continues on next page.)

$$C_T = [CO_2^*] + [HCO_3^-] + [CO_3^{2-}]$$
$$B_T = [B(OH)_3] + [B(OH)_4^-]$$
$$P_T = [H_3PO_4] + [H_2PO_4^-] + [HPO_4^{2-}] + [PO_4^{3-}]$$
$$Si_T = [SiO(OH)_2] + [SiO(OH)_3^-]$$
$$S_T = [H_2SO_4] + [HSO_4^-] + [SO_4^{2-}]$$
$$F_T = [HF] + [F^-]$$

$$\ln(K_0 / k^\circ) = 93.4517\left(\frac{100}{T/\mathrm{K}}\right) - 64.2409 + 23.3585\ln\left(\frac{T/\mathrm{K}}{100}\right) + S\left(0.023517 - 0.023656\left(\frac{T/\mathrm{K}}{100}\right) + 0.0047036\left(\frac{T/\mathrm{K}}{100}\right)^2\right)$$

$$\log(K_1 / k^\circ) = \frac{-3633.86}{(T/\mathrm{K})} + 61.2172 - 9.67770\ln(T/\mathrm{K}) + 0.011555 \cdot S - 0.0001152 \cdot S^{1/2}$$

$$\log(K_2 / k^\circ) = \frac{-471.78}{(T/\mathrm{K})} - 25.9290 + 3.16967\ln(T/\mathrm{K}) + 0.01781 \cdot S - 0.0001122 \cdot S^{1/2}$$

$$\ln(K_S / k^\circ) = \frac{-4276.1}{(T/\mathrm{K})} + 141.328 - 23.093\ln(T/\mathrm{K}) + \left(\frac{-13856}{(T/\mathrm{K})} + 324.57 - 47.986\ln(T/\mathrm{K})\right)\cdot\left(\frac{I}{m^\circ}\right)^{1/2} + \left(\frac{35474}{(T/\mathrm{K})} - 771.54 + 114.723\ln(T/\mathrm{K})\right)\cdot\left(\frac{I}{m^\circ}\right) - \frac{2698}{(T/\mathrm{K})}\left(\frac{I}{m^\circ}\right)^{3/2} + \frac{1776}{(T/\mathrm{K})}\left(\frac{I}{m^\circ}\right)^2 + \ln(I - 0.001005 \cdot S)$$

$$\ln(K_F / k^\circ) = \frac{874}{(T/\mathrm{K})} - 9.68 + 0.111 \cdot S^{1/2}$$

$$\ln\left(K_B / k^\circ\right) = \frac{-8966.90 - 2890.53 \cdot S^{1/2} - 77.942 \cdot S + 1.728 \cdot S^{3/2} - 0.0996 \cdot S^2}{(T/\mathrm{K})} + (148.0248 + 137.1942 \cdot S^{1/2} + 1.62142 \cdot S) + (-24.4344 - 25.085 \cdot S^{1/2} - 0.2474 \cdot S)\ln(T/\mathrm{K}) + 0.053105 \cdot S^{1/2}(T/\mathrm{K})$$

$$\ln(K_{Si} / k^\circ) = \frac{-8904.2}{(T/\mathrm{K})} + 117.385 - 19.334\ln(T/\mathrm{K}) + \left(\frac{-458.79}{(T/\mathrm{K})} + 3.5913\right)\cdot\left(\frac{I}{m^\circ}\right)^{1/2} + \left(\frac{188.74}{(T/\mathrm{K})} - 1.5998\right)\cdot\left(\frac{I}{m^\circ}\right) + \left(\frac{-12.1652}{(T/\mathrm{K})} + 0.07871\right)\cdot\left(\frac{I}{m^\circ}\right)^2 + \ln(1 - 0.001005 \cdot S)$$

$$\ln(K_{1P} / k^\circ) = \frac{-4576.752}{(T/\mathrm{K})} + 115.525 - 18.453\ln(T/\mathrm{K}) + \left(\frac{-106.736}{(T/\mathrm{K})} + 0.69171\right)\cdot S^{1/2} + \left(\frac{-0.65643}{(T/\mathrm{K})} - 0.01844\right)\cdot S$$

$$\ln(K_{2P} / k^\circ) = \frac{-8814.715}{(T/\mathrm{K})} + 172.0883 - 27.927\ln(T/\mathrm{K}) + \left(\frac{-160.340}{(T/\mathrm{K})} + 1.3566\right)\cdot S^{1/2} + \left(\frac{0.37335}{(T/\mathrm{K})} - 0.05778\right)\cdot S$$

$$\ln(K_{3P} / k^\circ) = \frac{-3070.75}{(T/\mathrm{K})} - 18.141 + \left(\frac{17.27039}{(T/\mathrm{K})} + 2.81197\right)\cdot S^{1/2} + \left(\frac{-44.99486}{(T/\mathrm{K})} - 0.09984\right)\cdot S$$

Figure 1-1 continued.

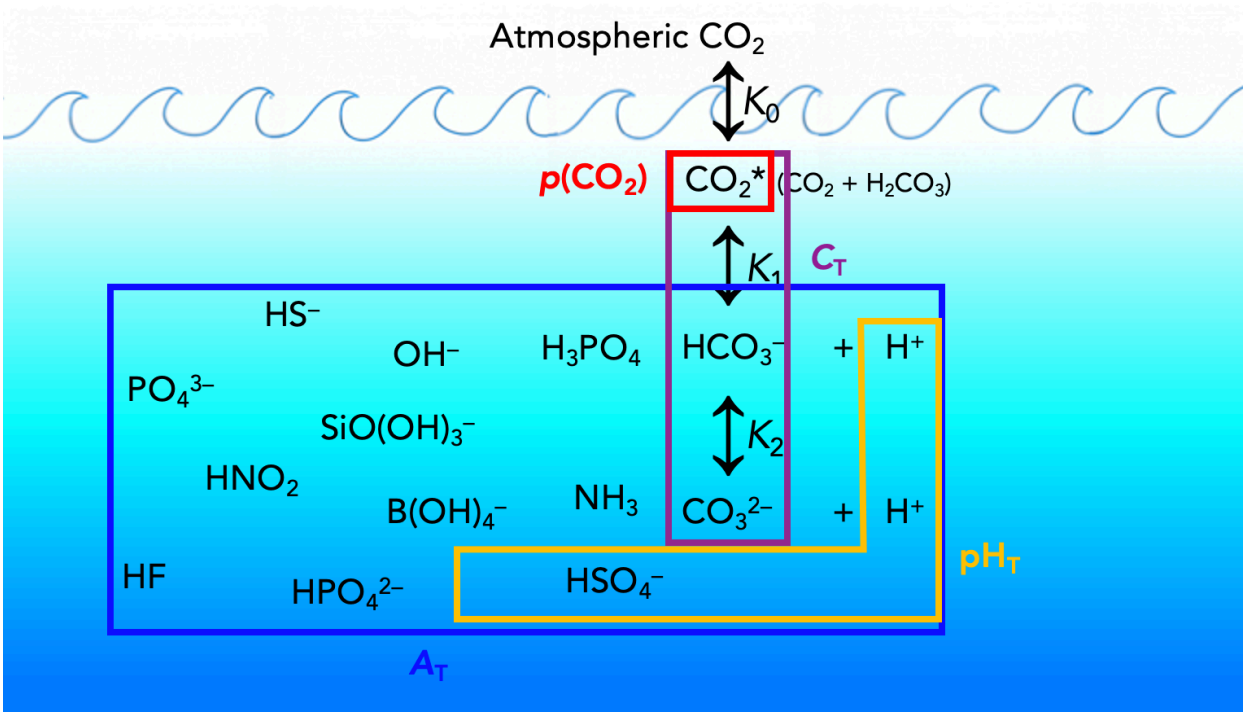

Figure 1-2 Schematic illustrating the relationships between A_T, C_T, pH_T, and $p(CO_2)$

The only way to improve the odds of making a useful assessment of the state of, or changes in, seawater CO_2 chemistry is to improve our understanding of the chemistry involved. The Global Ocean Acidification Observation Network (GOA-ON) has provided guidance in this question, as to "how good is good enough" and provided uncertainty goals to ensure measurements related to climate change and ocean acidification, made by different research groups in different parts of the world, are comparable and of sufficient quality (Newton et al. 2015).

1.3 Focusing on quality of measurements

GOA-ON defined two different uncertainty goals pertaining to CO_2 measurements, including a "climate" goal which is "defined as measurements of quality sufficient to assess long term trends with a defined level of confidence", and for A_T and pH implies an uncertainty

of 2 μmol kg^{-1} and 0.003, respectively (Newton et al. 2015). The "weather" uncertainty goal is "defined as measurements of quality sufficient to identify relative spatial patterns and short-term variation", and requires an uncertainty of 10 μmol kg^{-1} and 0.02 or better in A_T and pH_T, respectively. A study by Bockmon and Dickson (2015), however, showed that when a large proportion of relevant research labs were given the same solutions to analyze for A_T and pH_T (and C_T), the agreement between the values the various laboratories reported and "certified" values were largely only within the weather uncertainty goal of GOA-ON, and rarely within the climate goal. The results were particularly discouraging for electrometric pH_T measurement methods which are still widely used in marine research.

Two areas have been highlighted to improve the internal consistency and accuracy of studying the CO_2 system, namely the need for reliable standards that are easily accessible, and a full understanding of relevant acid-base equilibria. Of the former, the CO_2 certified reference materials (CRMs) (Dickson 2010) have paved the way for greater consistency in measuring C_T and A_T. While seawater-appropriate calibration solutions for pH_T measurements exist (DelValls and Dickson 1998), these are not widely available and pH_T is arguably one of the most commonly used measurements to describe the CO_2 system. As we shall see, the definition of A_T has evolved extensively throughout the years, and although there is general agreement on the contributions from inorganic acid-base systems, the likely contribution from organic acid-base systems has yet to be understood because there exists no unambiguous method of measuring such unidentified acids or bases.

1.4 Research objectives – quality of pH_T and A_T measurements

As mentioned, pH_T measured by electrometry has been and still is one of the easiest ways to measure pH_T, and the advent of pH_T sensors integrated into autonomous instrumentation have increased their geographical reach and applicability. A major issue with electrometric pH_T measurements, particularly those performed with a cell containing a liquid junction, is that the measurement itself is affected by the ionic matrix of the sample it is measuring. Therefore, it is paramount to calibrate the measurement using a calibration solution with an ionic strength and composition similar to that expected of the sample. While calibration solutions for low-ionic strength pH_T measurements are widely available (developed by the "National Bureau of Standards", now "National Institute of Standards and Technology") (Buck et al. 2002), for seawater they are not. Chapter 2 describes a method for preparing TRIS buffers in a synthetic seawater mixture which makes this an appropriate calibration solution for seawater pH_T measurements. Preparing such buffers have long been thought of as being a rather complex process and with a lack of confidence in their reproducibility. Key to the method described in Chapter 2 is the use of easily attainable supplies and that it relies on easy-to-learn calibration techniques. The method of preparation is accompanied by an estimate of its uncertainty, making this buffer an appropriate calibration solution for measurements expected to fulfil the "weather" uncertainty goal set by GOA-ON.

The measurement of A_T is another measurement that can be performed with simple materials and reagents, however, when estimating A_C from A_T uncertainty arise from calculating the contribution of other acid-base systems. As our measurement technology and sensitivity have improved it is evident that while we have probably identified all of the inorganic acid-base systems that might constitute a significant proportion of A_T, there are undoubtedly organic acid-

base systems that are not easily measured, understood, or accounted for. Chapter 3 will show a titration method designed to identify the presence of such unidentified "protolytes" and quantify the amount of unidentified protolyte (A_X) at a certain pH_T with an accompanying uncertainty. Chapter 4 will show examples of this titration method in use in simple laboratory mixed solutions to illustrate the success of the system when everything in a sample is identified and accounted for, and in a selection of seawater samples from various coastal environments.

1.5 Next steps

The research covered in this dissertation addresses some of the identified issues in regard to the quality of marine CO_2 measurements, namely calibrating seawater pH_T measurements and unambiguously measuring unidentified alkalinity components. In the case of seawater pH_T calibration, the buffer that will be presented is appropriate for open-ocean conditions where neither salinity nor pH_T changes all that much. Conversely, the coastal ocean can change rapidly and dramatically from e.g., storm events (Paulsen et al. 2017) and the importance of such events in climate modelling and other ecosystem assessments are hard to understand without an estimate of the uncertainty associated with the relevant measurements. Additionally, coastal and estuarine waters also cover a far wider salinity range. Moving ahead, work will be needed to carefully evaluate what salinity- and pH_T range of buffers are required for any given coastal or estuarine pH_T study. Further, both of these questions will have different answers depending on the admissible uncertainty. For example, pH_T might cover a wide range in an estuarine system and this could necessitate a multi-point calibration (the buffer presented in Chapter 2 is currently only tested to be prepared at one pH_T) as uncertainty in the calibration can increase rapidly if the sample pH_T is more than a few tenths of a unit away from the calibration pH_T (Buck et al. 2002;

Pratt 2014). Another question is whether or not synthetic seawater, which a simple mix of the six major ions in seawater, is sufficiently similar to seawater. Or, in other words, when does this simplification go from practical to inaccurate? Such questions can become particularly important in low-*S* environments, where nutrients and minor ions can represent a larger proportion of the ionic matrix than it would high-*S* environments (Pawlowicz 2015). Work is currently underway to determine a wider range of the relevant activity coefficients and will subsequently be used in ionic interaction modelling, such as the Pitzer equations (Humphreys et al. 2020).

In the estuarine realm we also face problems with A_T. With a higher influence of biology and (often) shallower waters that are disproportionally affected by run-off, there is a far greater chance for encountering unidentified alkalinity components. It would therefore be of interest to employ the titration method in Chapter 3 to such water masses as it will help determine how suitable A_T is as a CO_2 system parameter in these environments. As has already been hinted at, however, there are other sources of uncertainty in estuarine waters that need be resolved to be able to measure A_X in estuarine waters at the same, low level of uncertainty as for in open-ocean seawater (including, for example, determining acid dissociation constants over a wider range of *S*).

If the sensitivity of the titration system described in Chapter 3 proves high enough, it would be of great interest to collect samples for A_X analyses in the open ocean, for example along the GO-SHIP cruise lines seeing we currently don't know much about A_X except what can be inferred from comparing measured to calculated A_T (see, e.g., Fong and Dickson 2019). Creating an unambiguous base-line for the variation and magnitude of A_X will be helpful especially to help evaluate when A_T will be an appropriate CO_2 system parameter to use, or

when it is likely to be affected by A_X and thus a less favorable choice. It would further be desirable to create time-series of A_X in different kinds of environments, including from the open-ocean and towards more coastal waters. Furthermore, A_T is often used to infer changes biogeochemical processes such as coral reef calcification. It is commonly assumed that the only changes in A_T occurred related to the carbonate species and inorganic nutrients (Schoepf et al. 2017), although it is also known that a significant amount of organic matter is processed (Tanaka et al. 2011) and it is not clear whether or not some of the organic matter has acid-base qualities. What we can say, currently, about the presence of A_X in the ocean is that it is likely ubiquitous, but may vary significantly from ocean to ocean, or environment to environment. We cannot really know until we actually make the unambiguous measurements.

2 PREPARATION OF TRIS BUFFERS IN SYNTHETIC SEAWATER

2.1 Background

The process known as ocean acidification (OA) is causing a decrease of surface ocean pH and accompanying changes in acid-base chemistry. OA results from the uptake of anthropogenic CO_2 and there is a broad interest in monitoring and understanding how marine organisms respond to changes in ocean pH. While pH is one of the parameters most commonly used to describe seawater acid-base chemistry, other parameters that are not so easily measured are often more relevant for certain organisms (Orr et al. 2005). If pH is measured in conjunction with another parameter describing the CO_2 system it is possible to calculate such parameters, one example being the carbonate ion concentration, and hence the aragonite saturation state. However, for pH measurements to be appropriate for such calculations, and to enable comparison across time and space, it is important that the measurements are of a known uncertainty. It is also important to ensure that the choice of calibration buffer produces a pH value that is consistent with the relevant acid-base constants used in such calculations. Presently, this requires that the buffer is based on a synthetic seawater recipe intended to ensure that activity coefficients of acid-base species in the buffer are similar to what they would be in real seawater of the same nominal salinity, and using a pH scale that is appropriate for seawater: the total hydrogen ion scale, pH_T (Dickson et al. 2016). Access to suitable seawater pH_T calibration buffers is therefore key and, ideally, these should either be easily available or simple to prepare reproducibly.

The Global Ocean Acidification Observation Network (GOA-ON; http://www.goa-on.org) has proposed a standard uncertainty goal for the measurement of seawater pH of 0.02

(Newton et al. 2015). This uncertainty goal for pH will, when combined with the measurement of another CO_2 parameter such as total alkalinity or total dissolved inorganic carbon (C_T), allow for calculation of carbonate ion concentration with a relative standard uncertainty of ≤10%. This level of uncertainty (the "weather goal" of GOA-ON) is intended to be sufficient to identify relative spatial patterns and short-term variations, while also supporting mechanistic interpretation of the response to, and impact on, local and immediate ocean acidification processes. In the coastal ocean, the weather uncertainty goal is particularly relevant as the observed pH changes are usually much larger than those observed in the open ocean (see, for example, fig. 2 in Hofmann et al. 2011). This uncertainty goal for pH measurements will also enable laboratory studies of physiological processes potentially affected by OA such as calcification or primary production, and will allow comparison of similar studies performed at different locations.

The uncertainty of a pH measurement necessarily includes both the uncertainty of the sample measurement process and the uncertainty associated with the calibration. The combination glass/reference cell ("glass electrode" hereafter) which uses potentiometry to measure pH, is perhaps the most widely used pH measurement technique and can resolve changes in pH of ~0.003 depending on electrode design and sample handling procedure (Dickson et al. 2007; Easley and Byrne 2012), although 0.01 would be more usual. This suggests that with proper calibration, glass electrodes are able to fulfil the "weather" uncertainty goal proposed by GOA-ON. However, certain requirements of the calibration standard are necessary for the pH measurement to be useful in CO_2 system calculations. First, while glass electrodes measure the potential (E) of a solution, this measurement strictly depends on the unitless activity of hydrogen ions ($a(H^+)$) (Figure 2-1).

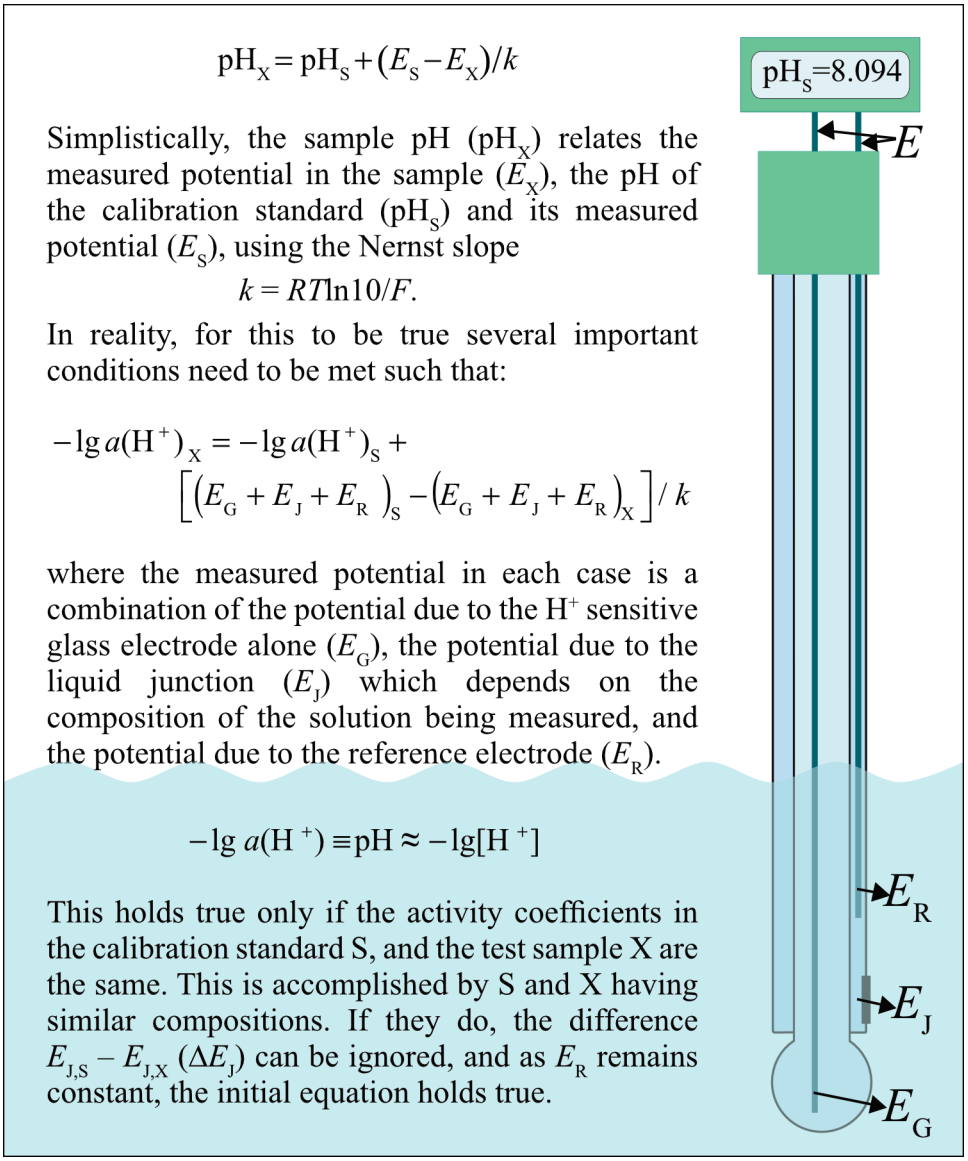

Figure 2-1 Schematic of a combination glass/reference electrode and what potentials are involved when measuring pH.

However, for seawater CO_2 system calculations it is the amount content of hydrogen ion expressed in moles per kilogram of solution ($[H^+]$) that is needed. $[H^+]$ and $a(H^+)$ are related by the activity coefficient of H^+, $\gamma(H^+)$, which is a function of solution ionic strength and composition. If $\gamma(H^+)$ is the same in both the calibration standard (S) and sample (X), the measured pH can be interpreted as $[H^+]$ instead of $a(H^+)$. In addition, the composition of the solution being measured also influences the potential of the glass electrode through the liquid

junction that connects the external measured solution (either calibration standard or sample) with the internal reference electrode solution (Figure 2-1). The potential across this junction (E_J) will likely be different in the calibration standard and in the sample, and this "residual liquid junction potential" (ΔE_J) is not easily quantified (see, for example, Buck et al. 2002 and citations therein). By calibrating the glass electrode in a standard with a similar ionic strength and composition to the sample, ΔE_J can be minimized (Hansson, 1973). Lastly, the expression used to convert the measured potential, E, to a pH value assumes "Nernstian behavior" of the electrode, meaning a change of one unit in pH results in a potential change equal to the temperature-dependent "Nernst factor" k (Figure 2-1). Ideal Nernstian behavior is unlikely for any given glass electrode system, and to account for this a "bracketing calibration" is often used. Bracketing means the electrode is calibrated with two or more standards of different pH values, where the expected sample pH value is between the highest and lowest calibration point (c.f. Buck et al. 2002). The pH range in the ocean is fairly narrow, however, and the pH range of the global surface ocean is less than one unit (Takahashi et al. 2014). Provided the one-point calibration standard has a pH within the observed ocean pH range (~8), the error associated with likely non-Nernstian behavior will be small.

A preferred calibration standard for seawater pH_T measurements has become the buffer formed from the base species: 2-amino-2-hydroxymethyl-1,3-propanediol (TRIS), and its conjugate acid: $TRIS{\cdot}H^+$, prepared in an ionic medium with a composition similar to that of seawater (Hansson 1973b; Ramette et al. 1977). At a temperature of 25 °C and a salinity (S) of 35 the 0.04 mol kg-H_2O^{-1} (or 0.03827 mol kg-solution^{-1}) equimolar buffer has a pH_T of 8.094, which is within the observed open ocean pH range (DelValls and Dickson 1998; Olsen et al. 2016). An equimolar buffer implies that the buffering species, TRIS and $TRIS{\cdot}H^+$ are present in

equal amounts. For such a buffer, the pH is determined by the acid dissociation constant (pK°) of the buffering substance and the quotient of the appropriate activity coefficients (Eq. 2-1). While the thermodynamic pK° is a function of temperature and pressure alone, the activity coefficient term is also a function of solution composition. TRIS, however, is an amine buffer, meaning that the activity coefficient term includes a singly-charged cation in both the numerator and the denominator (Eq. 2-1) (Bates 1961). Because of this, amine buffers offer the advantage of their pH not being very sensitive to changes in ionic strength and composition (S) at any given temperature.

$$\mathrm{pH(TRIS)} = \mathrm{p}K^{\circ}(\mathrm{TRIS}\cdot\mathrm{H}^{+}) - \log\left(\frac{[\mathrm{TRIS}\cdot\mathrm{H}^{+}]}{[\mathrm{TRIS}]}\right) - \log\left(\frac{\gamma(\mathrm{TRIS}\cdot\mathrm{H}^{+})}{\gamma(\mathrm{TRIS})\cdot\gamma(\mathrm{H}^{+})}\right)$$

Eq. 2-1

The assumption that is typically made when using a TRIS buffer is that the activity coefficient product in Eq. 2-1 is similar in value in the synthetic seawater (SSW; the ionic background) to what it would be the in natural seawater of the same nominal S. As a result, the activity coefficient product can be considered largely to be a function of S as well as temperature and pressure (a more detailed discussion of this can be found in Müller et al. 2018). A key consequence of this assumption when using such a buffer to calibrate the measurement of $[H^+]$ in seawater is that, if the calibration buffer and the measured sample differ significantly in S, a systematic error will be introduced. Its magnitude is not well-defined as it results from two factors: the changes in activity coefficient with solution composition, and the change in the liquid junction potential (E_J in Figure 2-1) between the calibration buffer and the sample – again a result of the changing composition. This has been evaluated empirically by Butler et al. (1985) for a particular junction design and a change of ~5 in S resulted in an error of ~0.01 in pH.

2.2 Buffer preparation

2.2.1 Background

Although a detailed method for the preparation of equimolar TRIS-TRIS·H^+ buffers in SSW has not been published, DelValls and Dickson (1998) presented a buffer solution composition (Table 2-1) to which they also assigned a pH_T. Their method of buffer preparation is intended to produce buffers for analysis by a high-precision electrometric method, and if followed carefully ensures buffers with highly reproducible pH_T values (e.g., Nemzer and Dickson 2005; Pratt 2014; Müller et al. 2018). The uncertainty and purity goals associated with the various buffer components (Table 2-1, column 4) used by DelValls and Dickson are quite stringent, however, and preparing a buffer to this high level might not only be impractical for many research groups, but even unnecessary. To simplify the buffer preparation method, it is important to keep in mind the two key features required for the resulting TRIS buffer to have the expected pH_T. This includes ensuring that the buffering species TRIS and TRIS·H^+ are present in a 1-to-1 ratio, and that the SSW background has the same composition as used by DelValls and Dickson. While the buffer ratio has the largest effect on the pH_T of TRIS, the composition of the SSW ensures that the activity coefficient term and E_J are comparable between the calibration standard and the seawater sample. As noted earlier, this consistency in activity coefficients for calibration and measurement provides the basis of using the pH_T measurement in further calculations dealing with other acid-base systems, including the CO_2 system. A discussion regarding to what extent the synthetic seawater needs to be "similar enough" to real seawater and its implication for relevant activity coefficients can be found elsewhere (Pratt 2014; Dickson et al. 2016).

Table 2-1 Composition of 0.04 mol kg-H_2O^{-1} equimolar TRIS–TRIS·H^+ buffers at a *S* of 35 by DelValls and Dickson

Component	mol kg-H_2O^{-1}	mol kg-solution^{-1}	Impurity specification (<) or relative uncertainty (±) in component amount [a]
HCl	0.04000	0.03827	±0.02 %
TRIS	0.08000	0.07654	±0.02 %
NaCl	0.38764	0.37089	< 0.1 % [b]
Na_2SO_4	0.02927	0.02801	< 0.1 % [b]
KCl	0.01058	0.01012	< 0.1 % [b]
$MgCl_2$	0.05474	0.05237	< 0.1 % [b,c]
$CaCl_2$	0.01075	0.01029	< 0.1 % [b,c]

[a] Reported values from DelValls and Dickson (1998); [b] Recrystallized for purification, exact impurity not characterized; [c] Added as solutions, see Method.

The SSW chosen to represent natural seawater for this purpose is a simple mixture comprising the six major ions of seawater (Cl^-, Na^+, SO_4^{2-}, Mg^{2+}, Ca^{2+}, and K^+). Minor components occurring in natural seawater, including acids and bases, have been replaced by an equivalent amount of one of the major ions of similar charge. Matching of ion charge helps to ensure that activity coefficients can be assumed the same in the SSW as in real seawater. The one exception to this is sulfate which reacts with hydrogen ion to form the hydrogen sulfate ion, and has proven hard to replace due to its relatively large amount and it being a double charged anion (Millero 1974). Instead of omitting sulfate from the SSW matrix, a pH scale intended for seawater use has been defined which implicitly includes the acid-base contribution of sulfate

(Hansson 1973b; Dickson 1993). This scale is known as the total hydrogen ion scale (pH_T; Eq. 2-2) and states that the pH_T of a solution is proportional to the free hydrogen ion amount content ($[H^+]_{free}$). The factor relating pH_T to $[H^+]_{free}$ depends on the total sulfate amount content $[SO_4^{2-}]_T$ of the solution and the stoichiometric acid dissociation constant of hydrogen sulfate, $K(HSO_4^-)$. Because sulfate is a conservative parameter in seawater, its total concentration $[SO_4^{2-}]_T$ can be estimated directly from *S*. As long as the $[SO_4^{2-}]_T$ in the calibration standard corresponds to *S*, the pH calibration can be made on the total H^+ scale:

$$pH_T = -\log\left(\left[H^+\right]_{free}\left(1+[SO_4^{2-}]_T / K(HSO_4^-)\right)\right)$$

Eq. 2-2

Preparing TRIS buffers according to the published component uncertainties and purities (Table 2-1) is not necessary for the calibration of glass electrodes, nor for the majority of research concerning marine organisms and their physiological response to changing ocean acid-base chemistry. There is nevertheless a need for an explicit method of buffer preparation that is reproducible to a known uncertainty, using materials that are easily available to the majority of laboratories with basic chemical equipment. The key focus is to ensure that the buffer ratio is 1, and the SSW composition ensures activity coefficients that are consistent with other relevant seawater acid-base constants. The goal of this work is to describe a method for TRIS buffer preparation that will result in a buffer pH_T equivalent to the value assigned by DelValls and Dickson (1998). This buffer will be appropriate to calibrate pH_T measurements expected to fulfil the GOA-ON "weather" uncertainty goal of 0.02.

2.2.2 Simplifying buffer preparation

The TRIS buffers used by DelValls and Dickson (1998) were prepared using highly purified and carefully characterized reagents. This included using doubly-distilled and coulometrically standardized HCl, using TRIS from the National Institute of Science and Technology (NIST) of certified purity, and SSW salts that had been purified by recrystallization (dissolving in de-ionized water followed by re-precipitation by partially evaporating the solution). Furthermore, NaCl, Na_2SO_4 and KCl were dried thoroughly following re-crystallization. The recrystallized $MgCl_2$ and $CaCl_2$ were prepared into solutions rather than dried salts, due to their highly hygroscopic nature which makes it difficult to know the exact amount of water in their crystal structure. These two solutions were subsequently calibrated by analyzing their chloride content through precipitation of AgCl from an addition of excess $AgNO_3$. All buffer components were weighed using a high-resolution (0.01 mg) balance and quantitatively transferred to the container. Finally, the buffer solution was brought to the desired total solution weight by adding de-ionized water.

To design a simplified method for preparing TRIS buffers, three areas of experiments were carried out. These included using a simple colorimetric acid-base titration to calibrate HCl directly against commercially available TRIS solid, thus ensuring a buffer ratio of 1, while avoiding having to use purified and carefully characterized TRIS and HCl. The buffer was further prepared to a total volume, eliminating the need for determining the weight of the final solution. Lastly, a combination of ionic interaction-modelling and simple experiments was used to investigate the sensitivity of the pH of the buffer to changes in the SSW matrix ($\Delta pH/\Delta salt$), changes that exceeded the likely errors that could occur during preparation of the synthetic seawater.

2.3 Methods

2.3.1 Calibrating the buffer ratio by titration

This method makes use of a simple colorimetric acid-base titration that is described in detail in appendix A1, together with all the calculations involved. Briefly, ~1 g (recorded to a resolution of 0.1 mg) of TRIS was dissolved in approximately 80 g of de-ionized water, to which six drops of 0.1 % methyl red indicator were added. The yellow-colored solution was titrated by weight with (approximately) 1 mol kg^{-1} HCl using disposable transfer pipettes until a distinct pink color was reached. The weights of TRIS and HCl were corrected to mass (Schoonover and Jones 2002) and the amount content of the HCl solution, $[HCl]_{titr}$, was calculated assuming the TRIS was 100 % pure. We performed these titrations primarily using TRIS from Macron (LOT 61548), NIST (SRM723e), and Fisher Scientific (LOT 144607), while a small number of titrations were carried out with TRIS from Sigma Aldrich (LOT 11K5445) and MP Biomedicals (LOT Q4553) for additional comparisons. The HCl solution was prepared by diluting 35–37 % ACS reagent grade HCl solution from Fisher Scientific.

Because this method assumes that the TRIS is 100% pure, any impurities in the TRIS (see Discussion) will result in an inaccurate amount content for the HCl, while still ensuring that an accurate buffer ratio of 1 can be obtained. To evaluate the accuracy of this titration approach we standardized one batch of HCl using coulometry ($[HCl]_{coul}$), as described in the appendix of Dickson et al. (2003), and compared this to the amount content determined by titration, $[HCl]_{titr}$.

2.3.2 Preparing the buffer

TRIS buffers were prepared in two ways, one set of more carefully prepared buffers ("primary buffers") to assess the success of calibrating the buffer ratio by titration, and one set of less carefully prepared buffers ("prepared volumetrically") to evaluate a simpler overall preparation approach. The SSW of the primary buffers were prepared using NaCl, Na_2SO_4, and KCl as dried salts, $MgCl_2$ and $CaCl_2$ as calibrated solutions, and the buffer solution was brought to a particular total mass. Buffers prepared volumetrically used salts that had not been dried, $MgCl_2$ and $CaCl_2$ solutions with manufacturer calibration, and the buffer solution was brought to a particular total volume rather than mass. For both kinds of buffer, the buffer ratio was calibrated as described in the section above. All salts used for the SSW conformed to the American Chemical Society reagent grade specification (ACS; Tyner and Francis 2017) and were used without further purification.

For the primary buffers, the salts were dried at 200 °C for at least 4 hours and cooled to room-temperature in a desiccator prior to preparing the buffer. Solutions of $MgCl_2$ and $CaCl_2$ were prepared in our laboratory and calibrated by titration against standardized ~0.3 mol kg-solution^{-1} $AgNO_3$ in the presence of a chromate/dichromate indicator as described in Vogel (1961), also known as a Mohr titration. The estimated relative standard uncertainty for this titration method is 0.5 %. For the volumetrically prepared buffers, the manufacturer's calibrations of ~1 mol kg^{-1} $MgCl_2$ and $CaCl_2$ solutions were used. No certificate of analysis was provided for the $MgCl_2$ solution (beyond being sold as a "1 mol L^{-1}" solution), while the $CaCl_2$ had a calibrated concentration of 1.04 mol L^{-1}.

Each type of buffer was prepared by first estimating the target weight of HCl solution that would be needed to prepare the desired quantity of buffer (either a particular weight of

primary buffer, or a particular volume otherwise). A quantity of HCl solution approximating this target value was then weighed out. The desired weights of TRIS, the various SSW salts, and the total solution weight (primary buffers only), were each scaled to correspond to the weight of dispensed HCl so as to produce a buffer of the relative proportions shown in table 1, and an effort was made to weigh out these desired amounts closely. The weights of HCl solution, TRIS, and the SSW salts, were recorded to a resolution of 0.1 mg. De-ionized water was used to quantitatively transfer all components into the buffer container and to dilute to the desired total buffer quantity. The total weight of the primary buffer solution was recorded using a high-capacity balance of 0.01 g resolution. A total of six buffers were prepared this way by one laboratory technician. Buffers prepared volumetrically were brought to a total volume of 1 L using a volumetric flask and a knowledge of the density of the resulting buffer (removing the need for a high-capacity balance). A total of ten buffers were prepared this way by two different laboratory technicians, and this buffer preparation approach is described in detail in appendix A2. Equations are provided that characterize the density of the resulting TRIS buffer, and that enable scaling of the desired weights of all components to the original dispensed weight of HCl.

2.3.3 Assessing effects of uncertainties in preparing the synthetic seawater

Errors can arise during the preparation of the buffer, and ACS grade chemicals are only provided with an upper-limit of impurities. While water is likely the main impurity, access to a drying oven (or other means of reducing the level of this impurity) might not always be available. It is possible to estimate the likely implications on the buffer pH_T of small compositional changes resulting from weighing errors or water contamination. The approach used here was to perform calculations with a Pitzer-type ionic interaction model similar to those used by Waters and Millero (2013) and by Gallego-Urrea and Turner (2017). These calculations

were carried out for us by Dr. Simon Clegg of the University of East Anglia, United Kingdom. The change in the molality (mol kg-H_2O^{-1}) of free hydrogen ion, $m(H^+)$ resulting from a 1% change in the total concentration of each of the various buffer components (Table 2-1) was calculated using a Pitzer model. The primary sensitivity was due to changes in the amounts of TRIS and of HCl, which in addition to affecting the buffer ratio (Eq. 2-1) have a comparatively minor effect on the relevant activity coefficients. In fact, for a 1 % change in the buffer ratio, the buffer pH will change by about 0.004 pH units, due almost entirely to the change in buffer ratio. The next most significant change in $m(H^+)$ resulted from an error in the amount of NaCl where a 1 % change resulted in a small change of <0.001 in pH_T. A 1% error in the amount of Na_2SO_4 results in a very small change in $m(H^+)$ (<0.04 %), but as can be seen from Eq. 2-2 the change in the sulfate ion concentration can have an additional effect when considering (as we do here) the total H^+ concentration. We estimate the overall effect from a 1 % error in amount of Na_2SO_4 to be ~0.3 %, or an error of a little more than 0.001 in pH_T, using Eq. 2-2. For the other components, the largest effect is for a 1 % change in the amount of $MgCl_2$ which results in an estimated change of pH_T of 0.0001 (i.e. a negligible amount).

This Pitzer-modelling approach was supplemented with a simplistic experiment where six buffers were prepared with an identical buffer ratio but slightly different SSW compositions. These six buffers were prepared similarly to the primary buffers described above, with the exception that an HCl-TRIS mixture was prepared and divided into the six bottles before adding the remaining components (scaling them to the weight of HCl in the mixture). This ensured identical buffer ratio in the six buffers. While one of the six buffer solutions was prepared as a regular, “unaltered” TRIS buffer, the amount of one the SSW salts: NaCl, Na_2SO_4, KCl, $MgCl_2$, or $CaCl_2$ was increased by approximately 15 % in each of the remaining five bottles. This

resulted in five different buffers which all had a different composition from that of a regular TRIS buffer, and a different composition from one another. This simplistic experiment was repeated a total of three times.

The unaltered and altered buffer solutions were subsequently examined spectrophotometrically at 25 °C using the (purified) pH-sensitive dye *meta*-cresol purple (mCP) and the method described by Carter et al. (2013). The pH of the unaltered and altered TRIS buffers were calculated based on the equations of Liu et al. (2011). It is, however, important to recognize that the changes in the ionic composition of the TRIS solution will also affect the activity coefficients of the mCP dye. This would result in a calculated pH value, obtained spectrophotometrically, that is likely not consistent with other relevant acid-base parameters in seawater. Thus, this calculated "pH" will not be identical to the actual pH_T of the buffer, and the pH values from these experiments are referred to here as pH_{spec}.

2.4 Results and discussion

2.4.1 Using and acid-base titration to ensure the buffer ratio

For one batch of HCl, $[HCl]_{titr}$ was determined using Macron TRIS on five separate days, as the mean of ≥ 3 titrations each day, and on each day that particular value was used to prepare a batch of primary TRIS buffer. This particular batch of HCl had been standardized previously using coulometry, $[HCl]_{coul}$, which enabled an estimate of the accuracy of the titration method (or, largely, of TRIS impurities). The relative percent difference between $[HCl]_{titr}$ and $[HCl]_{coul}$, was small for each of the five days, and within the relative standard deviation, 0.1 %, of the titration method (Figure 2-2a).

The resulting pH_T of the buffer, measured spectrophotometrically, was within 0.002 of the value originally assigned by DelValls and Dickson (1998) (Figure 2-2b). Furthermore, the range of pH_T values was within the expected range resulting from the $[HCl]_{titr}$ calibration uncertainty, and within the uncertainty estimated for the spectrophotometric measurement technique itself (<0.004; Müller and Rehder 2018). There appeared to be no correlation between the deviation in buffer pH_T from the assigned value (8.094) and %Δ[HCl].

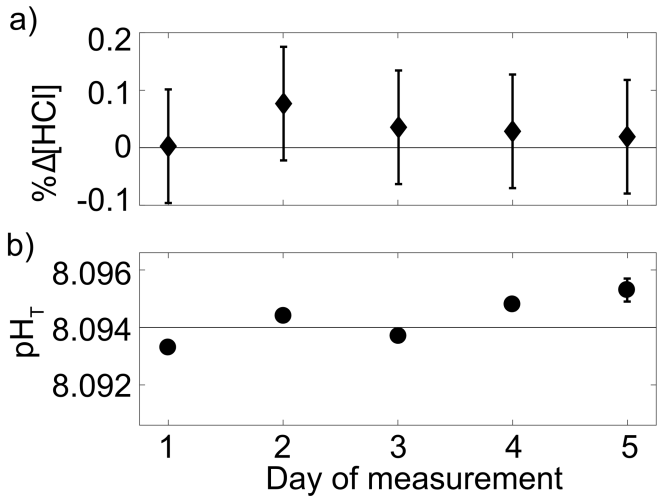

Figure 2-2 %Δ[HCl] and corresponding pH_T on five different occastions. a) shows mean %Δ[HCl] = 100· ([HCl]titr – [HCl]coul)/ [HCl]coul %, (n ≥ 3) for the five different days of measuring [HCl]titr while the bars represents one relative standard deviation of the titration technique and not for each individual set of titrations. Panel b) shows the mean pHT (n ≥ 4) of each of the five TRIS buffers, the bars represent one standard deviation of each set of the pHT measurements and the black drawn line indicates the value 8.094.

Calibrating the HCl solution against TRIS solid will likely not yield the true [HCl] because TRIS crystals can have varying levels of water occluded in their crystal structure (Koch et al. 1975). This will act to over-estimate [HCl] relative to the true value, as our approach assumes the TRIS is 100 % pure. This value of [HCl] is however appropriate for use to prepare the TRIS buffer (e.g., Figure 2-2b), as the presence of a (small but unknown amount of) water impurity in the TRIS solid will be accounted for in this calibration. This implies that it is important to treat the TRIS similarly prior to HCl calibration and to preparing the buffer, e.g., it

should either be dried for both purposes or not at all. Thoroughly drying TRIS can be difficult and requires careful homogenization of the crystals. Furthermore, drying at high temperatures can decompose the molecule and while drying the salt over a hygroscopic substance, such as phosphorus pentoxide, in vacuum is preferred, most laboratories do not have easy access to this approach. It is therefore more practical to use TRIS solid "as is" without any further treatment. Any additional water added to the buffer solution in this way, (< 2 % of the total weight of TRIS according to the reagent grade specification), will decrease the total buffer amount by < 2 %, and the *S* of the resulting solution by < 0.02 %. Neither of these effects will change the pH_T of the buffer appreciably (see e.g., fig. 1 and 2b in DelValls and Dickson 1998).

It should be pointed out that the SSW composition used here is slightly different from that of "pure" SSW. The addition of HCl increases the ionic strength of the solution, and this effect is compensated for by reducing the amount of NaCl. Thus, while the calibrated $[HCl]_{titr}$ might achieve the correct buffer ratio, if it is higher or lower than the true amount content, the amount of NaCl will also be in error by the same amount and of opposite sign. This error is likely much smaller than the likely uncertainty introduced by using reagent-grade NaCl (≤ 1 % impurity; see "Preparing synthetic seawater" below).

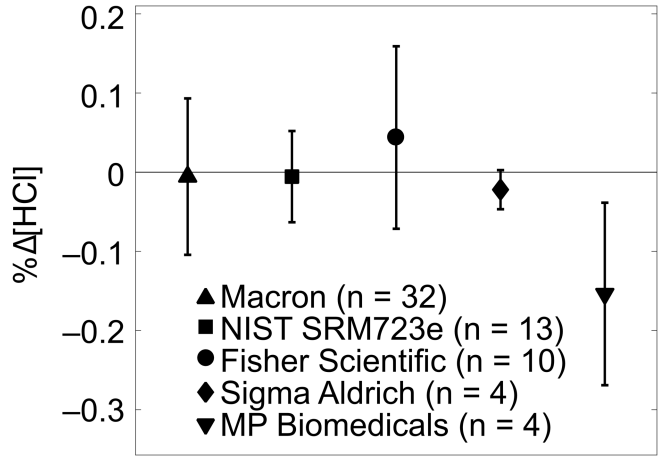

Figure 2-3 %Δ[HCl] as determined with TRIS from various manufacturers. Number of titrations are indicated in the parentheses in the legend.

The relative purity of TRIS from various commercial manufacturers is suggested in Figure 2-3, which shows %Δ[HCl] for a single batch of HCl calibrated against TRIS from five different manufacturers. Four of these, Macron, Fisher Scientific, Sigma Aldrich and MP Biomedicals, were all of "reagent grade", reported a water content of 2 % or less, and were used "as is". TRIS from NIST is far more homogenized than the other commercial sources, and it is sold with a certificate of purity for both with and without drying and further homogenization. As such, NIST SRM723e TRIS would be appropriate when it is necessary to accurately determine [HCl]. However, the high level of purity does not increase the quality of the buffer for the purposes described herein. NIST SRM723e is also more than 30 times as expensive as TRIS from the other commercially available sources.

A potential drawback to the less expensive sources of TRIS is increased crystal heterogeneity, where the weights used for titration (~1 g) may not necessarily be representative for the average water impurity of the amount of salt used for a 1 L buffer (~10 g). In terms of calibrating $[HCl]_{titr}$, this would result in an increased standard deviation, which is perhaps the

case when comparing e.g., $[HCl]_{titr}$ of TRIS from Macron versus from NIST in Figure 2-3. Although the titration data using TRIS from other commercial suppliers than Macron is limited, there appears to be little difference between the various commercially available sources of TRIS with the exception of MP Biomedicals. It is hard to ascertain whether the significantly lower $[HCl]_{titr}$ determined using TRIS from this source is due to the crystals being more heterogeneous, an overall higher amount of impurities, or just an artefact of the limited number of titrations performed.

2.4.2 Preparing synthetic seawater

There was a measurable increase in pH_{spec} (ΔpH_{spec}) between the unaltered TRIS buffers and those altered with 15 % of any single salt of the SSW matrix. ΔpH_{spec} correlated to the total amount of salts in solution (Figure 2-4; Table 2-1), in other words, ΔpH_{spec} seemed to be largely a function of change in the ionic strength of the buffer. ΔpH_{spec} did not, however, scale linearly to the change in ionic strength.

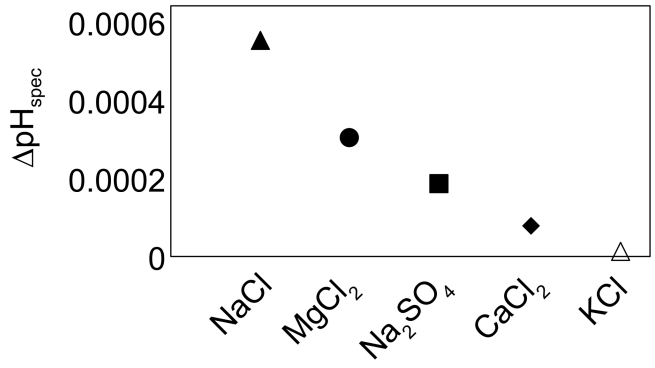

Figure 2-4 Estimated increase in pH_{spec} (ΔpH_{spec}) for the experimental buffers caused by the addition of salt, including 1 % extra of the salts NaCl (▲), $MgCl_2$ (●), Na_2SO_4 (■), $CaCl_2$ (◆), or KCl (△). ΔpH_{spec} was estimated by the observed change in pH_{spec} from adding 15 % extra salt and scaled to 1 %, to better represent likely preparation errors.

The change caused by salts containing divalent ions (Mg^{2+}, Ca^{2+}, and SO_4^{2-}) was larger than might be expected from the change in ionic strength their respective salts caused, compared

to the salts that only contained monovalent ions. This was likely caused by stronger interactions of the divalent ions with TRIS, $TRIS \cdot H^+$, and with the spectrophotometric dye mCP.

This simplistic view on buffer pH_T sensitivity to changes in the background ionic composition suggests NaCl and KCl can be added to the SSW as salts of 99 % purity or higher, without changing the buffer pH_T by more than ~0.0005 (Table 2-2), a view that is supported by the Pitzer modelling. $MgCl_2$ and $CaCl_2$ solutions used for this particular experiment were calibrated to ±0.5 % in our laboratory.

Table 2-2 Suggested specifications of reagents for the preparation of 1 L[a] TRIS buffers at a *S* of 35, and contributions to buffer pH_T uncertainties from the various components.

Component	Weight of component (g)	Tolerable impurity (<) or uncertainty (±) in relative component amount	Contribution to buffer pH_T uncertainty
HCl (1 mol kg-solution^{-1})	39.270[b]	±0.1 %	0.002
TRIS	9.517[b]	≤ 2 %	
NaCl	22.254	< 1 %	0.0005
Na_2SO_4	4.085	< 1 %	0.001
KCl	0.775	< 1 %	~0
$MgCl_2$ (1 mol L^{-1})	58.862	±1.5 %	0.0004
$CaCl_2$ (1 mol L^{-1})	11.726	±1.5 %	0.0001
De-ionized water	"Fill to line"	±1 %[c]	0.001
Accumulated maximum uncertainty relative to 8.094			0.005

[a] Assumes that volume is calibrated (and measured) at 20 °C; [b] Weights of HCl and TRIS subject to the measured $[HCl]_{titr}$; [c] Includes error in weighing HCl to the desired amount, and implications of subsequent scaling amounts of remaining components.

Our results suggest that they can be used successfully as the commercially available 1 mol L^{-1} solutions (provided these are calibrated to ±2 % or better from the manufacturer), producing an accumulated buffer pH_T uncertainty of less than 0.0005 (Table 2-2). While it is possible to add $MgCl_2$ and $CaCl_2$ directly as solids ($MgCl_2 \times \sim 6H_2O$ and $CaCl_2 \times \sim 2H_2O$), their exact level of hydration would need to be known. The number of H_2O in their crystal structure can vary significantly depending on the environmental conditions in the laboratory where the salts are stored, and determining the level of hydration would involve additional analysis. While increasing the amount of Na_2SO_4 did not have a large effect on observed pH_{spec}, a 1 % change in $[SO_4^{2-}]_T$ has implications for the use of the pH_T scale. Increasing $[SO_4^{2-}]_T$ by 1 % at a constant $[H^+]_{free}$ changes pH_T by nearly 0.001 unit (using Eq. 2-2), which is much larger than the observed ΔpH_{spec} from such an increase in the amount of Na_2SO_4 (Figure 2-4). Nevertheless, carefully adding Na_2SO_4 as a salt of 99 % purity or better should not cause an error in pH_T of more than 0.001.

As was pointed out earlier, this simplistic experiment necessarily illustrates that the change in observed pH is not only caused by the actual buffer pH changing as a consequence of the extra salt, but also because the mCP dye behaves differently in the altered ionic background. The difference between ΔpH_{spec} and the ΔpH implied by the Pitzer model is particularly large for $MgCl_2$ and it is believed that the base form of mCP, a doubly charged anion, interacts more strongly with the divalent Mg^{2+} compared to the other SSW ions. Despite the slightly different results from the two approaches, the likely error in a normal buffer preparation will be small.

An altered ionic composition may also affect measurements made with glass electrodes, although it is a less sensitive measurement than the spectrophotometric pH method. The pH of the experimental buffer with the largest change to its ionic composition (+ 15 % NaCl) was

measured and compared to the unaltered buffer using a glass electrode in our laboratory. This observed "ΔpH" was 0.01, which was the reported resolution of the glass electrode pH meter. Therefore, no other altered solutions were tested in this way as this indicated small errors in the SSW matrix are unlikely to produce a measurable difference when using a glass electrode.

2.4.3 Reproducibility in preparing TRIS buffers

Volumetrically prepared TRIS buffers were analyzed over the course of a couple of weeks, where several but not all buffers were analyzed on the same day. The ten buffers agreed very well with one another and their mean pH_T, measured spectrophotometrically, was 8.088 ± 0.001 (mean ± one standard deviation; n = 43) showing that our method is highly reproducible. Alongside these were also measured the pH_T of four batches of primary TRIS buffers, where the mean pH_T was 8.089 ± 0.001 (n = 50). It should be noted here that the expected pH_T of TRIS is 8.094, as determined by DelValls and Dickson (1998). This discrepancy of 0.005–0.006, if real, has many potential sources including the spectrophotometric measurement itself. To confirm that our buffers were consistent with historical Harned cell measurements made in our laboratory we made a small number of additional measurements on a subset of the TRIS batches. Two batches of primary buffers and one volumetrically prepared batch were analyzed in a spectrophotometric cell whose values for TRIS pH_T measurements had been previously cross-checked using the Harned cell. The average pH_T for all three batches using this cell was 8.092 (±0.001; n = 16), which is in good agreement with the value published by DelValls and Dickson.

Preparing the buffer by total volume rather than total weight removes some flexibility. If the first component added (i.e., HCl) is slightly wrong, you cannot straightforwardly prepare the

buffer to a scaled volume without gaining some uncertainty. Because the provided calculations will scale the weight of the remaining components to the added weight of HCl, the buffer might be prepared to a *S* that is slightly different than 35. As mentioned previously, the pH_T of a TRIS buffer is quite insensitive to changes in *S*, and from a *S* of 25 to 35 the change in $pK(TRIS{\cdot}H^+)$ is a little less than 0.02 at 25 °C (Bates and Hetzer 1961; DelValls and Dickson 1998). Provided the weight of HCl deviates less than 1 % from what would be required for a 1 L solution, the final error in the *S* of the sample would not be more than 1 %. This, in turn, should cause an error of less than 0.001 in the pH_T of the buffer solution according to equation 18 of DelValls and Dickson (1998). Any small errors caused by preparing the buffer to a certain volume are therefore largely outweighed by the benefit of only needing one high-resolution analytical balance and not an additional high-capacity balance.

2.4.4 Modification of the buffer for use with external chloride-sensitive reference electrodes

While the buffer prepared according to our proposed method is largely intended for the calibration of glass electrodes and similar pH sensors incorporating a liquid junction, it may also be suitable for other seawater pH_T measurements as long as its limitations are recognized. In particular, the use of the SeaFET™ sensor is becoming more widespread and integrated in sensor packages such as the SeapHOx (Bresnahan et al. 2014). Unlike the glass electrode pH cell, the SeaFET sensor utilizes a solid-state H^+ electrode, a reference electrode with a gel-filled junction, and an additional external chloride-sensitive reference electrode (Martz et al. 2010) which is also sensitive to bromide ion concentration. For those interested in calibrating such a sensor with TRIS buffers it will be necessary to add an appropriate amount of NaBr or KBr to

their buffer during preparation. For 1 L of TRIS buffer 0.103 g of KBr is needed, which has a trivial effect on the ionic strength.

2.4.5 Storage of TRIS solutions

Nemzer and Dickson (2005) monitored TRIS buffers stored in borosilicate bottles sealed with greased ground glass stoppers over several years, showing that these buffers experienced less than 0.0005 drift in pH per year. What exactly causes this drift is unknown, although preliminary analysis in our laboratory suggest that TRIS buffers do absorb some CO_2 from the atmosphere. Buffers analyzed for C_T within two months of preparation and bottling (in greased borosilicate bottles) had a C_T of 30–60 μmol kg^{-1}. This would increase the buffer ratio term in Eq. 2-1 by ~0.2 % and thus lower the pH_T by ~0.001. Part of this buffer C_T is likely caused by de-ionized water being in equilibrium with lab atmosphere. For example – at a mole ratio of 1000 ppm CO_2 in lab air, the C_T of de-ionized water will be approximately 40 μmol kg^{-1} which is consistent with the lower C_T values measured in the buffers. The level of C_T in TRIS buffers over time will further depend on the amount of time the buffer has been exposed air and could vary depending on the headspace of the storage container. Most plastic containers (e.g., low- or high-density polyethylene) are permeable to gases, suggesting that TRIS buffers stored in such a container will almost certainly take up CO_2 from the atmosphere over time.

2.5 Conclusion

With access to standard laboratory equipment, including a balance readable to ±0.1 mg, it is possible to prepare TRIS buffers in synthetic seawater to a pH_T that has an uncertainty of 0.006 relative to the expected value of 8.094 at 25 °C (DelValls and Dickson 1998). The

proposed colorimetric acid-base titration technique used to calibrate the HCl directly to the TRIS allows for significant savings on the materials used to prepare the buffer. This level of uncertainty in the buffer pH_T is more than sufficient for seawater pH measurements that are expected to fulfil the GOA-ON *weather* uncertainty goal of 0.02 in pH, and the buffer ionic composition provides consistency with various acid-base equilibrium constants appropriate for seawater.

2.6 Acknowledgements

The authors are grateful for the help of Lauren Briggs in preparing several TRIS batches, and George C. Anderson for coulometric analysis of the HCl. The authors would also like to thank Dr. Simon Clegg for his work with the Pitzer modelling of TRIS in synthetic seawater. Comments from two anonymous reviewers greatly enhanced the manuscript. This work was supported by the US National Science Foundation Grant OCE-1657799 and by a grant from the NOAA Ocean Acidification Program, NA15OAR4320071.

2.7 Appendix

2.7.1 Appendix 1 Estimation of the amount content of HCl solutions by titration against TRIS.

Materials

Magnetic stirrer and magnetic stir bar; 250 mL pyrex low-form beaker(s), small beaker (e.g., 50 mL) to hold pipettes during weighing, disposable Samco™ Narrow Stem Transfer Pipettes of 4.5 mL and 15.3 mL capacity, Tygon® tubing of 3/32″ inner diameter, analytical balance (0.1 mg

resolution), white paper and light source. A list of suggested materials and their catalogue numbers can be found in Appendix 3.

Chemicals

1.0 mol L^{-1} HCl, TRIS solid, 0.1 % methyl red indicator in alcoholic solution. A list of suggested chemicals and their catalogue numbers can be found in Appendix 3.

Modification of disposable pipettes

The tip of the 4.5 mL disposable pipette is modified to deliver a smaller drop size by carefully melting and stretching the tip over an ethanol flame, so it is able to deliver a drop size of less than 0.01 g (Figure 2-5 c and d). A cap for the 15.3 mL disposable pipette is prepared by tying a knot in the Tygon® tubing and cutting it to an appropriate length (Figure 2-5 b). Over the course of several hours, evaporation from the modified-tip 4.5 mL pipette is minimal, and a cap is not necessary.

Figure 2-5 Pipettes used for titration, including a) A 15.3 mL pipette with b) Tygon®-tubing cap, c) modified tip of a d) 4.5 mL pipette.

Titration

a) One gram of TRIS solid is weighed into a 250 mL beaker, deionized water is added to a total solution weight of about 80 g, and a magnetic stir bar placed in the solution.
b) Six drops of indicator are added, turning the solution yellow (Figure 2-6 a). The 250 mL beaker is placed on a magnetic stirrer with a white paper as a background and a light shining down directly on the beaker (this allows for easier perception of the color change).
c) The two disposable pipettes are filled with the ~1.0 mol L^{-1} HCl solution, the 15.3 mL pipette is capped, they are both placed in a small beaker which is then weighed to ±0.1 mg.
d) HCl is added, as the solution is stirring, from the 15.3 mL pipette until the solution shows a hint of pink that persist for less than a couple of seconds. At this point, the larger pipette is again capped and returned to the small beaker.
e) HCl is then added slowly using the modified 4.5 mL pipette until one drop changes the solution from an orange-pink color to a distinct pink color (Figure 2-6 b).
f) The beaker with the two pipettes is again weighed, and the difference from the first weighing equals the weight of HCl added. For a 1.0 mol L^{-1} solution of HCl and 1 g of tris, the weight of HCl used should be close to 8 g.
g) Make sure to practice this method until you feel confident you can identify the appropriate color change. At this point, proceed to use the method for calibrating $[HCl]_{titr}$.

Figure 2-6 Color of sample after a) addition of indicator and after b) reaching the titration endpoint.

Calculations

The amount content (in mol kg-solution^{-1}) of HCl is calculated based on the mass (m) in g of TRIS and HCl used in the titration. Their weights (w), in g, are corrected to mass by applying an air buoyancy correction as shown in Eq. 2-3, where the densities (ρ) of TRIS and HCl are 1.33 g cm^{-3} and 1.02 g cm^{-3}, respectively.

$$m\,(\mathrm{g}) = w\,(\mathrm{g}) \cdot \left(1 + 0.0012 \cdot \left(1/\rho - 1/8\right)\right)$$

Eq. 2-3

The amount content of HCl, based on this titration technique, $[HCl]_{titr}$, is then calculated according to Eq. 2-4, using the molar mass (M) of TRIS of 121.14 g mol^{-1}.

$$n_{\mathrm{HCl}} = n_{\mathrm{TRIS}}$$

$$[\mathrm{HCl}] \cdot m_{\mathrm{HCl,\,solution}} = \frac{m_{\mathrm{TRIS}}}{M_{\mathrm{TRIS}}}$$

$$[\mathrm{HCl}]_{\mathrm{titr}}\ (\mathrm{mol\ kg\text{-}solution}^{-1}) = \frac{m_{\mathrm{TRIS}}\ (\mathrm{g})}{M_{\mathrm{TRIS}}\ (\mathrm{g\ mol}^{-1})} \cdot \frac{1000\ (\mathrm{g\ kg}^{-1})}{m_{\mathrm{HCl,\,solution}}\ (\mathrm{g})}$$

Eq. 2-4

A spreadsheet implementation of this calculation is included as a supplement ("Preparing TRIS buffers.xlsx", sheet #1 Calibrating HCl and TRIS).

2.7.2 Appendix 2 Preparation of 1 L TRIS buffer in synthetic seawater

Materials

Clean volumetric flask (1 L), funnel, analytical balance (±0.1 mg), seven glass beakers (< 250 mL) or weighing dishes/pouring boats, three disposable Samco™ Narrow Stem Transfer Pipettes of 15.3 mL capacity, two spatulas, magnetic stir bar and stir plate. A list of suggested materials and their catalogue numbers can be found in Appendix 3.

Chemicals

1.0 mol L^{-1} HCl, TRIS solid, NaCl, Na_2SO_4, KCl, 1.0 mol L^{-1} $MgCl_2$, 1.0 mol L^{-1} $CaCl_2$.

A list of suggested chemicals and their catalogue numbers can be found in Appendix 3.

The desired weight of HCl ($w(HCl)_{desired}$) depends on $[HCl]_{titr}$ as determined in Appendix 1, and is calculated based on Eq. 2-5, where $[HCl]_{buffer\ solution}$ is the target HCl (and thus $TRIS{\cdot}H^+$) amount content of 0.03827 mol kg-solution^{-1} (equivalent to 0.04 mol kg-H_2O^{-1}) in the buffer and $w(\text{buffer solution})_{desired}$ the weight of 1 L of the buffer solution at 20 °C.

$$w(\mathrm{HCl})_{\mathrm{desired}}\ (\mathrm{g}) \approx w(\text{buffer solution})_{\mathrm{desired}}\ (\mathrm{g}) \cdot \frac{[\mathrm{HCl}]_{\text{buffer solution}}(\text{mol kg-solution}^{-1})}{[\mathrm{HCl}]_{\mathrm{titr}}(\text{mol kg-solution}^{-1})}$$

Eq. 2-5[1]

[1] While this equation should strictly be in terms of mass (m), and not weight (in air), the ratio of the air buoyancy correction term for the buffer solution and the HCl solution approximately equals one and can be omitted. In the supplementary spreadsheet, however, this air buoyancy correction is explicitly included in the calculation.

Mixing the buffer

a) *Weigh out HCl*: Place the funnel in the neck of the volumetric flask and start by weighing out HCl into a beaker (or weighing boat) to within 0.3 g or better of the desired weight from table A1, using a disposable transfer pipette to adjust the final weight. Record the dispensed weight of HCl and transfer the HCl quantitatively into the volumetric flask by rinsing the weighing vessel directly into the flask with de-ionized water (~100 mL).

b) *Scale desired weights to the dispensed weight of HCl*: Calculate by what proportion the dispensed HCl weight ($w(\mathrm{HCl})_{\mathrm{dispensed}}$) is different from the weight in Table 2-3($w(\mathrm{HCl})_{\mathrm{desired}}$). To ensure the ratio of moles between all components remain the same, this factor is used to adjust the desired weights ($w(\mathrm{X})_{\mathrm{desired}}$) of the remaining components to re-calculate a target weight of each ($w(\mathrm{X})_{\mathrm{target}}$) as shown in equation Eq. 2-6. As long as HCl is added to within 0.3 g of the desired weight (for a 1 L buffer), and the remaining components are added in proportion to that, the resulting 1 L buffer will have a *S* of < 0.3 units different than the desired *S* of 35.

$$w(\mathrm{X})_{\mathrm{target}}\ (\mathrm{g}) = w(\mathrm{X})_{\mathrm{desired}}\ (\mathrm{g}) \cdot \frac{w(\mathrm{HCl})_{\mathrm{dispensed}}\ (\mathrm{g})}{w(\mathrm{HCl})_{\mathrm{desired}}\ (\mathrm{g})}$$

Eq. 2-6

c) *Weigh out the remaining components*: weigh out the target weights, $w(\mathrm{X})_{\mathrm{target}}$, of the remaining components in individual beakers or weighing boats (disposable transfer pipettes can be used to adjust the final weights of the $MgCl_2$ and $CaCl_2$ solutions), and transfer each of these quantitatively into the volumetric flask by rinsing each individual weighing vessel into the flask, using ~100 mL de-ionized water per rinse.

d) *Add water and mix*: Once all components have been added, rinse the funnel into the flask with de-ionized water and fill the flask to a few centimeters below the 1 L mark. Replace the flask stopper and mix by hand by inverting the bottle a few times to dissolve the majority of the salts. This will increase the density and thus decrease the volume slightly. Fill the flask carefully with de-ionized water (using e.g., a transfer pipette) until the bottom of the solution meniscus is level with the etched 1-L mark on the bottle. Place a stir bar in the flask, replace the stopper, and set to stir for at least four hours.

Table 2-3 Desired weights to prepare 1 L of 0.04 mol kg-H_2O^{-1} equimolar TRIS-TRIS·H^+ buffer at a S of 35

Component	Weight of component (g)
HCl	$39.270/[HCl]_{titr}$
TRIS	9.517
NaCl	22.254
Na_2SO_4	4.085
KCl	0.775
$MgCl_2$ (1.0 mol L^{-1})	58.862
$CaCl_2$ (1.0 mol L^{-1})	11.726
De-ionized water	"Fill to line"

A spreadsheet implementation of the calculations involved is included as a supplement ("Preparing TRIS buffers.xlsx", sheet #2 Mixing buffer).

2.7.3 Appendix 3 Suggested list of chemicals and materials, and their catalogue numbers

Chemicals

1.0 mol L^{-1} HCl: Fisher Scientific catalogue number (FS#) 60-007-56.

TRIS solid: FS# T395-100.

NaCl: FS# S271-500.

Na_2SO_4: FS# S421-500.

KCl: FS# P217-500.

1.0 mol L^{-1} $MgCl_2$: FS# 50-751-7456/Amresco E525-500ml.

1 mol L^{-1} $CaCl_2$: FS# 50-751-7510/Amresco E605-500ml.

0.1 % methyl red indicator in alcoholic solution: RICCA catalogue number 5045-4.

Materials

Weighing dishes: FS# 08-732-113.

Disposable Samco™ Narrow Stem Transfer Pipettes of 4.5 mL capacity: FS# 13-711-34/ThermoFisher Scientific 251PK.

Disposable Samco™ Narrow Stem Transfer Pipettes of 15.3 mL capacity: FS# 13-711-36/ ThermoFisher Scientific 252PK.

Tygon® tubing of 3/32″ inner diameter: Fisher Scientific catalogue number FS# 14-171-130/Saint Gobain ADF00004.

3 A TITRATION METHOD THAT UNAMBIGUOUSLY MEASURES UNIDENTIFIED COMPONENTS OF TOTAL ALKALINITY IN SEAWATER MEDIA

3.1 Introduction

Seawater is a complex mixture including inorganic and organic acids over a range of concentrations, whose amounts and speciation can have implications for a range of biogeochemical processes such as air-sea CO_2 gas exchange and shellfish calcification. The total alkalinity (A_T) of seawater is generally thought of as the quantitative excess of bases over acids, and while complex in nature is simplistically the measure of how much acid is needed to bring a sample of seawater to a given titration end-point. Since the development of the alkalinity concept there has been a long string of researchers slowly uncovering this acid-base black box, where measurement methods and data processing tools have developed alongside a changing definition of A_T (Dickson 1992).

Early on in oceanography, it was recognized that carbonate and bicarbonate were major buffer components of seawater, and as such the measurement of alkalinity was taken to mean the base contribution of the carbonate system (Dittmar 1880; Krogh 1904). This was measured by titration, initially by acidifying a seawater sample, rendering it "CO_2-free" by boiling it, and titrating the excess acid with a strong base like NaOH or KOH in the presence of a colorimetric pH indicator. The advent of electrometric pH measurement methods enabled more flexibility in measuring pH, and thus, choice of titration end-point and titration method (McClendon et al. 1917).

It was also recognized that the measured values of total alkalinity (A_T), pH, and total CO_2 (C_T) for a particular seawater sample are correlated, and two can be used to calculate the third. This picture was complicated, however, by the realization that different methods of measuring and calculating alkalinity did not always agree (McClendon 1917). Further, studies suggested that besides the carbonate contribution to alkalinity (which could vary between different sample locations), there seemed to be some proportion of the buffering capacity that was nearly constant across the oceans.

> "The carbonates and the bi-carbonates are the predominating ions affecting the buffer capacity of sea water, but from a study of the data given, the authors are of the opinion that the buffer capacity is also a function of some inherent basic property of the sea" – Thompson and Bonnar (1931)

Borate, phosphate, and silicate were explicitly recognized as possible contributors, but borate (which is conservative with respect to salinity; Moberg and Harding 1933) was the only identified "non-volatile" base that was accounted for regularly and explicitly due to its large contribution to alkalinity relative to phosphate and silicate (Buch 1933).

At the same time as the concepts of marine acid-base chemistry were developing, so were methods for determining total amounts of, and equivalence points for, inorganic acids and bases in the field of analytical chemistry (Gran et al. 1950; Gran 1952). The intercept of progress in analytical and marine chemistry led to the understanding that ocean acid-base chemistry is likely to be even yet more complex than just including carbonate, borate, and nutrient bases and likely seawater contains additional, as yet, unidentified acid-base systems. In the solution chemistry world, such protolytic impurities were referred to by some as "dirt acid" recognizing that it in theory could be formalized as one or more monoprotic acids (e.g., "HX")

(Rossotti et al. 1971; Hansson 1973a). Referring to unidentified acid-base contamination in such a way was later used by marine researchers as well (Bradshaw and Brewer 1988b), and may have aptly hinted at the frustration of not yet having fully characterized the ocean acid-base mixture.

Additional insight into the complex nature of ocean acid-base chemistry came with the improvement and innovation of relevant measurement methods. For example, a titration of seawater performed in a closed system became commonplace for the simultaneous measurements of C_T and A_T (Edmond 1970; Bradshaw et al. 1981) . This titration method was widely employed for the Geochemical Ocean Sections Study (GEOSECS) where it was revealed that phosphate was not only contributing significantly to A_T, but by not explicitly including its amount content in the closed-cell titration analysis C_T was erroneously over-estimated (Bradshaw et al. 1981). The amount of unidentified acid-base systems in seawater had by now been reduced significantly by explicitly accounting not only for borate and phosphate, but all other identified inorganic acid-base systems in seawater (Eq. 3-1) (Dickson 1981). The definition of A_T is based on considering acids to be those with a $pK_A \leq 4.5$ and bases as having a $pK_A > 4.5$, where the pK_A values are at zero ionic strength and 25 °C. (The use of square brackets, [], indicates the amount content of any species in mol kg-sol^{-1} or mol kg^{-1})

$$\begin{aligned} A_T = {} & [HCO_3^-] + 2[CO_3^{2-}] + [B(OH)_4^-] + [SiO(OH)_3^-] + 2[PO_4^{3-}] + [HPO_3^{2-}] + \\ & [HS^-] + [OH^-] + [NH_3] + [\text{unidentified bases}] - \\ & [H_F^+] - [HSO_4^-] - [HF] - [H_3PO_4] - [HNO_2] - [\text{unidentified acids}] \end{aligned}$$

Eq. 3-1 (a slightly expanded version of Eq. 1-3)

Still, within a few years comparisons had been made of C_T inferred from titration data, and C_T measured directly by a careful gas extraction-manometric method or a coulometric

approach (Brewer et al. 1986; Bradshaw and Brewer 1988a). The C_T estimated from closed cell titrations exceeded that determined by extraction-manometry or coulometry by up to 21 μmol kg^{-1}, and the authors noted that the depth-dependence of this discrepancy strongly suggested this may be caused by the presence of an unknown protolyte. They proposed the "dirt acid" (Eq. 3-2) in seawater to be due to acid-base groups associated with dissolved organic matter, as well as noting that errors in equilibrium constants and the summation of other random errors can affect these measurements and calculations. It is therefore convenient to express the alkalinity contribution of these "unknown protolytes" as

$$A_X = [\text{unidentified bases}] - [\text{unidentified acids}]$$

Eq. 3-2

It is worth noting that at a typical seawater pH, such acids defined in the sense of Eq. 3-1 can be ignored because they are fully protonated. Their presence may however matter during a titration, if titration data is interpreted over a wide pH_T range.

One approach to estimating A_X is thus to compare A_T measured by titration (which would include identified and unidentified species) to that calculated from e.g., pH_T, C_T, B_T, and other identified components as shown in Eq. 3-1 (which would *not* include unidentified alkalinities) (Eq. 3-3).

$$A_X = A_T - A_T(C_T, pH_T, S, T, K_1, K_2 ...)$$

Eq. 3-3

Because A_X consists of one or more acid-base systems, it should be possible to estimate it by direct titration. However, A_X in seawater is one or more acid-base systems in a complex mixture of other identified acids and bases, and it is impractical, if not impossible, to try to isolate A_X as its composition is not known.

The points regarding measurement and calculation errors made by Bradshaw and Brewer are key. Errors in equilibrium constants cannot be avoided, and although glass/reference combination electrodes and automated burettes have greatly improved with time, they are still prone to uncertainties in their readings. If the apparent values of A_X estimated for seawater samples (using equation 3) were comprised only of random uncertainties, one would expect there to be an average of zero with both positive and negative scatter. Instead, the measured alkalinity is nearly always greater than the calculated one (see, e.g., Figure 3-1). In the open ocean this discrepancy seems to be on the order of 4–8 μmol kg^{-1} (Millero et al. 2002; Fong and Dickson 2019), while it has shown to be >15 μmol kg^{-1} in the coastal ocean (Kuliński et al. 2014; Patsavas et al. 2015; Yang et al. 2015). Importantly, these discrepancies are larger than the desired uncertainty goals for A_T set forth by the Global Ocean Acidification Observation Network (Newton et al. 2015). Such calculations are subject to uncertainties particularly those associated with the acid dissociation constants K_1 and K_2 of the CO_2 system and the uncertainties of the three independent measurements of the CO_2 system (A_T and two others, e.g., C_T and pH_T).

Another approach is to attempt to measure A_X "directly" either by titrating a seawater sample with a strong acid, or by strong acid followed by strong base. In both cases assumptions are made about the "volatile alkalinity" that can enter or leave the solution in the form of a gas, i.e., carbonate and bicarbonate (carbonate alkalinity, $A_C = [HCO_3^-] + 2[CO_3^{2-}]$).

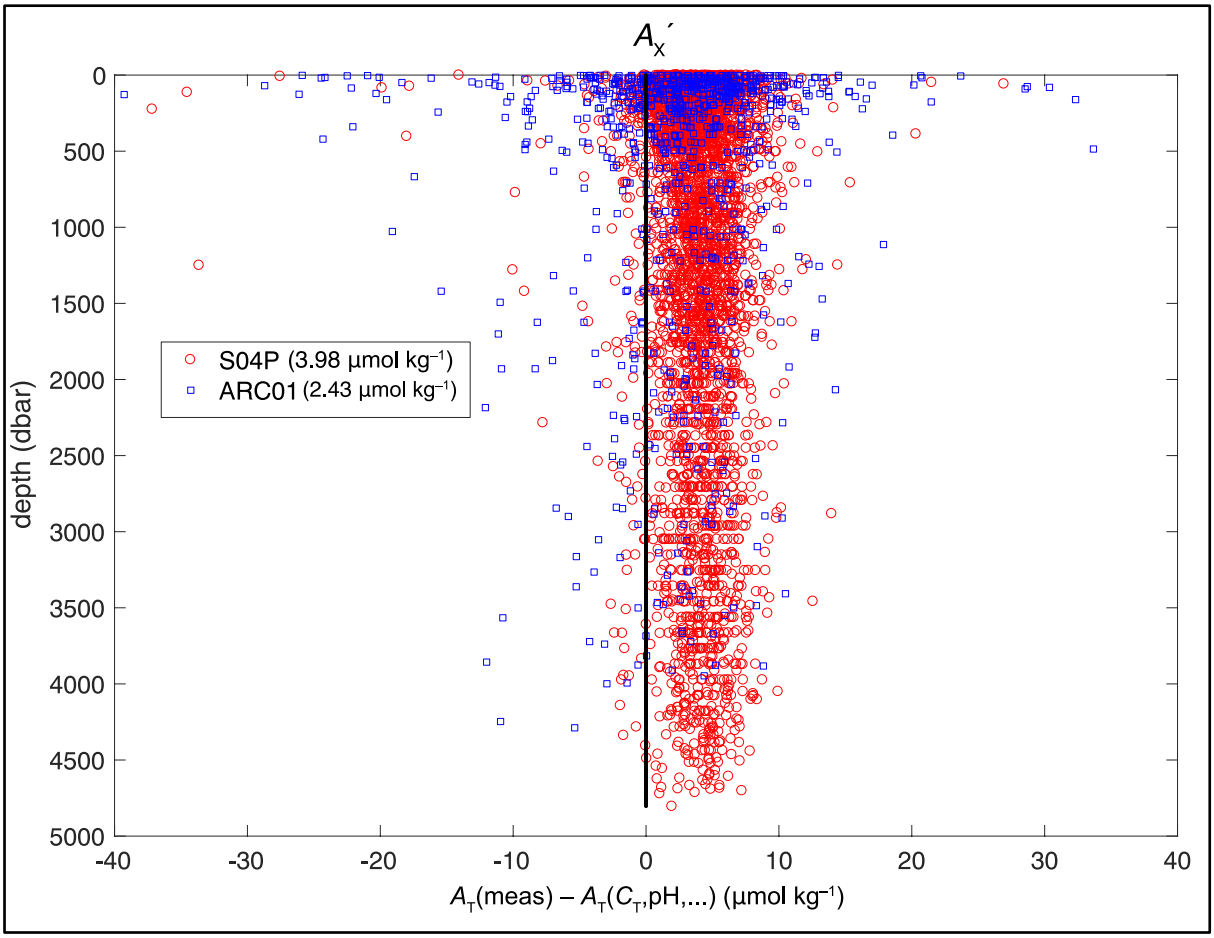

Figure 3-1 A_X from the GO-SHIP cruises ARC01 (Arctic Ocean, 2015) and S04P (Southern Ocean, Pacific section, 2018) across depth, average value for each cruise is presented in the parenthesis of the legend. pH_T was measured at 25 °C, and all constants used for these calculations are listed in Table 3-2. (Dickson et al. 2018; Millero and Swift 2018)

Assumptions about A_C can have significant implications for the uncertainty analysis of the measurement. For example, Hernández-Ayón et al. (2007) and Muller and Bleie (2008) performed the closed-cell titrations mentioned above, while also measuring C_T independently. This allowed them to subtract out A_C and other identified bases and acids from each titration curve and ascribe the remaining titration curve response to one or more unknown protolytes. With this approach though, uncertainty related to estimating and subtracting A_C will be quite large as the contribution to A_T from the carbonate system is usually an overwhelming majority (> 95 %; Eq. 3-1). Uncertainty of A_C will include errors from both the C_T measurement and from

calculating its speciation using K_1 and K_2 where particularly K_2 is believed to have a large uncertainty relative to K_1 and K_B (borate is usually the second most abundant alkalinity species at ~400 μmol kg^{-1}; see Table 3-2 on page 77). There is also uncertainty in how to estimate B_T from salinity (S), as the two published B_T/S ratios disagree by 4 % (Uppström 1974; Lee et al. 2010). Furthermore, it can be difficult to keep a titration cell perfectly closed and without any headspace, so it is possible for some C_T to be lost from the solution at e.g., low pH_T values when $p(CO_2)$ is high. It can also be difficult to ascertain that no C_T was added or removed when transferring the sample into the closed titration cell, meaning that an independently measured sample C_T may or may not be identical to the C_T inside the closed cell.

Cai et al. (1997) and Hunt et al. (2020) chose another approach, where they aimed to acidify the seawater sample and remove CO_2 by de-gassing (e.g., bubbling with N_2 for some period of time), followed by a titration with a strong base for which an attempt had been made to remove contamination by carbonate (which is very common, see e.g., Sipos et al. 2000). Such an open-cell titration approach has the potential of reducing uncertainty related to A_C, which would greatly reduce the overall measurement uncertainty. However, no convincing evidence was put forth showing C_T had been adequately removed from the sample before titration against a strong base, nor that the strong base was CO_2-free. Furthermore, in neither of these examples of A_X measurements nor in other examples (e.g., Muller and Bleie 2008; Ko et al. 2016; Hunt et al. 2020; Sharp and Byrne 2021) was any effort focused on random instrumental uncertainties, errors in equilibrium constants, or errors from accounting for other alkalinities (e.g., a knowledge of the total amounts of borate, silicate, or phosphate). A point not mentioned by Bradshaw and Brewer, and one that should be obvious but is often overlooked, is the purity and quality of calibration of the titrants. It is desirable that they are prepared in an ionic background,

so they do not significantly alter the ionic composition of the sample in a way that changes relevant activity coefficients and the electrode liquid junction potential. **Without careful detail to the titrants and all the other sources of uncertainty mentioned above, it is not possible to make an unambiguous measurement of A_X.**

3.2 Approach

Because A_X consists of one or more acid-base systems, it will be measurable by titration, but as has been discussed above – it is not as simple as it might seem at first. The overall method that will be described here is acidification of a seawater sample followed by titration using a strong base. It would of course be possible to only titrate the sample with acid, but as the sample necessarily must be stirred this would lead to loss of CO_2 (and thus C_T) unless the titration is performed in a closed system. There are additional complications to performing a titration in a closed cell that will be discussed briefly, but first it is necessary to look at how the data is best evaluated. Since this chapter primarily focuses on the titration of acidified seawater with NaOH, I will also present the approach in this way, but please note that performing a titration across the full pH_T range would also be applicable to an HCl titration in a closed cell.

3.2.1 Titration data visualization

A common way of evaluating titration data of a simple system is by looking at the change in pH_T as a function of added titrant as shown in the black drawn line in Figure 3-2. At the same time as titrant is added, the alkalinity in the sample at any given point is increasing proportional to how much base has been added (blue dashed line). At any titration point (i) during this simulated titration, Eq. 3-4 will be true (which is a simplified version of Eq. 3-1.

$$A_{\mathrm{T},i} = [\mathrm{HCO_3^-}]_i + 2[\mathrm{CO_3^{2-}}]_i + [\mathrm{B(OH)_4^-}]_i + [\mathrm{OH^-}]_i - [\mathrm{H_F^+}]_i - [\mathrm{HSO_4^-}]_i - [\mathrm{HF}]_i$$

Eq. 3-4

The change at each titration point is a consequence of a) titrant has been added so that the original total amount content of any species, e.g., B_T or S_T, has been multiplied by a factor d_i to account for the dilution from the addition of the acid ($m(\mathrm{HCl})_\mathrm{T}$) and base ($m(\mathrm{NaOH})_\mathrm{i}$) to the original mass m_0 of the sample (Eq. 3-5), and b) the titrant also added hydroxide ions, so that the $A_{\mathrm{T},i}$ increases. If the total amount contents of carbonate, boron, silicate, sulfate, and fluoride are the same as in the original sample and dilution is ignored throughout the titration, the titration curve will look like the one presented in Figure 3-2.

In other words, even during a titration A_T always equals the sum of bases with a $\mathrm{p}K_\mathrm{A} > 4.5$ minus sum of acids with $\mathrm{p}K_\mathrm{A} \leq 4.5$, but the contribution of any species to A_T changes with $\mathrm{pH_T}$. The change in what species are currently being titrated and dominating $A_{\mathrm{T},i}$ at any titration point can be better illustrated by visualizing A_T and each of the individual alkalinity species as a function of $\mathrm{pH_T}$. Figure 3-3 shows two simulations of base titrations of an acidified seawater sample. In Figure 3-3a) the following has occurred: a HCl solution of mass $m(\mathrm{HCl})_\mathrm{T}$, and with an amount content of $C(\mathrm{HCl})$, was added to a seawater sample with an initial $\mathrm{pH_T}$.

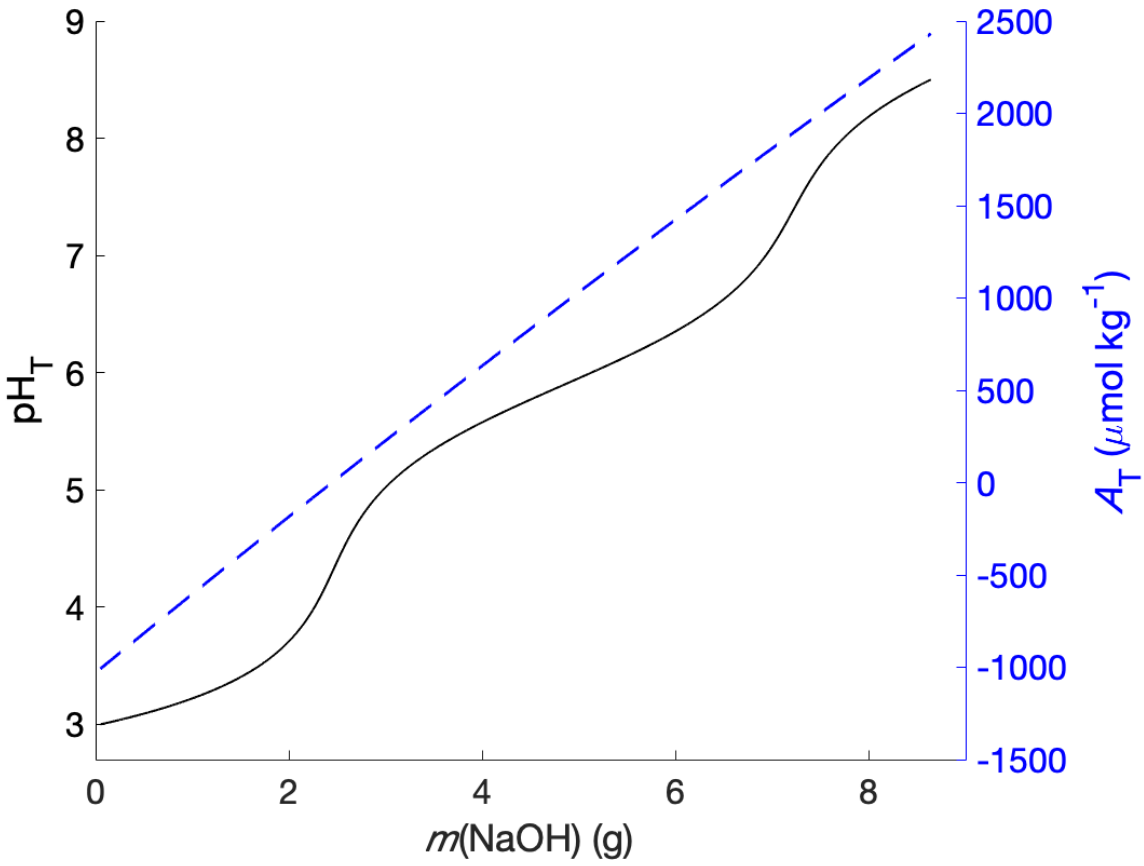

Figure 3-2 A simulated titration curve showing change in pH_T and A_T as a function of titrant mass. The titration curve was simulated assuming a closed cell titration on an acidified solution, using the conditions in Table 3-2

$$d_i = \frac{m_0}{m_0 + m(\mathrm{HCl})_\mathrm{T} + m(\mathrm{NaOH})_i}$$

Eq. 3-5

$$A_{\mathrm{T},i} == \frac{A_{\mathrm{T},0} m_0 - C(\mathrm{HCl}) m(\mathrm{HCl})_\mathrm{T} + C(\mathrm{NaOH}) m(\mathrm{NaOH})_i}{m_0 + m(\mathrm{HCl})_\mathrm{T} + m(\mathrm{NaOH})_i}$$

Eq. 3-6

This sample is then titrated with NaOH (m(NaOH)), with an amount content of C(NaOH), from $pH_T \sim 3$ to $pH_T \sim 8.5$. The black drawn line in Figure 3-3 shows $A_{T,i}$ that was calculated in the same manner as shown in Figure 3-2, but in this figure it is a shown as a

function of pH_T as opposed to m(NaOH). The various dashed and colored lines shows the contribution to A_T from individual species, including hydrogen sulfate, hydrogen fluoride, and hydrogen ions (which are all contributing negatively to alkalinity), and hydrogen carbonate, carbonate, borate, and hydroxide ions, which are all contributing positively to A_T. It is clear that the carbonate alkalinity (A_C) dominates A_T in seawater around typical ocean pH_T values, and borate a smaller proportion. In this graph is also included an "unidentified" alkalinity component HX with a total amount content of X_T = 10 μmol kg^{-1} and a pK_X = 4.5.

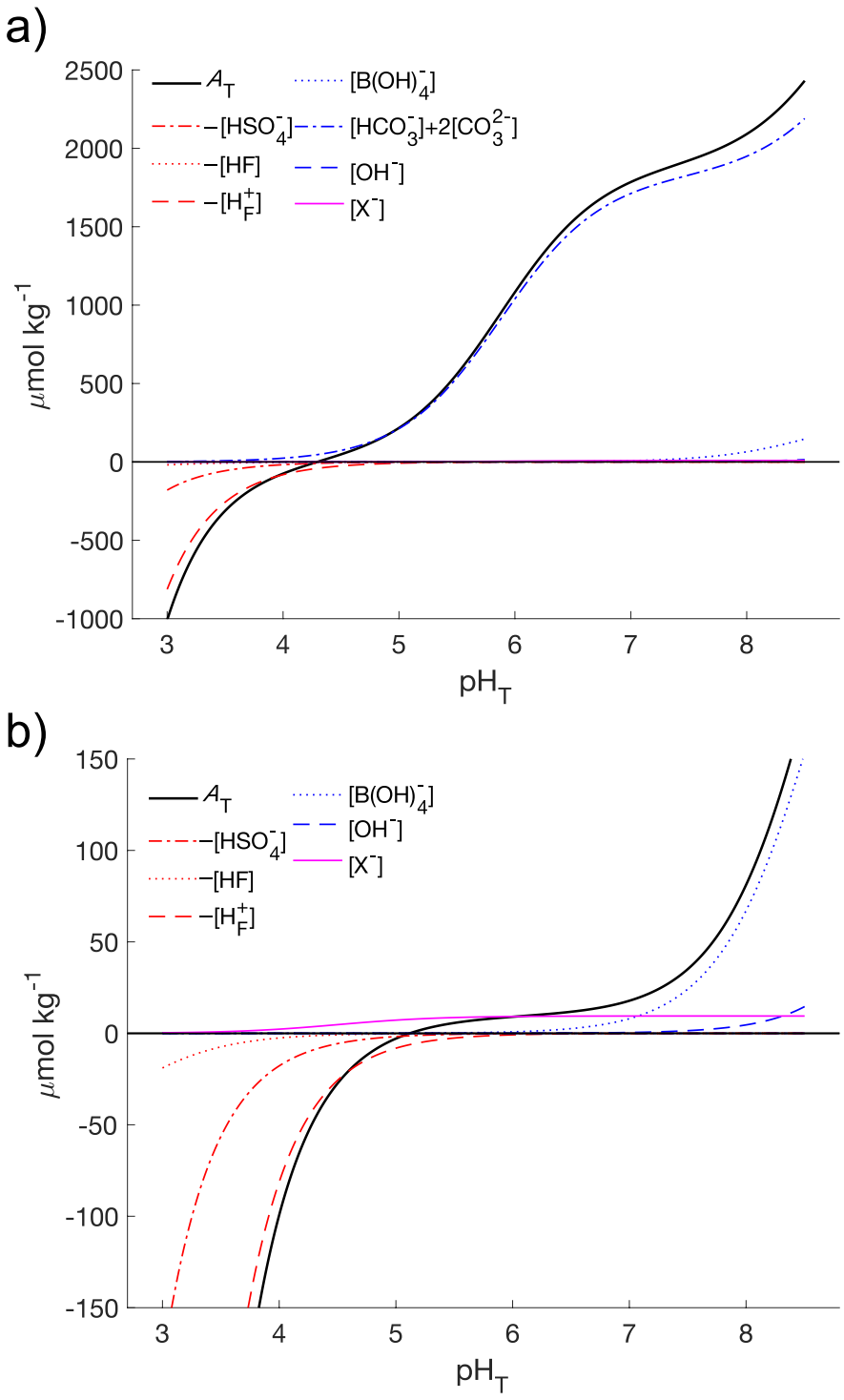

Figure 3-3 Simulated titration curves for a back titration in a simplified seawater solution with 10 µmol kg^{-1} of HX with a pK_A of 4.5 in the a) presence of C_T (2000 µmol kg^{-1}) and b) absence of C_T (0 µmol kg^{-1}), and the amount content of each alkalinity species as a function of pH$_T$. Note that the figure includes dilution of each species by the titrants. For the species defined as acids, the negative of their amount content is shown. Values for total amount contents, and acid dissociation constants were calculated using the expressions in Figure 1-1 and the exact values can be found in Table 3-2).

Although it contributes ~0.5 % to the initial value of A_T, it is barely visible in the presence of A_C at natural amounts, and it is well outside the desired uncertainty goal for A_T set by GOA-ON. This value is however well within the range of A_X observed in the coastal ocean (Yang et al. 2015; Song et al. 2020), and with a pK_A that can be considered typical for organic acids (Reusch 2020). Notably, X_T is large enough that if not accounted for, using this A_T value in CO_2 system calculations, it will cause an error that is borderline or larger than the uncertainty goals set by the global ocean acidification observation network (GOA-ON) both for long-term, open ocean monitoring (2 μmol kg^{-1}) and near-shore, high-frequency changing environments (10 μmol kg^{-1}) (Newton et al. 2015).

3.2.2 Removal of C_T

The advantage of acidifying the seawater sample before starting the titration against NaOH is that nearly all C_T will be in the form of dissolved unionized CO_2 (CO_2^*), and if the sample is bubbled and stirred with N_2 gas it will drive out CO_2 gas (i.e., lowering C_T). Figure 3-3b) shows the same titration as described above, with the exception that C_T was completely removed by degassing prior to titrating the sample with NaOH, and no CO_2 was introduced to the sample during the titration. All other amount contents than C_T are the same as in a), and while borate is now the dominating species, the contribution from HX (X^-) is now a much larger proportion, about 10 %, of the A_T of the sample. **With such an "amplification" of the signal of minor species, by removal of C_T, it will be much easier to extract quantitatively useful information about unidentified species.**

3.2.3 Focus on the titrants

Now, the basis of any successful titration is careful control and calibration of the titrants, and removing A_C is just one important aspect into an unambiguous measurement of A_X. In our

laboratory we have been preparing and carefully (coulometrically) calibrating HCl titrants (Dickson et al. 2003) for A_T analyses for over 25 years. An accurately characterized HCl titrant will be used not only as part of the titration routine, but also to calibrate the NaOH titrant using a Gran function (Gran 1952) to find the equivalence point. Both titrants are prepared in a NaCl background to achieve an ionic strength similar to seawater (~0.7 mol kg^{-1}) so the dilution of the sample by the titrants does not change activity coefficients appreciably. Further, the amount content of the titrants is chosen to balance how much the sample is diluted by the added titrants (higher concentration equals less dilution), against the resolution of data points collected across the full pH range of the titration (lower concentration equals higher resolution).

With accurately calibrated titrants we are one important step closer to extracting quantitatively useful information from a titration. Even after we remove C_T, however, A_X will not be the only contribution to A_T. It is desirable to not add any C_T back into the system once it has been removed (or, as we shall see, greatly reduced), so the sample needs to be continually bubbled by N_2 throughout the titration. Furthermore, the purity control of the NaOH titrant is important as its strongly basic nature makes it prone to carbonate contamination, often reaching > 100 μmol CO_3^{2-} kg^{-1} for a dilute NaOH (< 1 mol kg^{-1}) solution. Preparing and ensuring CO_2-free NaOH titrant is a key step for the titration method, as a constant supply of additional C_T and thus A_C throughout the titration will increase the uncertainty of the measurement. Removing and reducing C_T in the system not only increases sensitivity to measure A_X, but also limits any uncertainty associated with the carbonate system equilibrium constants.

3.2.4 Accurate monitoring of sample pH_T and acid titration

In addition to pure and accurately calibrated titrants, and a sample without volatile alkalinity components, we also need a precise method for measuring and monitoring pH_T of the

sample during the titration. The pH_T measurement device needs to be as sensitive as possible, as the resolution with which pH_T can be measured will affect the resolution at which the data can be interpreted. We have extensive experience with a particular design of combination glass/reference cell (Metrohm Ecotrode) which has shown itself to be very reliable especially in the low-pH_T region. Strictly we do not monitor pH_T but rather the emf, E, of this cell in a particular solution, which should be proportional to pH_T if the electrode response is perfectly Nernstian (see section 2.1 and Figure 2-1 for details). And, while a change in E should be proportional to a change in pH_T, the $E°$ of the electrode still needs calibrating so that the absolute pH_T is known.

To acidify the sample being studies, I use a typical open-cell A_T titration, where the sample is titrated to a pH_T of ~3.0, and both A_T and the $E°$ of the pH_T cell are estimated (SOP 3b in Dickson et al. 2007). Because this acid titration occurs between pH_T 3.5 and 3.0, only two of the acid species in Eq. 3-1, sulfate and fluoride, in addition to hydrogen carbonate are not yet fully titrated (Figure 3-3). In that pH_T range C_T is present predominantly as CO_2^*, and if the solution is given a short time (~5 minutes) to degas at pHT ~ 3.5 by stirring it and bubbling it with CO_2-free gas, C_T will reach < 100 μmol kg^{-1} and the amount of hydrogen carbonate that remains to be titrated is negligible.

Since this titration is done in an open cell, as acid is added and $p(CO_2)$ increases, CO_2 is likely to escape solution. It is therefore futile to attempt collecting any titration points before reaching the low-pH_T range. Instead, a large aliquot of acid is added until a pH_T of nearly 3.5 is reached. After the short degassing period, the sample is titrated with some number of small increments until it is below pH_T 3. Because the HCl is added as a volume (v(HCl)), it needs to

be converted to mass by multiplying by its density. The mass of HCl used at any point (i) during the titration can be described by Eq. 3-7.

$$m(\mathrm{HCl})_i = v(\mathrm{HCl})_i \cdot \rho(\mathrm{HCl})$$

Eq. 3-7

At any titration point, then, the original A_T ($A_{T,0}$) of the sample of a mass m_0 can be related to the change in $[H_T^+]_i$ measured by the combination glass/reference electrode relative to $m(\mathrm{HCl})_i$ according to Eq. 3-8, where dilution by addition of the titrant has been corrected for.

$$\frac{A_{T,0} \cdot m_0 - C(\mathrm{HCl}) m(\mathrm{HCl})_i}{m_0 + m(\mathrm{HCl})_i} \approx -[\mathrm{HSO}_4^-]_i - [\mathrm{HF}]_i - \frac{[\mathrm{H}_T^+]_i}{Z}$$

Eq. 3-8

As described by Dickson et al. (2003) a simple Gran approach is used to estimate initial values of $A_{T,0}$ (the alkalinity of the original seawater) and $E°$ (the apparent standard potential for the pH_T cell). These are then used in a non-linear least squares fitting process based on Eq. 3-8 and titration data (E and m(HCl) pairs) from the region $3.0 \leq pH_T \leq 3.5$. As part of this procedure the $E°$ of the electrode is also calibrated. Rather than rewriting Eq. 3-8 in terms of the Nernst equation,

$$E = E° - \frac{RT}{F} \ln[\mathrm{H}_T^+]$$

Eq. 3-9

it is simpler to fit another parameter f that is a multiplier between the true value of $[H_T^+]$ and an estimate, $[H_T^+]'$, which is calculated from the Nernst equation for a particular E using the initial estimate of $E°$ ($E°'$) in Eq. 3-9:

$$[H_T^+] = f\,[H_T^+]'$$

Eq. 3-10

The final $E°$ of the pH_T cell in that particular solution can then be calculated according to:

$$E° = E°' - \frac{RT}{F}\ln(f)$$

Eq. 3-11

3.2.5 Further refining E° and the basis of the base titration

It is straightforward to get an estimate of $E°$ prior to starting the titration, using e.g., a TRIS buffer prepared in synthetic seawater (see previous chapter) or other appropriate reference material, but by calibrating it in the sample itself prior to the base titration it is possible to perform a titration in a much more well-known pH_T interval. A similar calibration is possible from the base titration data as well. The $E°$ might have changed slightly as the sample was sitting and degassing for 45 minutes, and the $E°$ calculated from the acid titration data will be a good initial guess for this value before the nonlinear fitting routine. In this case, the total amount of acid added ($m(HCl)_T$) is used instead and the active titrant is now NaOH ($m(NaOH)_i$). In the same low pH_T range, 3–3.5, we can then re-write Eq. 3-8 in terms of adding base to the already acidified solution (Eq. 3-12).

$$\frac{A_{T,0}\cdot m_0 - C(HCl)m(HCl)_T + C(NaOH)m(NaOH)_i}{m_0 + m(HCl)_T + m(NaOH)_i} \approx -[HSO_4^-]_i - [HF]_i - \frac{[H_T^+]_i}{Z}$$

Eq. 3-12

Now, Eq. 3-12 will only hold true in the low pH_T region ($pH_T < 3.5$) and only if there aren't any other acid species being titrated. For the rest of the titration with base it is necessary to include all identified alkalinity species. Eq. 3-13 does just that and accounts for the dilution from the addition of titrant. Eq. 3-13 further assumes that all C_T was removed during degassing,

and while it does account for the dilution, it recalculates the total amount contents relative to the original mass of the undiluted sample m_0. By simply multiplying the entire equation with the dilution factor d_i in Eq. 3-5 one would get each species as presented in the progressively diluted solution (pH_T, and thus $[H_T^+]$ and $[OH^-]$ is always measured in the diluted solution).

$$A_{T,i} = \frac{A_{T,0} \cdot m_0 - C(\mathrm{HCl}) m(\mathrm{HCl})_T + C(\mathrm{NaOH}) m(\mathrm{NaOH})_i}{m_0 + m(\mathrm{HCl})_T + m(\mathrm{NaOH})_i}$$
$$= [\mathrm{B(OH)_4^-}]_i + [\mathrm{OH^-}]_i - [\mathrm{HSO_4^-}]_i - [\mathrm{HF}]_i - \frac{[\mathrm{H_T^+}]_i}{Z}$$

Eq. 3-13

If the titrants were calibrated perfectly, and all acid-base species in the sample identified and accurately accounted for, one should be able to subtract the right-hand side/bottom alkalinity species term from the left-hand side/top and have the value be zero at each titration point. If there were unidentified species (e.g., A_X) releasing or taking up protons however, the change in recorded pH_T and thus $[H_T^+]$ would not be appropriately represented by Eq. 3-13, and subtracting one side from the other would produce a non-zero value. If that is the case, one could add an extra term which essentially describes unidentified alkalinity component(s), ΔA_X (Eq. 3-14).

$$A_{T,i} = \frac{A_{T,0} \cdot m_0 - C(\mathrm{HCl}) m(\mathrm{HCl})_T + C(\mathrm{NaOH}) m(\mathrm{NaOH})_i}{m_0 + m(\mathrm{HCl})_T + m(\mathrm{NaOH})_i}$$
$$= [\mathrm{B(OH)_4^-}]_i + [\mathrm{OH^-}]_i - [\mathrm{HSO_4^-}]_i - [\mathrm{HF}]_i - \frac{[\mathrm{H_T^+}]_i}{Z} + \frac{\Delta A_X}{d_i}$$

Eq. 3-14

An example titration curve based on Eq. 3-14 multiplied with d_i is shown in Figure 3-3b), where an example extra acid HX with a total amount content of 10 μmol kg^{-1} and a pK_X of 4.5. The

base form, X^-, is plotted in pink and if this were treated as an unidentified component a plot of ΔA_X would take on this form (ignoring any other errors).

3.2.6 Treatment of identified alkalinity components

Since it is currently not possible to isolate A_X our approach necessarily involves correctly accounting for identified alkalinities remaining in the sample. The total amount contents of sulfate, fluoride, and borate in seawater are usually assumed to be proportional to S of the original sample; we follow that approach here (see Table 3-2). Silicate and phosphate, included in Eq. 3-1 but not included in the simple example in Figure 3-3 for simplicity, are commonly accounted for by discrete measurements of their total amount contents (typically as part of the standard seawater nutrients "panel"). Nitrite, ammonia, and sulfide are rarely present at total amount contents above 1 μmol kg^{-1} in oxygenated seawater, and, thus, their individual contributions to alkalinity are less than this. Therefore, they are usually neglected in carbonate system calculations. Uncertainties are however associated both with estimating total amount contents from S as well as these discrete measurements, in addition to the uncertainty of their acid dissociation constants.

Borate and silicate are of particular concern. Silicate has been found to leach from even high-quality glass in solutions that are only slightly alkaline, and as such, the silicate amount present in a sample stored in a glass bottle for any amount of time will exceed the natural silicate amount content in the sample at the time it was collected in the field. Borate poses another problem, for although it is generally conservative with respect to S, there are currently two published B_T/S and they disagree by ~4 % (Uppström 1974; Lee et al. 2010). Further, there is evidence that borate can behave non-conservatively in estuarine environments (Shirodkar and Sankaranarayanan 1984; Narvekar and Zingde 1992; Kuliński et al. 2018). Considering that

borate is the largest alkalinity component following A_C, this could be problematic. (Work to accurately measuring total boron in all samples was well under way before the pandemic-induced lock-down started, but came to a halt as a result and was thus impossible to finish within the given timelines.)

As will be shown below in section 3.4.2.2, silicate was explicitly accounted for and also ended up being a contaminant in the base titrant. The total amount content of silicate ($Si_{T,i}$) used to calculate the amount of silicate in the sample at any titration point can be described by Eq. 3-15 and is a product of the original total silicate of the sample ($Si_{T,0}$) and the silicate amount content of the NaOH titrant ($Si_{T,NaOH}$).

$$Si_{T,i} = \frac{Si_{T,0} \cdot m_0 + Si_{T,NaOH} m(\mathrm{NaOH})_i}{m_0 + m(\mathrm{HCl})_T + m(\mathrm{NaOH})_i}$$

Eq. 3-15

Similarly, as will be shown below, it proved impossible to remove 100 % of C_T (the remaining fraction being $C_{T,degas}$), and while carbonate contamination of the NaOH titrant could be greatly reduced there were still low levels of C_T in the titrant ($C_{T,NaOH}$). $C_{T,i}$ in the sample at any given titration point can then be described by Eq. 3-16.

$$C_{T,i} = \frac{C_{T,de\text{-}gas}(m_0 + m(\mathrm{HCl})_T) + C_{T,NaOH} m(\mathrm{NaOH})_i}{m_0 + m(\mathrm{HCl})_T + m(\mathrm{NaOH})_i}$$

Eq. 3-16

The base titration processing equation can then be amended to represent these contaminants as shown in Eq. 3-17, where the total amount contents of borate, sulfate, and fluoride are those of the original sample ($B_{T,0}$, $S_{T,0}$, and $F_{T,0}$) as calculated from the sample

salinity. If we re-write it in terms of ΔA_X being the residual of the two sides of the equation we have a straight forward equation that can be used to calculate A_X in the sample at any given pH_T.

$$\Delta A_X = \frac{A_{T,0} \cdot m_0 - C(\mathrm{HCl})m(\mathrm{HCl})_T + C(\mathrm{NaOH})m(\mathrm{NaOH})_i}{m_0 + m(\mathrm{HCl})_T + m(\mathrm{NaOH})_i} - [\mathrm{B(OH)_4^-}]_i - [\mathrm{OH^-}]_i - [\mathrm{HCO_3^-}]_i - 2[\mathrm{CO_3^{2-}}]_i - [\mathrm{SiO(OH)_3^-}]_i + [\mathrm{HSO_4^-}]_i + [\mathrm{HF}]_i + \frac{[\mathrm{H_T^+}]_i}{Z}$$

Eq. 3-17

A_X of a sample will be the point on the ΔA_X curve, corrected for the dilution by the titrants, where pH_T equals the initial pH_T of the sample and is therefore calculated according to Eq. 3-18 where i and i+1 are the points before and after pH_T, respectively.

$$A_X = \frac{\Delta A_{X,i}}{d_i} + (\mathrm{pH_T} - \mathrm{pH_{T,}}_i)\frac{\Delta A_{X,i+1} - \Delta A_{X,i}}{\mathrm{pH_{T,}}_{i+1} - \mathrm{pH_{T,}}_i}$$

Eq. 3-18

However, if the titrants are not perfectly calibrated, C_T not fully removed, $E°$ poorly calibrated, or borate or other identified alkalinity species not accurately accounted for, any combination of these errors could produce a non-zero value for ΔA_X without actually being composed of unidentified acid-base species.

3.3 Methods

3.3.1 Titration set-up

The titration set-up was a modified version of that by Dickson et al. (2003) described as SOP 3b in Dickson et al. (2007) where the main difference is the addition of another titrant delivery method. In short, the system consists of a temperature-controlled (20 ± 0.05 °C) water-

jacketed beaker of 250 mL fitted with a lid to hold the tips of two automated burettes (Metrohm Dosimat 876), a combination glass/reference electrode cell (Metrohm Ecotrode Plus), a temperature probe (±0.01 °C), and a fritted tube delivering N_2 gas (see Figure 3-4). *E* of the solution is measured using a Metrohm Ecotrode plus whose signal is passed through a custom-built high-impedance voltage-follower amplifier, and acquired using an Agilent 34970A multimeter.

3.3.2 Acid titration

1. A sample of mass m_0 (~120 g) is quantitatively transferred to the sample beaker.
2. A large aliquot, $m(\mathrm{HCl})_a$, of 0.1 mol kg^{-1} HCl (C(HCl)) in a sodium chloride background (0.6 mol kg^{-1}) is added based on an estimate of sample A_T from m_0 and sample S, aiming to reach a pH_T of ~3.6.
3. The sample is stirred for 30 seconds, and if pH_T is above 3.6 a second aliquot of acid is added ($m(\mathrm{HCl})_b$), whose mass is calculated from the distance of the current $pH_{T,a}$ from 3.6 relative to C(HCl) (Eq. 3-19).

$$m(\mathrm{HCl})_b = \frac{(10^{-3.6} - 10^{pH_{T,a}})(m_0 + m(\mathrm{HCl})_a)}{C(\mathrm{HCl})}$$

Eq. 3-19

4. To remove CO_2 produced during acidification, and to reach a stable desired temperature, the sample is stirred vigorously and bubbled with N_2 for 5 minutes.
5. HCl is added in increments of approx. 0.05 g until a $pH_T < 3$.
6. $E°$ of the electrode is estimated from the acid titration data and used to monitor pH_T during the base titration.

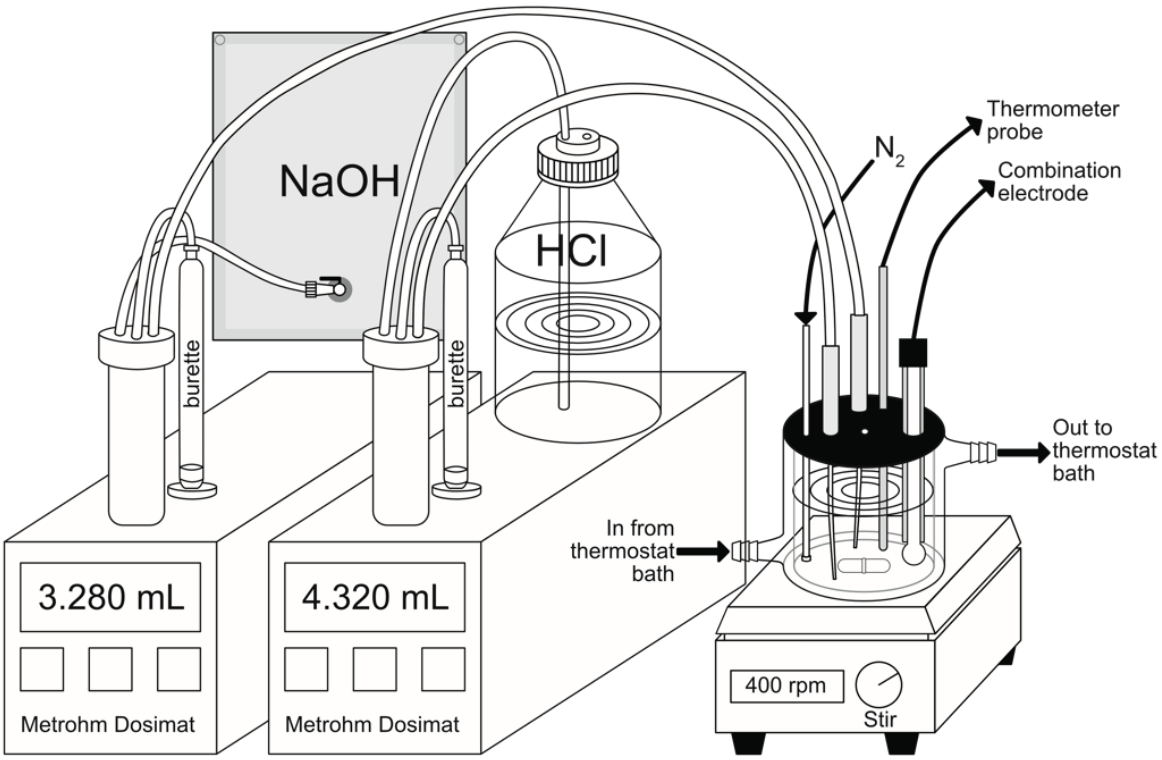

Figure 3-4 Titration set-up, including two automated burettes for HCl and NaOH and the titrant storage methods, a stirred temperature controlled beaker, and semi-enclosing lid holding the burette tips, thermometer, electrode, and N_2 gas line.

3.3.3 Base titration

7. The sample, now at pH ~3, is stirred and de-gassed for an additional 40 minutes (> 45 minutes total) to remove as much CO_2 as is practical (see discussion below).
8. 0.05 mol kg^{-1} NaOH prepared in 0.65 mol kg^{-1} NaCl is added in increments of 0.05 g until $pH_T > 9.5$. The increment size is reduced to about a third of the original size, from 0.05 g to 0.015 g, when pH_T lies between 4.5 and 9 to increase resolution, after which it was again increased.

a. There are other physical interactions that sets an upper limit for the titration end pH_T. These include interactions of Na^+ with the H^+ electrode, and formation of Mg^{2+} and Ca^{2+} hydroxides, as will be discussed in section 3.4.4.3.

3.4 Minimizing and understanding A_X measurement uncertainty

3.4.1 Titrant characterization

3.4.1.1 Calculating titrant mass

The volume delivered by the automated burettes is calibrated by dispensing de-ionized water and measuring the mass of dispensed water. The burettes are fitted with temperature probes on the outside of the burette glass which allows for conversion from water mass to water volume, thus assigning accurate dispensed volumes to the burette. The burettes have a resolution of 0.0005 cm^3, which has been found to be the precision of the burettes according to many years of in-house calibration in our laboratory. Since the titrants have a different composition than de-ionized water, a temperature-dependent density equation is calibrated for each new batch of either titrant using a Mettler Toledo DE45 Delta Range densitometer (±0.00005 g cm^{-3}). With an accurate burette volume, and knowledge of the titrant density we can process the titration data using titrant masses.

3.4.1.2 HCl preparation and composition

The HCl titrant is prepared by diluting 36.5–38 % HCl to 0.1 mol kg^{-1} in a 0.6 mol kg^{-1} NaCl background. The acid is standardized by coulometry as described in the appendix of Dickson et al. (2003), and is also used to calibrate the NaOH titrant (see below). Because the HCl titrant has a very low pH, neither carbonate contamination from the air nor silicate contamination from the glass dissolving will be a concern. Independent measurements for Si_T

were performed and was shown to be ~3 μmol kg^{-1}, essentially at the detection limit. While the HCl may have some C_T in solution, any C_T added from HCl during titration will be part of the C_T that is removed during de-gassing so this amount is not relevant.

3.4.1.3 NaOH preparation

To minimize the risk of CO_2 contamination while preparing the NaOH titrant, as much as possible of the work was performed in a N_2 atmosphere provided by a glove-box, Cleatech® 2200-2-A, where a Green Eye CO_2 meter was used to monitor the replacement of air/CO_2 in the box by N_2 gas. Although initially, I tried using a method similar to that described by Sipos et al. (2000), which involved removing carbonate ion from a NaOH solution as $CaCO_3$ by addition of CaO, it proved hard to produce NaOH with C_T values below 50 μmol kg^{-1}, likely because the filtration part of the process was quite difficult seeing as the solution was both viscous and had large amounts of precipitate in it. Consequently, an alternate approach was used (still inside the glove-box): 10 M NaOH (Fisher Scientific cat.no. SS25-1, contained in a polyethylene bottle) was diluted in CO_2-free de-ionized water without filtration. The advantage of using concentrated NaOH that has been stored for a while is that Na_2CO_3 is insoluble in such a background and will settle out of solution with time (Sipos et al. 2000). (While the concentrated NaOH should ideally be filtered, this proved very difficult with a PE syringe and capsule PTFE filter but fortunately using the unfiltered concentrate to produce dilute solutions produced a suitably low $C_{T,NaOH}$ in the titrant.) The de-ionized water had been rendered CO_2-free by boiling for > 1 hour in air and was then cooled down inside the N_2-filled glove-box. NaCl was added to the NaOH solution to achieve an ionic strength of approx. 0.7 mol kg^{-1}. The resulting dilute NaOH solution (~0.05 mol kg-sol^{-1}) was filled into gas sampling bags (Calibrated Instruments Inc.) fitted with alkaline-resistant polysulfone stop-cocks, before being removed from the N_2 atmosphere.

3.4.1.4 Calibration of C(NaOH)

Calibration of C(NaOH) is performed by titration against a large aliquot of HCl titrant in a NaCl background. While the NaCl background is necessary to maintain activity coefficients, there is ample evidence that even highly purified inorganic salts can have micromolar levels of acid/base impurities (pers. comm. G. Anderson; Ciavatta 1963). By performing at least two titrations such an impurity will be titrated, and thus accounted for, during the first titration, and therefore not be relevant in any subsequent titrations.

The overall procedure involves adding one large weighed aliquot of acid (~1 g; $m(\mathrm{HCl})_T$) to a ~120 g 0.7 mol kg^{-1} NaCl solution to reach a $pH_T < 3.5$, after which the sample is allowed to de-gas for 45 minutes to remove any C_T. The C_T-free acidic solution is then titrated with the NaOH titrant, m(NaOH), to a $pH_T > 7$, i.e., beyond the equivalence point of a strong base-strong acid titration. This is repeated at least three more times (one to account for impurities, and at least three replicates), with the exception that the de-gassing time is reduced to 10 minutes for each subsequent titration. For each new batch of NaOH, at least eight titrations were performed, while four titrations were used for periodic checks of the C(NaOH) calibration.

A Gran function (Eq. 3-21) was used to process the data and calculate C(NaOH) (Gran 1952), and is based on the Nernst equation (Eq. 3-9) and the fact that the solution is diluted as titrant is added as shown in Eq. 3-20.

$$[\mathrm{H}_T^+] = \exp\left(\frac{E - E^\circ}{RT / F}\right)$$

Eq. 3-20

Since E° is a constant, this can be moved to the left-hand side of the equation which will change the slope of the function F_1 (Eq. 3-21), but not the intercept.

$$F_{1,i} = \left(m_0 + m(\mathrm{HCl})_\mathrm{T} + m(\mathrm{NaOH})_i\right)\exp\left(\frac{E_i}{RT/F}\right)$$

Eq. 3-21

F_1 is zero at the intercept which also corresponds to the mass needed of the NaOH to reach the equivalence point, $m(\mathrm{NaOH})_{eq}$:

$$C(\mathrm{NaOH})\cdot m(\mathrm{NaOH})_{eq} = C(\mathrm{HCl})\cdot m(\mathrm{HCl})_\mathrm{T}$$

Eq. 3-22

This holds true as long as there are no impurities and the sample started at the equivalence point before any acid or base was added, and $m(\mathrm{NaOH})_{eq}$ is estimated using a linear least-squares fit of $F_{1,i}$ against $m(\mathrm{NaOH})_i$. However, chances are that the NaCl solution might not be completely free of protolytic impurities, or in other words the NaCl solution is likely to have some impurity. For the first titration, therefore, the moles of added HCl will appear smaller or bigger if the impurity is a base ([impurity] negative) or an acid ([impurity] positive), respectively. Consequently, the $C(\mathrm{NaOH})$ calculated from this first titration will also be smaller or bigger than its true value (Eq. 3-23).

$$C(\mathrm{NaOH})\cdot m(\mathrm{NaOH})_{eq} = C(\mathrm{HCl})\cdot m(\mathrm{HCl})_\mathrm{T} + [\mathrm{impurity}]\cdot m_0$$

Eq. 3-23

If the first titration is perfectly terminated at the equivalence point, and if a second titration is performed in the same NaCl solution by adding another aliquot of acid ($m(\mathrm{HCl})_{T,II}$) and again titrated with the NaOH ($m(\mathrm{NaOH})_{eq,II}$) the amount content of the impurity will have been accounted for in the previous titration. However, it is unlikely that the titration terminated at the equivalence point meaning that titration II will leave the solution slightly more acidic or basic, or in other words the solution will have an excess moles of acid (H_{ex}) that can be either negative

or positive. The H_{ex} in the solution following the first titration I ($H_{ex,I}$) will be the starting H_{ex} for the second titration II and can be calculated according the data from titration I:

$$H_{ex,I} = C(\mathrm{NaOH})_I \cdot \left(m(\mathrm{NaOH})_{T,I} - m(\mathrm{NaOH})_{eq,I} \right)$$

Eq. 3-24

For each subsequent titration C(NaOH) can then be calculated according to the remaining H_{ex} from the previous titration (Eq. 3-25).

$$C(\mathrm{NaOH})_{II} = \frac{C(\mathrm{HCl})m(\mathrm{HCl})_{T,II} - H_{ex,I}}{m(\mathrm{NaOH})_{eq,II}}$$

Eq. 3-25

The method repeatedly produced a relative standard deviation of 0.1 % or better, and calibration checks performed within up to four weeks from NaOH batch preparation agreed to within 0.1 % of the originally assigned C(NaOH).

Table 3-1 Sample set of eight titrations for *C*(NaOH) calibration

Titration	C(NaOH) (mol kg^{-1})
I	0.05110
II	0.05039
III	0.05042
IV	0.05037
V	0.05044
VI	0.05042
VII	0.05039
VIII	0.05041

Table 3-1 shows a sample of C(NaOH) titration data with a mean of 0.05041 mol kg^{-1} with a relative standard deviation of 0.05 % (excluding $C(\mathrm{NaOH})_\mathrm{I}$). $C(\mathrm{NaOH})_\mathrm{I}$ in this titration set was higher than the subsequent ones, as was typical for these titrations and likely indicated an acid impurity in the NaCl salt used to prepare the 0.7 mol kg^{-1} solution.

3.4.2 Contaminants

3.4.2.1 Sample C_T removal and titrant contamination

Between the acid and base titrations the sample is stirred vigorously and CO_2 removed by bubbling of N_2 for some period of time. The appropriate period of time was determined from a series of low-volume C_T measurements made out of an acidified seawater sample. A seawater sample of a 120 g was acidified to pH_T 3 using the HCl titrant (where the sample would be after the acid titration). The sample was then stirred (vigorous without splashing, dial had no metric) and de-gassed (200 mL/min), the same rates used for a titration, and C_T measured in increments of 5–60 minutes for up to three hours. Measurements were made with a CO_2 gas analyzer (Li-COR LI-7000 CO_2/H_2O analyzer) using a 5 mL sample volume, and the system was calibrated using the certified reference materials (CRMs) for C_T measurements. At most, eight measurements (40 mL) were drawn from one single sample, and these were spaced out at various intervals. The first measurement was taken within a couple of minutes after the acid being added, and at most the sample was de-gassed for two hours and twenty minutes.

A composite of these ten sets of measurements are shown in Figure 3-5, and a de-gassing time of 45 minutes was determined, at which point C_T was 6 (±2) μmol kg^{-1} (n = 8; Figure 3-5). These sets of measurements did reduce the sample volume somewhat throughout the de-gassing period, and while it did how when C_T reached the lowest and stable value it is not clear that this value would be accurate. To confirm the results a different measurement system was used based

on coulometric CO_2 detection (SOMMA, Johnson et al. 1993). This system uses 30 mL of sample, so only a single sample could be extracted from the original seawater sample. In this case, an actual acid titration was performed, followed by the allotted time for de-gassing (45 minutes total), after which the sample was transferred to a glass bottle for immediate C_T analysis. While this method runs the risk of taking up CO_2 from the laboratory air during the liquid transfer step, these measurements confirmed a C_T of 3.5 (± 0.6) µmol kg^{-1} (n = 3).

It is worth noting that neither of these systems have been thoroughly tested to measure C_T that far below typical seawater amount contents (~2000 µmol kg^{-1}), but their level of agreement is reassuring. The $C_{T,degas}$ determined using the coulorimetric measurement (3.5 µmol kg^{-1}) was used for all sample processing and titration simulation (Table 3-2).

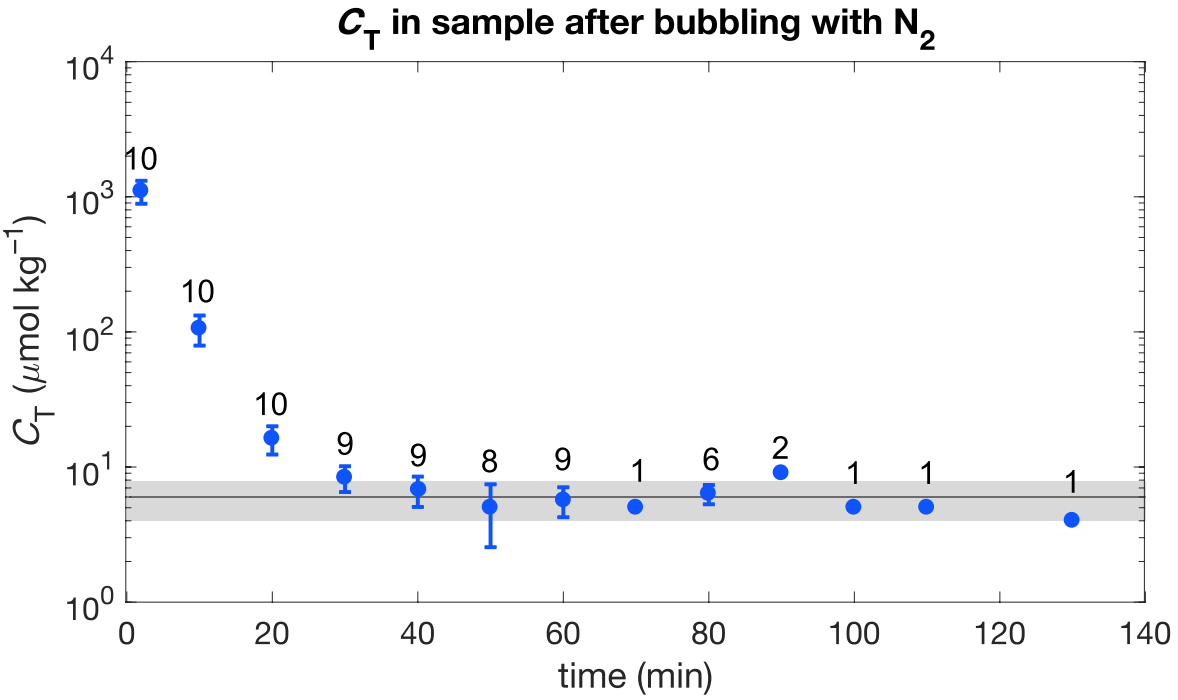

Figure 3-5 C_T removal by degassing, where each point is the mean of measurements in the number of samples indicated above each point. Ten de-gassing samples total were measured. The error bars represent one standard deviation of the mean and appear asymmetrical due to the y-axis being logarithmic. The horizontal line represents the average lowest value reached (6 µmol kg^{-1}), and the shaded grey bands the one standard deviation of these (2 µmol kg^{-1}).

3.4.2.2 Silicate contamination

It became apparent that silicate leaches from storage glass bottles at amounts that were detected during the titration procedure. Even during preparation of the NaOH titrant, it was detected that some Si dissolved although only the dilute solution was in contact with glass, and for less than 30 minutes. To account for this, samples for silicate analysis were collected from all samples analyzed by the titration system, as well as from the NaOH titrant. The appropriate estimate of total silicate was then included in the data processing (Eq. 3-15). All silicate samples were analyzed manually using the protocol described in chapter 12 of Knap et al. (1993), with the modification that all work was done by weight and not by volume. The method involved spectrophotometric analysis of samples reacted with molybdate and reduced with a metol sulfite-oxalic acid-sulfuric acid mixture for at least 2 hours. A subset of the samples was analyzed by Ocean Data Facilities (ODF) at SIO using an autoanalyzer method (Armstrong et al. 1967) as a cross-check, and the two methods agreed to within the reported uncertainty of 2–4 μM (pers. comm. S. Becker).

3.4.3 Titration simulation

Although the titration method presented here is a more direct estimate of A_X than calculating A_X from Eq. 3-3, it is still technically an estimate based on subtracting the contribution from other acid-base species, though now at each titration point, rather than only at the pH of the original sample. As a result, it can be affected by random errors in the titration system to a greater degree. To explore these uncertainties a titration simulation and chemical equilibrium model was written and run using matlab R2016b.

Table 3-2 Amount contents and constants used for modelling, including their estimated uncertainty and source, based on a seawater sample of a salinity of 33.5 and a sample temperature of 20 °C, and calculated using the equilibrium expressions in Figure 1-1

Quantity	Value	Uncertainty	Source
$C_{T,\,sample}$	2000 µmol kg^{-1}		
$C_{T,degas}$	3.5 µmol kg^{-1}	1.5 µmol kg^{-1} [a]	(Measurements and experience in our laboratory using a SOMMA system)
$C_{T,NaOH}$	20 µmol kg^{-1}		
$Si_{T,\,sample}$	20 µmol kg^{-1}	4 µmol kg^{-1} [a]	(Armstrong et al. 1967; pers. comm S. Becker)
$Si_{T,NaOH}$	30 µmol kg^{-1}		
B_T	397 µmol kg^{-1}	2 % [b]	(mean of Uppström 1974; Lee et al. 2010)
F_T	65.4 µmol kg^{-1}	3 % [c]	(Riley 1965)
S_T	27.03 mmol kg^{-1}	0.16 % [c]	(Morris and Riley 1966)
P_T	0 µmol kg^{-1}	0.004 µmol kg^{-1} [a]	(Armstrong et al. 1967; pers. comm S. Becker)
pK_W	13.43	0.01 [c]	(Millero 1995)
pK_1, pK_2	5.897; 9.06	0.007, 0.02 [c]	(Lueker et al. 2000)
pK_{Si}	9.47	0.02 [c]	(Millero 1995)
pK_B	8.665	0.004 [c]	(Dickson 1990)
pK_F	2.63	0.02 [c]	(Perez and Fraga 1987)
pK_{P1}, pK_{P2}, pK_{P3}	1.61; 6.01, 8.9	0.02, 0.09, 0.2 [c]	(Millero 1995)

[a] Measurement uncertainty; [b] Half difference between the two ratios; [c] Uncertainty reported by authors

The titration simulation model is thus based on the same equations used to process the titration data, Eq. 3-8 and Eq. 3-13 as described in “Approach”, but instead of calculating what

the initial $A_{T,0}$ and $E°$ were, the model starts with a known A_T (and C_T and thus pH_T) which is re-calculated every time acid or base is added.

3.4.3.1 Simulating the acid titration

First, the initial pH_T of the sample is calculated using a given $A_{T,0}$, typically 2200 μmol kg^{-1}, and total amount contents and equilibrium constants of other acid-base systems as listed in Table 3-2. The initial $[H_T^+]$ is calculated by rearranging Eq. 3-26 as a polynomial equaling 0 and solving for a positive solution with a reasonable initial guess of 10^{-8}. (The species HS^-, NH_3, and HNO_2 were not included in these titration simulations, but they could just as easily be included as any of the other species.)

$$A_{T,i} = [HCO_3^-]_i + 2\cdot[CO_3^{2-}]_i + [B(OH)_4^-]_i + [SiO(OH)_3^-]_i + [OH^-]_i + 2[PO_4^{3-}]_i + [HPO_3^{2-}]_i - [HSO_4^-]_i - [HF]_i - [H_3PO_4]_i - ([H_T^+]_i / Z)$$

Eq. 3-26

Each time titrant is added to the sample, the total amount contents of all constituents, save $[H_T^+]$ and $[OH^-]$, are diluted according to Eq. 3-27, and the diluted amount content is used to calculate the species amount content at titration point i in Eq. 3-26 and using the expressions in Figure 1-1. At the initial state of the sample $i = 0$, the dilution d_i equals 1 as $m(HCl)_i = 0$. The $[H_T^+]/Z$ that is calculated is therefore equal to the current amount content of free hydrogen ions in the sample, just as a combination glass/reference electrode would measure it in a real sample.

$$d_i = \frac{m_0}{m_0 + m(HCl)_i}$$

Eq. 3-27

The simulated acid titration then proceeds similar to the real titration, starting with the addition of one large aliquot to bring pH_T to ~3.5. For $i = 1$, the mass of the large acid titrant

aliquot is calculated using Eq. 3-28, which is an approximation of the amount of acid is needed to reach a pH_T of 3.5. The reason to approximate it is that a real titration will not necessarily perfectly reach pH_T 3.5, so by approximating the mass of HCl necessary to reach this pH_T it is more reflective of the real titration processes.

$$m(\mathrm{HCl})_1 = \frac{(-10^{-3.5} - A_{\mathrm{T},0})m_0}{10^{-3.5} - C(\mathrm{HCl})}$$

Eq. 3-28

$A_{T,1}$ is then calculated as the initial $A_{T,0}$ minus the addition of acid from $m(\mathrm{HCl})_1$ according to Eq. 3-29. Next, C_T is set to 100 μmol kg^{-1} which is the estimated C_T after five minutes of degassing. $[H_T^+]_1$ is calculated according to Eq. 3-26 where the total amount contents B_T, Si_T, P_T, S_T, and F_T have been diluted and C_T now equals 100 μmol kg^{-1}.

$$A_{\mathrm{T},i} = \frac{A_{\mathrm{T},0}m_0 - C(\mathrm{HCl})m(\mathrm{HCl})_i}{m_0 + m(\mathrm{HCl})_i}$$

Eq. 3-29

The next part of the titration is simulated with m(HCl) increments of 0.05 g where $A_{T,i}$ and $[H_T^+]_i$ are calculated at each point until $pH_T < 3$ (and the lower C_T is diluted as are the total amount contents of the other species).

3.4.3.2 Simulated base titration

The base titration is simulated next, using the same equations with a minor modification to account for the fact that base (i.e., positive alkalinity) is being added to an acidified (i.e., negative alkalinity) sample. Another difference is that C_T and Si_T increase throughout the titration due to them being contaminants in the NaOH titrant. Also, between the acid and base titration the sample was simulated to have degassed for 40 minutes and thus C_T has been

reduced to $C_{T,degas}$ = 3.5 μmol kg^{-1}. At each point during the base titration, therefore, Si_T and C_T are calculated according to Eq. 3-15 and Eq. 3-16, and the total amount contents of the other species are diluted according to Eq. 3-5.

The base titration is simulated by adding m(NaOH) increments of 0.01 g (smaller than what is possible for the real titrations to increase resolution of the models, and without changing the increment size in the middle pH_T values) until pH_T = 10, and $A_{T,i}$ in the sample is now calculated according to Eq. 3-30 (the first half of Eq. 3-14) while $[H_T^+]_i$ is still calculated according to Eq. 3-26.

$$A_{T,i} = \frac{A_{T,0} m_0 - C(\mathrm{HCl}) m(\mathrm{HCl})_T + C(\mathrm{NaOH}) m(\mathrm{NaOH})_i}{m_0 + m(\mathrm{HCl})_T + m(\mathrm{NaOH})_i}$$

Eq. 3-30

These two titrations produce four data vectors – m(HCl) and $[H_T^+]$(HCl), and m(NaOH) and $[H_T^+]$(NaOH). The two $[H_T^+]$ vectors are converted to E vectors via the Nernst equation (Eq. 3-9) using an $E°$ of 0.4 V. Resulting vectors of E from acid and base titrations, and of m(HCl) and m(NaOH) together with m_0, S, and T are saved in the same format as the real titration data. This enables using the exact same data processing equations and matlab scripts as are used for the real data, meaning it is possible to verify the data processing approach using perfectly characterized (simulated) data.

3.4.3.3 Simulation of titrations with A_X present

As in Eq. 3-17, it is possible to simulate a titration of a sample with one or more HX in it. This can be done by defining one (or more) HX according to Eq. 3-31 and including the relevant term(s) $[X^-]$ in Eq. 3-26, as shown in Eq. 3-32. When adding an extra component to the simulated sample, $A_{T,0}$ was kept the same (i.e., 2200 μmol kg^{-1}).

$$[\mathrm{X}^-] = \frac{X_\mathrm{T}}{1 + [\mathrm{H}^+_\mathrm{T}] / K_\mathrm{X}}$$

Eq. 3-31

$$A_{\mathrm{T},i} = [\mathrm{HCO}^-_3]_i + 2\cdot[\mathrm{CO}^{2-}_3]_i + [\mathrm{B(OH)}^-_4]_i + [\mathrm{SiO(OH)}^-_3]_i + [\mathrm{OH}^-]_i + 2[\mathrm{PO}^{3-}_4]_i + [\mathrm{HPO}^{2-}_3]_i + [\mathrm{X}^-] - [\mathrm{HSO}^-_4]_i - [\mathrm{HF}]_i - [\mathrm{H_3PO_4}]_i - ([\mathrm{H}^+_\mathrm{T}]_i / Z)$$

Eq. 3-32

3.4.4 Uncertainty assessment

Before exploring the various uncertainties, it is useful to illustrate how they will be presented, and what "zero uncertainty" looks like. One way of handling this is to look at the base titration shown in Figure 3-3b), and to subtract each of the individual species from A_T as is done in Eq. 3-17. As long as there is no contamination of the titrants, C_T was completely removed from the sample during de-gassing, all other alkalinities are known, and $E°$ is well characterized this should produce a horizontal line that is 0 μmol kg^{-1} at any $\mathrm{pH_T}$ during the titration.

This "residual curve" representation gives the advantage that if there are unidentified alkalinity components present (i.e., A_X), these should show up by making the curve non-zero. A few examples have been simulated and are shown in Figure 3-6, with a range of amount contents and acid dissociation constants. Another advantage by processing the titration data this way is that one can easily estimate X_T and K_X by looking at this type of figure, i.e., the top of the curve estimates X_T and the middle of the steep slope estimate pK_X. Any errors present, however, could falsely present as A_X or add noise to the data which would make interpreting information about A_X more difficult. In the next section this kind of plot will be used to demonstrate the potential bias caused by random and systematic errors in the absence of A_X. To assess these

types of errors a perfect titration is simulated (including acid and base titration), error is added, and the titration data is processed according to Eq. 3-8–Eq. 3-17.

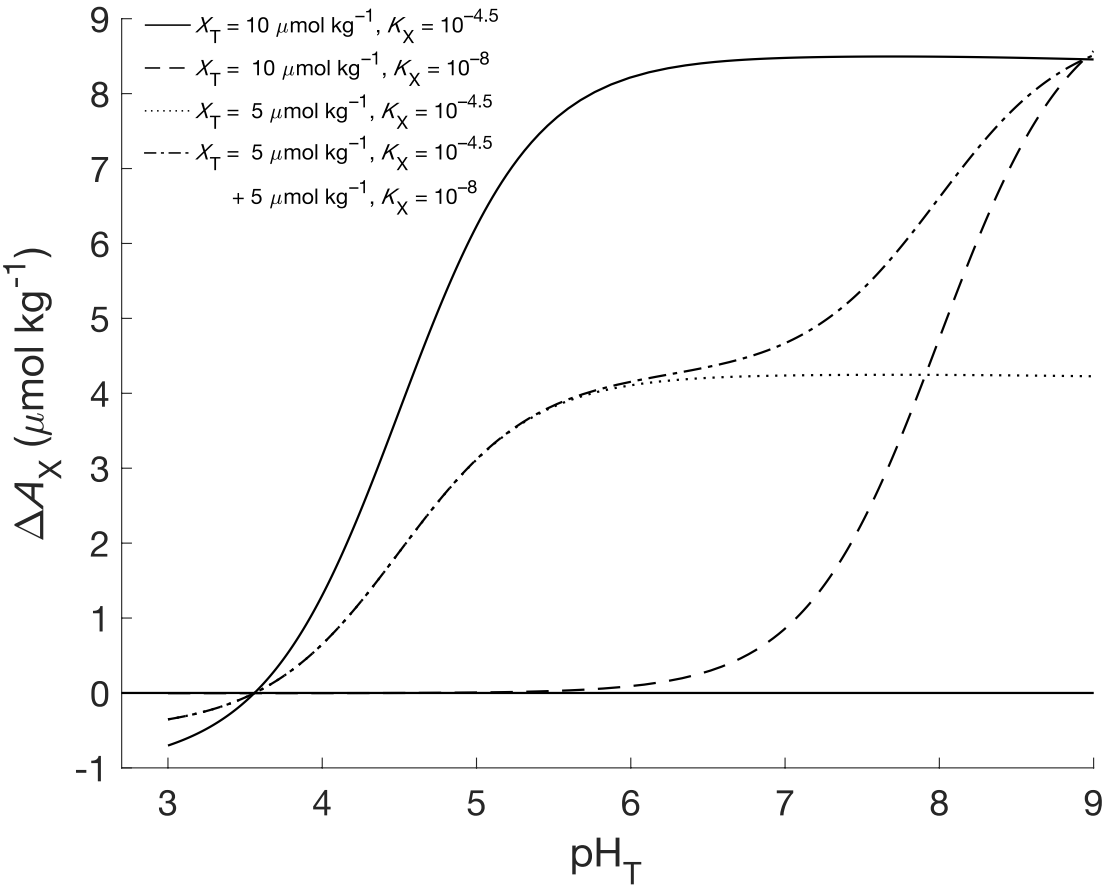

Figure 3-6 Four simulated titrations of a simple seawater sample each with a different A_X content, including 5 amd 10 µmol kg^{-1}, and pK_X values of 4.5 and 8, and a mixture of both.

3.4.4.1 Incorrectly accounting for the total amount content of identified alkalinities

Since it was not possible to remove 100 % of sample C_T, the small level of remaining C_T plus that being added from the titrant was included in the data processing according to Eq. 3-16. Additionally, some silicate and carbonate are introduced to the sample during titration via

contamination of the NaOH titrant (both contaminants were negligible in the HCl titrant). Although the content of these two in the sample and titrants were determined independently, the numbers still have uncertainties associated with them and the values used are shown in Table 3-2. Another alkalinity component present at a relatively large amount content (> 10 μmol kg^{-1}) is borate. While B_T is usually estimated from S using either of the two published ratios (Uppström 1974; Lee et al. 2010), the two B_T/S ratios disagree by approx. 4 %. While both ratios have precisions associated with their measurements (2 % and 0.4 % for Uppström and Lee et al., respectively), it is not clear which ratio is correct (see, e.g., Fong and Dickson 2019). Instead, it was chosen to consider their 4 % difference as twice the relative uncertainty for either measurement, so the standard value (as has been considered for all other errors) would be 2 %. Hydrogen sulfate is not included here, as its uncertainty can be mostly ignored by using $[H_T^+]$ rather than $[H_F^+]$. While fluoride is present at an amount content > 10 μmol kg^{-1}, its pK is small, and thus it is only interacting with the titrants in the pH_T range where $E°$ is calibrated. If there is an error in F_T a large proportion of this will be accounted for in the $E°$ calibration. Nutrients such as phosphate are rarely present at > 5 μmol kg^{-1}, and the measurement error is small enough that it was not included in this uncertainty assessment.

A titration was simulated using "total amount content plus uncertainty" for each identified alkalinity component, and the data was processed using just the amount content, thus creating a positive bias in the ΔA_X curve (performing the same operation but subtracting the uncertainty would lead to a negative bias of the same magnitude). In Figure 3-7 the errors in ΔA_x contributed by each of the individual biases have been added in quadrature (solid line). It is worth noting that the effect of titrant contamination is less than 1 % of the signal for both

silicate and carbonate. At a typical initial sample pH_T of ~8, the effect of errors of this magnitude constitutes an overall bias of approx. 3 μmol kg^{-1}, although it is important to note that in samples where silicate is higher (> 100 μmol kg^{-1} in some instances, see next chapter) the silicate uncertainty contribution will be higher.

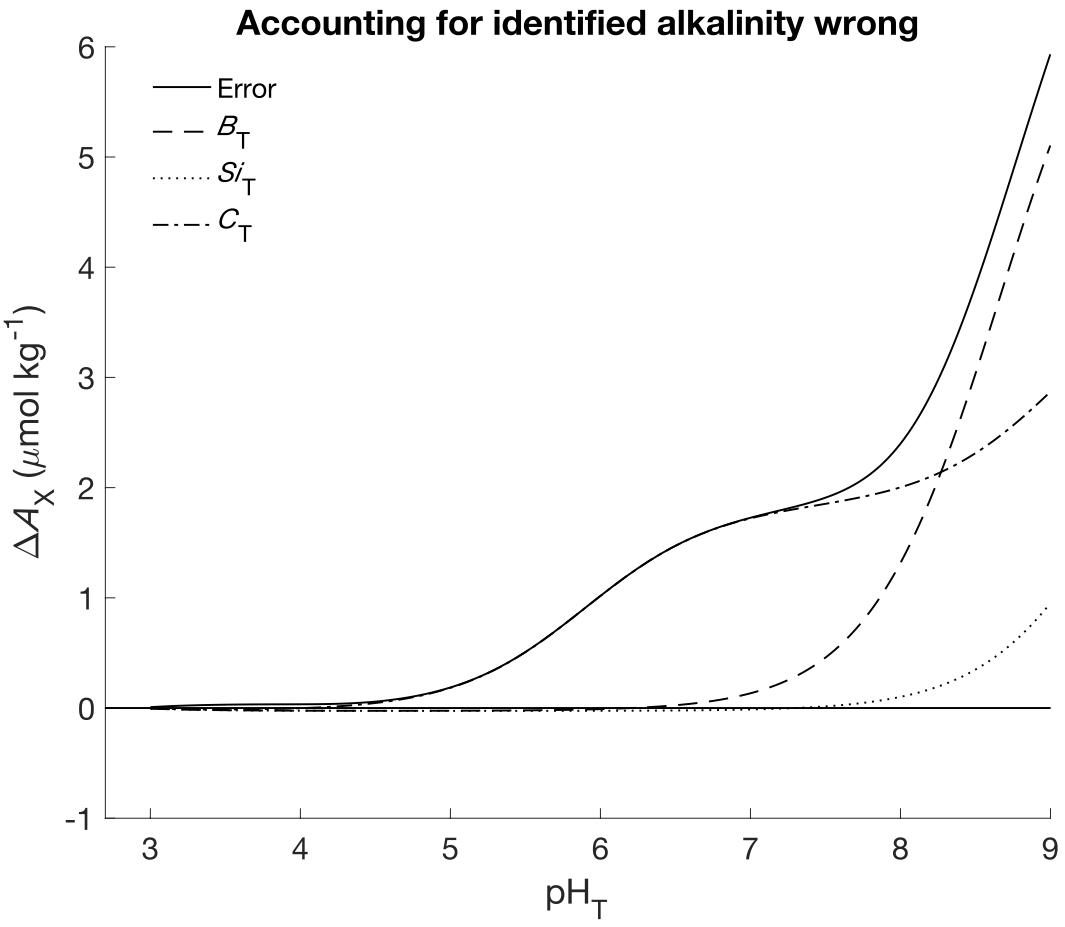

Figure 3-7 Accounting for identified alkalinities wrong and the observed positive signal in ΔA_X, including the effect from error in estimating total borate, total silicate, and total carbonate..

3.4.4.2 Incorrectly accounting for the speciation of identified alkalinities

There are also uncertainties in acid dissociation constants, whose effect will have a pH_T dependence. To assess these errors, a set of titrations were simulated using a biased set of K_A values for water (K_W), the carbonate system (K_1 and K_2), silicate (K_{Si}), borate (K_B), and fluoride (K_F). These biased values were the conventionally accepted K_A value plus the reported uncertainty for all constants. When interpreting the titration data, the K_As were used without adding the uncertainty value. Including the uncertainty in this way led to a positive error while interpreting the data, and subtracting the K_A uncertainty would likely produce the same error in ΔA_X but with opposite sign. The result of this is shown in Figure 3-8, where the solid line results from adding the other lines in quadrature.

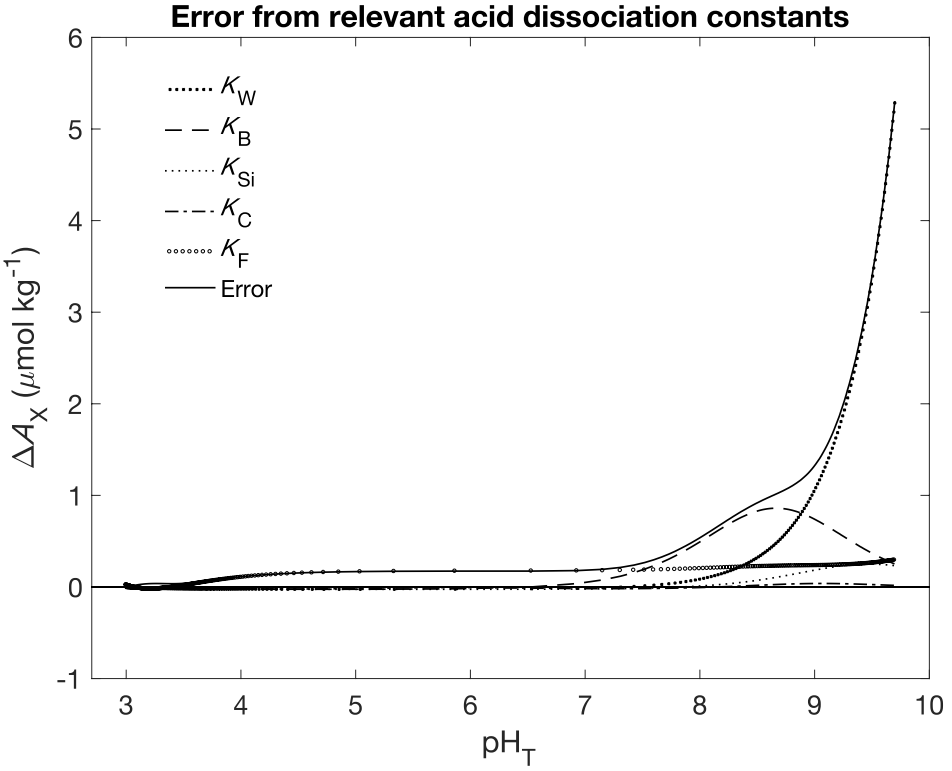

Figure 3-8 Error from bias in the K_A of water, borate, silicate, carbonate and hydrogen carbonate, fluoride, and their error added in quadrature and squared is shown in the drawn line.

The largest effect is caused by an assumed error in K_W and only shows at high pH values. For example, for a change in pH_T of 0.01 the error in correcting for $[OH^-]$ using K_W is ~0.023$[OH^-]$, and $[OH^-]$ of course increases logarithmically at higher pH values. The uncertainty contributions from K_1 and K_2 of the carbonate system are so small that they are not visible because the amount content of C_T in this simulation (and during the real titrations) is so small. In this scenario, the alkalinity contribution from borate is the highest which explains its large contribution relative to the other K_A values.

3.4.4.3 Upper pH_T limit for the titration

To measure the A_X of a sample, it is necessary to titrate to its initial pH_T. There is a benefit of titrating to an even higher pH_T value because a broader pH_T range will potentially allow for more quantitative information about A_X if it includes material with higher-pKs. There are however complications with the chemical composition of the sample that sets an upper pH_T limit, including precipitation of magnesium hydroxides, and sensitivity of the glass electrode in the pH_T cell to sodium ions.

Magnesium (and, to a lesser extent calcium) can cause problems during titration because they form precipitate in the form of hydroxides, such as $Mg(OH)_2$, at higher pH_T values. This can act as to remove alkalinity from solution where the amount removed depends on the solubility constant (K_{SP}). There are also potential complications from forming solid gel-like hydroxides and their interaction with the surface of the electrode. With a K_{SP} for $Mg(OH)_2$ of 3.4×10^{-11} in de-ionized water (Vogel 1961) and a typical seawater magnesium concentration, it suggests that altered magnesium activity is likely to occur starting at $pH_T \sim 9.4$, although it is

worth noting that a higher ionic strength and more complex ionic matrix such as seawater K_{SP} could be different. While the precipitation of Mg hydroxides is bound to affect the sample acid-base balance, the soluble $MgOH^+$ will form first. It should be noted that formation of such mono-hydroxides will have affected K_W during its determination (either in real or synthetic seawater media which both contain magnesium) and as such the effect of mono-hydroxides are likely accounted for (Dickson and Riley 1979). The precipitation of magnesium hydroxide sets a practical upper limit for the titration in solutions containing Mg.

Combination glass/reference electrodes for pH_T measurements have difficulties at higher pH_T values. This is due to the electrode having a slight sensitivity for Na^+, so that when H^+ is present at sufficiently low levels Na^+ will interact with the electrode (also known as "alkali error"). The manufacturer of the electrode used in this work reports a selectivity constant of $K_{Na+/H+}$ of 10^{-13}, suggesting that there can be a bias in $[H_T^+]$ of approx. 1 % at a $-\log([H_F^+])$ of 11 (Haider 2004), or an error of ~0.004 in pH_T. Since this happens well above the limit imposed by the precipitation of hydroxides, this should not be an issue in seawater solutions although it does set a limit for titrations performed in simple salt solutions such as KCl or NaCl.

3.4.4.4 Errors in estimating A_X at initial pH_T

A_X of a sample is evaluated using Eq. 3-17 at the initial pH_T of the sample. It is unlikely that there will be a titration point exactly at this pH_T, and therefore a small error will be associated with interpolating to this number between two titration points. The distance between two titration points will be large if the initial pH_T is in an area of low buffering (i.e., a steep slope), but in this case the pH_T changes fairly linearly (as a result of the presence of the boric acid-system) so that a linear interpolation between two points would be appropriate (Figure 3-9).

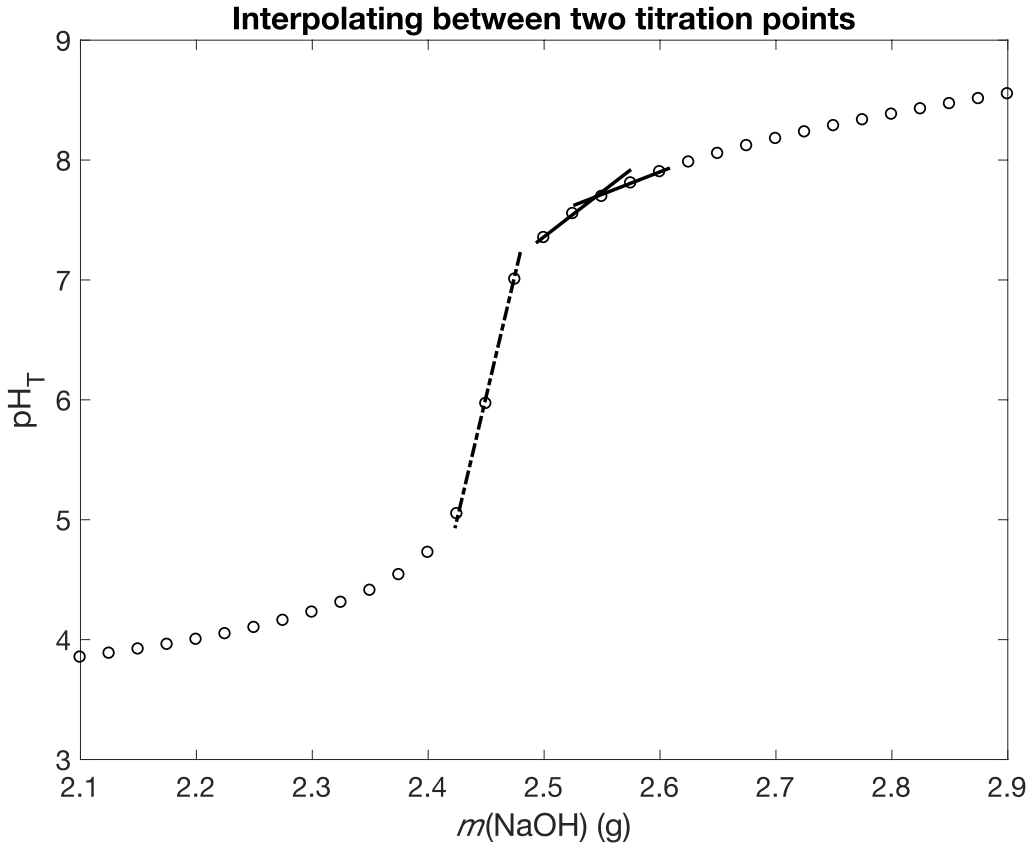

Figure 3-9 Lines suggesting the appropriateness of linear interpolation between two titration points at high buffering (solid line) and low buffering (dash-dot line).

If the initial pH_T is in a region with higher buffering and where pH_T changes slowly, the distance between two points will be very small and as such the uncertainty in linear interpolation between two points will be small. Interpolating to the initial pH_T from two titration points can likely be improved by the use of a polynomial interpretation, but time did not permit this improvement for this dissertation.

3.4.4.5 Random errors in voltage and titrant mass

Random errors occur during the titration from noise in voltage (E) measurements and in the mass (m) of dispensed titrant due to imperfections in the burette. The errors from these were

estimated by including the error in either E or m while simulating a titration and processing the titration data without accounting for this random error. This simulation was followed by data processing using Eq. 3-17, and was repeated 1000 times each for E and m using the matlab code described in an earlier section. For m, during simulation, a randomly distributed number with a mean of 0 g and a standard deviation of 0.0005 g was added at each titration point. This vector was used to calculate $[H_T^+]$ for the next titration step and resulted in an E vector. An error free m vector was recorded alongside this and used in the titration data processing together with the error-affected E vector.

The resulting error in ΔA_X is shown in Figure 3-10, which shows one standard deviation of the 1000 simulations. It is worth noting that random error occurred in m(HCl) during the acid titration will appear as a systematic error in each base titration, explaining the slightly larger error at the first titration point. For random error in E, a perfect titration was simulated, after which a random number with a mean of 0 μV and a standard deviation of 20 μV was added to each of the points of the resulting E vector (this error is the observed standard deviation for our pH_T cell from the 10 average values that goes into the final E during a measurement). No error was added to the m vector. 1000 titrations were simulated, and the resulting effect in ΔA_X is shown in Figure 3-10.

Changes in T and S throughout the titration from e.g., room temperature fluctuations or evaporation of the sample during de-gassing were small ($\Delta T < 0.1$ °C and $S < 0.1$), had no significant effect on the speciation calculations.

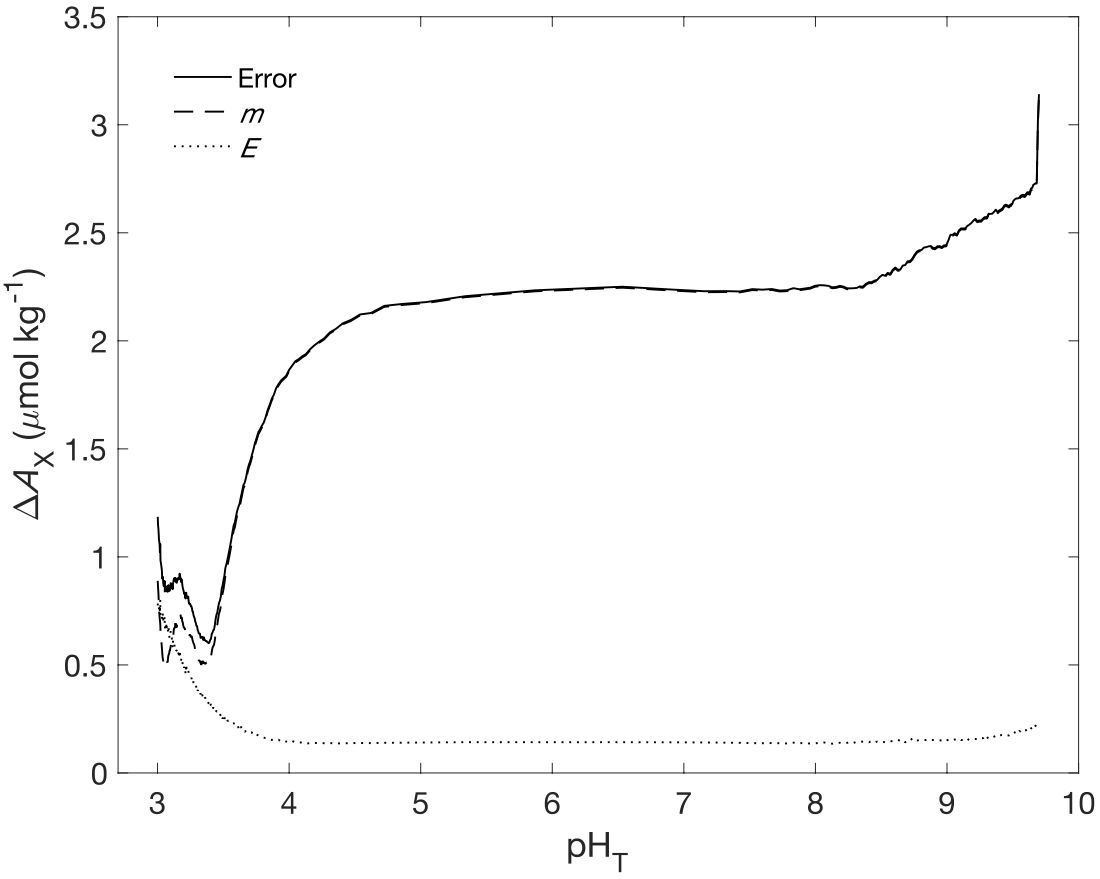

Figure 3-10 The effect of random error in m and E on ΔA_X shown as the standard deviation of the ΔA_X curve from 1000 simulations with random error in either m or E, and the drawn line shows these two lines added in quadrature.

3.5 What is the uncertainty in measuring A_X?

The A_X uncertainty contribution from random errors adds up to 2.3 μmol kg^{-1} at most pH_T values, and should be considered the repeatability of the titration method. The systematic errors from accounting for identified alkalinities clearly affect the accuracy of measuring A_X, with approximately 0.6 μmol kg^{-1} being added from uncertainty in the acid dissociation constants at a pH_T of ~8 and 1.9 μmol kg^{-1} from accounting for the amount contents of identified alkalinities in error. One last error not added to the figure is the uncertainty in the

calibration of C(NaOH), at a 0.1 % uncertainty and 3.5 g of NaOH titrant needed to reach a pH_T of 8 in a 120 g sample this error is 1.7 μmol kg^{-1}. When all these errors are added in quadrature, the accuracy of this method is estimated as 3.4 μmol kg^{-1} at pH_T of 8 (Figure 3-11). It is worth noting that if the sample is not allowed ample time for de-gassing, the uncertainty contributions from C_T will be even larger. For example, if C_T is not driven to a stable minimum it could still be degassing as the sample is titrated, and at C_T < 700 μmol kg^{-1}, uncertainties in K_1 and K_2 will add ± ~3 μmol kg^{-1} at various pH_T values. Extracting quantitatively useful information at pH_T > 8 is associated with larger uncertainties largely as a consequence of uncertainties in K_W.

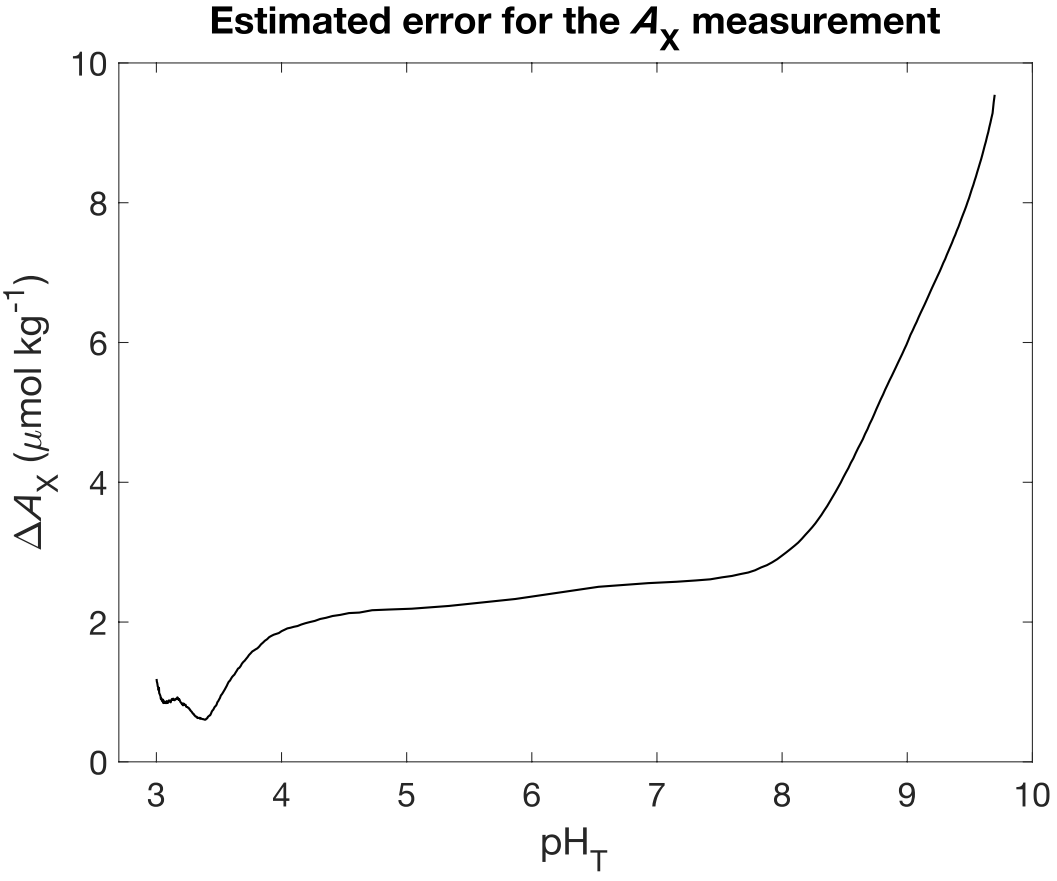

Figure 3-11 Total error in calculating ΔA_X across the titration pH_T range from adding all the individual errors in quadrature, except for uncertainty associated with C(NaOH).

4 MEASUREMENTS OF A_X IN SYNTHETIC AND REAL SEAWATER SAMPLES

For this chapter, a range of samples from simple salt solutions to samples collected off the coast of California were analyzed for A_X according to the method described in Chapter 3 (in addition to analysis of their silicate content). However, this chapter will start out by discussing what an ΔA_X curve might look like in the absence of A_X.

4.1 What does "no A_X" looks like

To be able to say unambiguously that the titration method works it is desirable to show that when titrating a sample where everything has been characterized, ΔA_X at each titration point (Eq. 3-17) is zero within the uncertainties of the measurement. To start with, a simple salt solution consisting of NaCl at an ionic strength similar to that of seawater (~0.7 mol kg^{-1}) was titrated. This makes it practical to assess the two processes that are likely to set an upper pH_T limit for the titrations. As identified in the previous chapter, there are two known issues that can obscure an electrometric pH_T measurement: the sodium error and issues related to the formation of magnesium hydroxides (section 3.4.4.3).

4.1.1 Will the sodium error be visible in the titration data?

To evaluate if the effects of the sodium error could be seen in the titration curve, two solutions were prepared of NaCl and KCl, where both were of the same ionic strength. These simple salt solutions were prepared from ACS reagent grade salts (Tyner and Francis 2017) without any purification, to approx. 0.7 mol kg^{-1} by dissolving the background salt in 17.9 MΩ de-ionized water in screw-cap borosilicate bottles. If sodium error is a meaningful concern, it

should be obvious in the NaCl solution and not the KCl solution. Note however, that combination glass/reference electrodes can have an affinity for other alkali metals as well, such as potassium, but the error will be smaller than for sodium (Isard 1967). The A_X curves obtained for three such titrations in each of NaCl and KCl are shown in Figure 4-1.

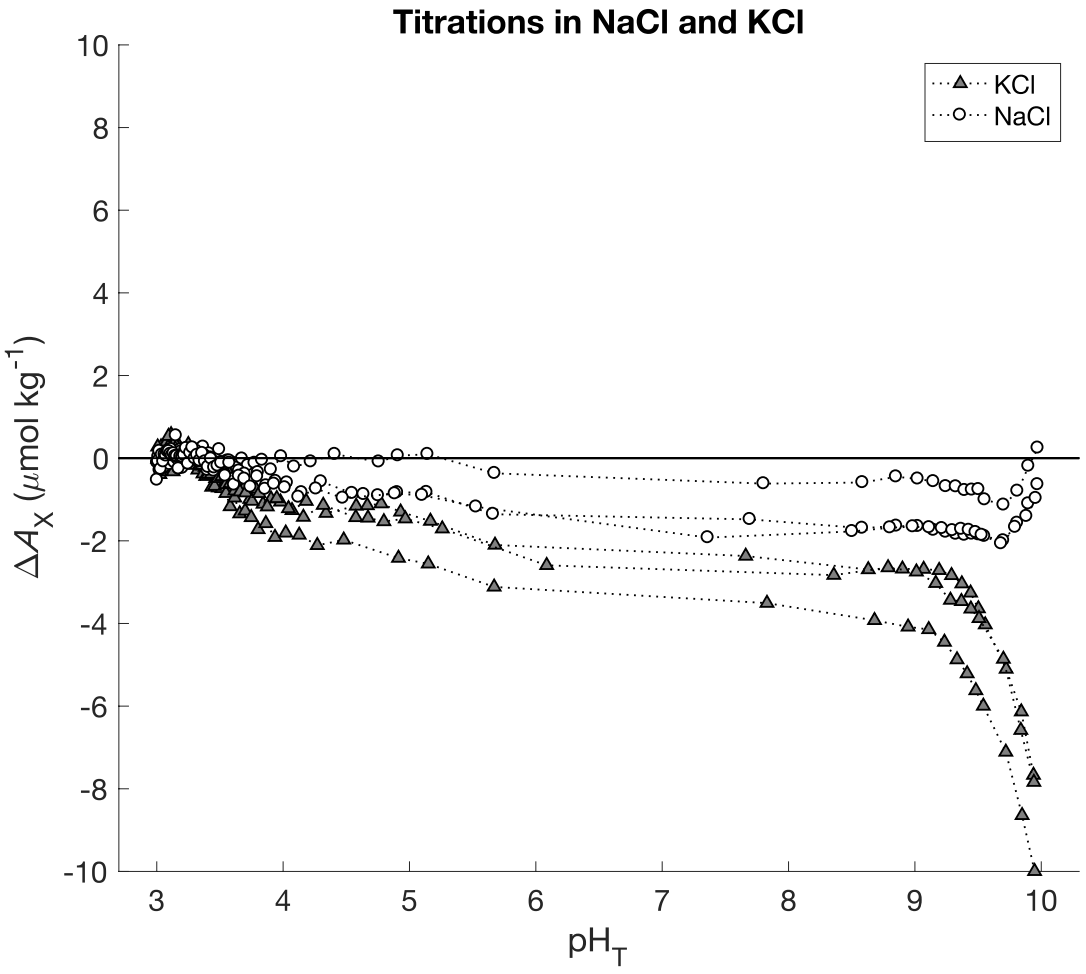

Figure 4-1 ΔA_X in titrations of 0.7 mol kg^{-1} solutions of NaCl (n = 3) and KCl (n = 3), calculated using $C_{T,degas}$ = 3.5 µmol kg^{-1} (the value measured for seawater in Chapter 3) and measured at 20 °C.

The only identified alkalinity components in these two solutions were silicate that has leached from the glass during storage (which was estimated from independent measurements of

total dissolved silicate), and C_T from contact of the solution with air although most of this should have been removed during the degassing. Considering, therefore, the uncertainty of the titration system (~2.3–3.4 μmol kg^{-1} from pH_T 4–8) these titrations are showing that the system does indeed works. It is striking that for both NaCl and KCl, the curves are just below zero for the entire titration pH_T range, suggesting (at lower pH_Ts) that the value of C_T chosen may be too high. This is likely, because the $C_{T,degas}$ used to process the titration data (Eq. 3-16) was originally measured in seawater, and the simple salt solutions used here started out with little to no alkalinity and little C_T. It is therefore likely that after the de-gassing period of 45 minutes the final C_T was lower than had been found in seawater. Using different $C_{T,degas}$ inputs during data processing suggested that more appropriate $C_{T,degas}$ for the NaCl and KCl solutions would be 3 and 1 μmol kg^{-1}, respectively. Unfortunately, this was not tested as there was no access to a working C_T measurement system available to me at the time of this discovery.

Nearing a pH_T of 10 both ΔA_X curves start to deviate, increasing for NaCl and decreasing for KCl. As noted earlier (in Figure 3-8) this is where any uncertainty due to K_W really starts to show up, suggesting that this deviation could, perhaps, be caused by a slight error in the K_W used. The value measured by Harned and Hamer (1933) was used for KCl, and that by Harned and Mannweiler (1935) for NaCl. In the higher pH_T range, i.e., well beyond the equivalence point, one can use Gran function Eq. 4-3 which is similar to the approach described in 3.4.1.4, to calculate K_W (Gran 1952). Eq. 3-20 can be rearranged to represent [OH^-] instead of [H_T^+] since

$$[OH^-][H_T^+] = K_W$$

Eq. 4-1

$$[\mathrm{OH}^-] = \frac{K_W}{\exp\left(\frac{E - E^\circ}{RT/F}\right)} = K_W \exp\left(\frac{E^\circ - E}{RT/F}\right)$$

Eq. 4-2

F_2 can then be fitted linearly against m(NaOH) as for F_1, and solved for the intercept value of $m(\mathrm{NaOH})_i$ at the point where the analytical concentration of [OH^-] is zero relative to the equivalence point ($m(\mathrm{NaOH}_{eq})$).

$$F_{2,i} = \left(m_0 + m(\mathrm{HCl})_\mathrm{T} + m(\mathrm{NaOH})_i\right)\exp\left(\frac{-E_i}{RT/F}\right)$$

Eq. 4-3

Since E° is known, K_W can be calculated as the mean of the $K_{W,i}$ calculated at each titration point according to **Eq. 4-4**:

$$K_{\mathrm{W},i} = \frac{C(\mathrm{NaOH})(m(\mathrm{NaOH})_i - m(\mathrm{NaOH})_{\mathrm{eq}})}{\left((m_0 + m(\mathrm{HCl})_\mathrm{T} + m(\mathrm{NaOH})_i\right)}\exp\left(\frac{E_i - E^\circ}{RT/F}\right)$$

Eq. 4-4

The resulting ΔA_X curves using the estimate of K_W obtained directly from the titration are shown in Figure 4-2, where K_W was calculated in the range where F_2 was linear. This example shows that the deviations from a straight line have been reduced in the case of KCl, or reversed direction in the case of NaCl. What these measurements show is that while the system is operating within the estimated precision (2.3 μmol kg^{-1}; Figure 3-10), K_W is likely not known well enough to establish a high level of accuracy of data collected in the higher pH_T range.

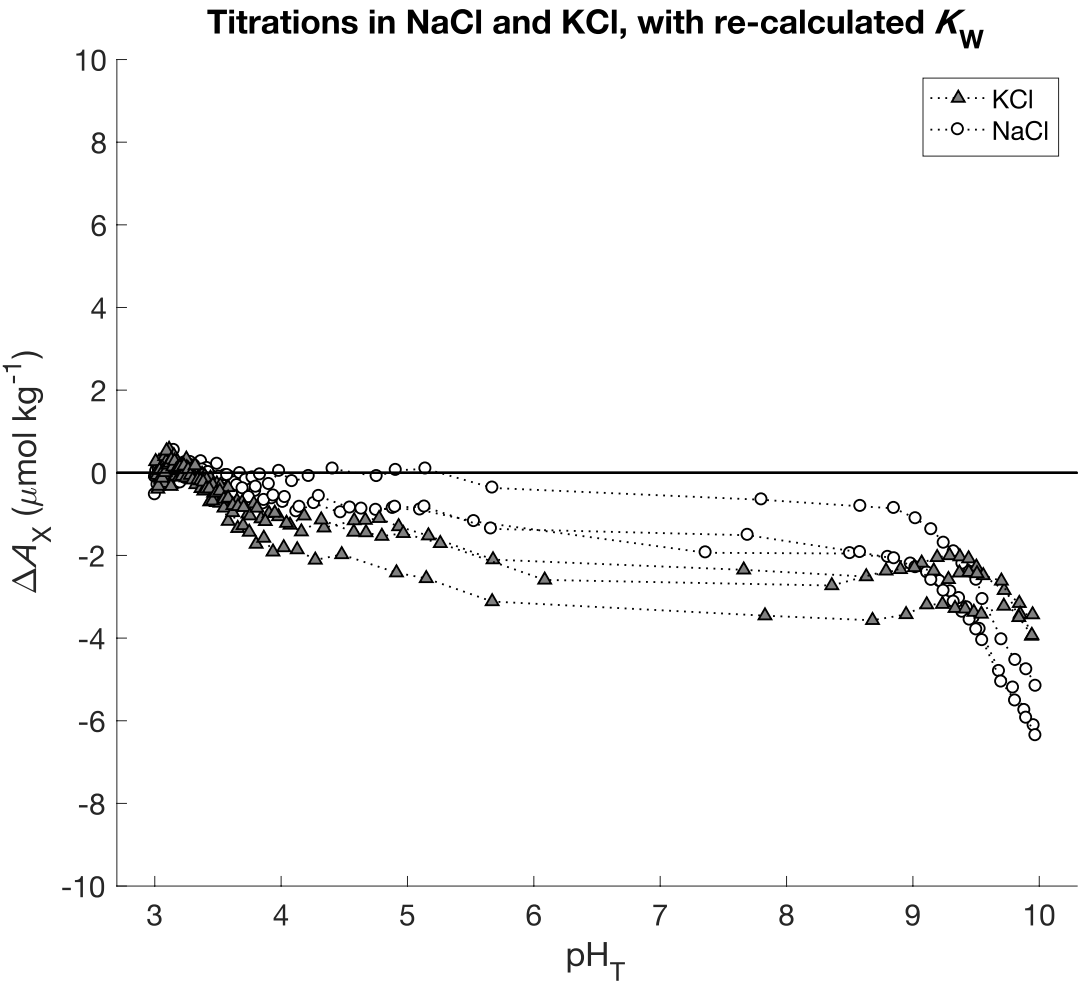

Figure 4-2 ΔA_X in titrations of 0.7 mol kg^{-1} solutions of NaCl (n = 3) and KCl (n = 3), using $C_{T,degas}$ = 3.5 µmol kg^{-1}, and re-calculating K_W from the titration data.

In this case, the K_W by Harned and Mannweiler (1935) for NaCl was 13.852 at 20 °C for the given amount content of NaCl, while the K_W calculated using Eq. 4-4 was 13.840 ± 0.003. Similarly, for KCl Harned and Hamer (1933) measured a pK_W of 13.887 while the same value calculated from our titration data was 13.895 ± 0.04. For both salt solutions, a change in pK_W of ~0.01 changed the ΔA_X curve of more than 5 µmol kg^{-1} above pH$_T$ 9, and this level of disagreement of the calculated K_W and the value found in literature is in line with the reported measurement uncertainty for K_W. This set of titrations shows that an error in K_W is likely to

decrease the quality of the data in the higher pH_T range well before the "alkali error" can affect the pH_T measurement cell.

4.1.2 The effect of the formation of magnesium hydroxides

That the formation of magnesium hydroxides and precipitation of $Mg(OH)_2$ can affect the balance of hydroxide ions in a solution during titration has been pointed out previously in section 3.4.4.3, and could also contribute to setting an upper pH_T titration limit. To test this, $MgCl_2$ was added to the 0.7 mol kg^{-1} NaCl solution at a similar level that one might expect to find in seawater (~0.05 mol kg^{-1}). The resulting solution was titrated and the effect on the titration curve is shown in Figure 4-3, where the open circles are the same NaCl titrations as shown in Figure 4-2. By adding magnesium chloride at a high amount content relative to the total ionic strength of the solution (in this case > 7 %), it is bound to affect K_W, and the K_W used for pure NaCl solutions is not be appropriate. Therefore, K_W was calculated for the $MgCl_2$-spiked NaCl solution in the same manner as in the previous section, and the resulting titration curve is shown in the filled grey circles. The resulting pK_W was 13.504 ± 0.002, more than 0.3 units lower than for a NaCl solution of comparable ionic strength. When K_W in seawater has been determined, this has been in the presence of magnesium (as well as the other major ions, see e.g., Dickson and Riley 1979). Therefore, the formation of dissolved $MgOH^+$ should be reflected in the K_W while the beginning of the precipitation of $Mg(OH)_2$ might not be. As such, it would make sense that a drop in the ΔA_X curve and suggests OH^- is being removed form the solution by precipitation of $Mg(OH)_2$. An increase of A_X of no more than 1 μmol kg^{-1} was observed at $pH_T = 8$, suggesting perhaps a small impurity in the $MgCl_2$ salt but well within the limits of the uncertainty of the system.

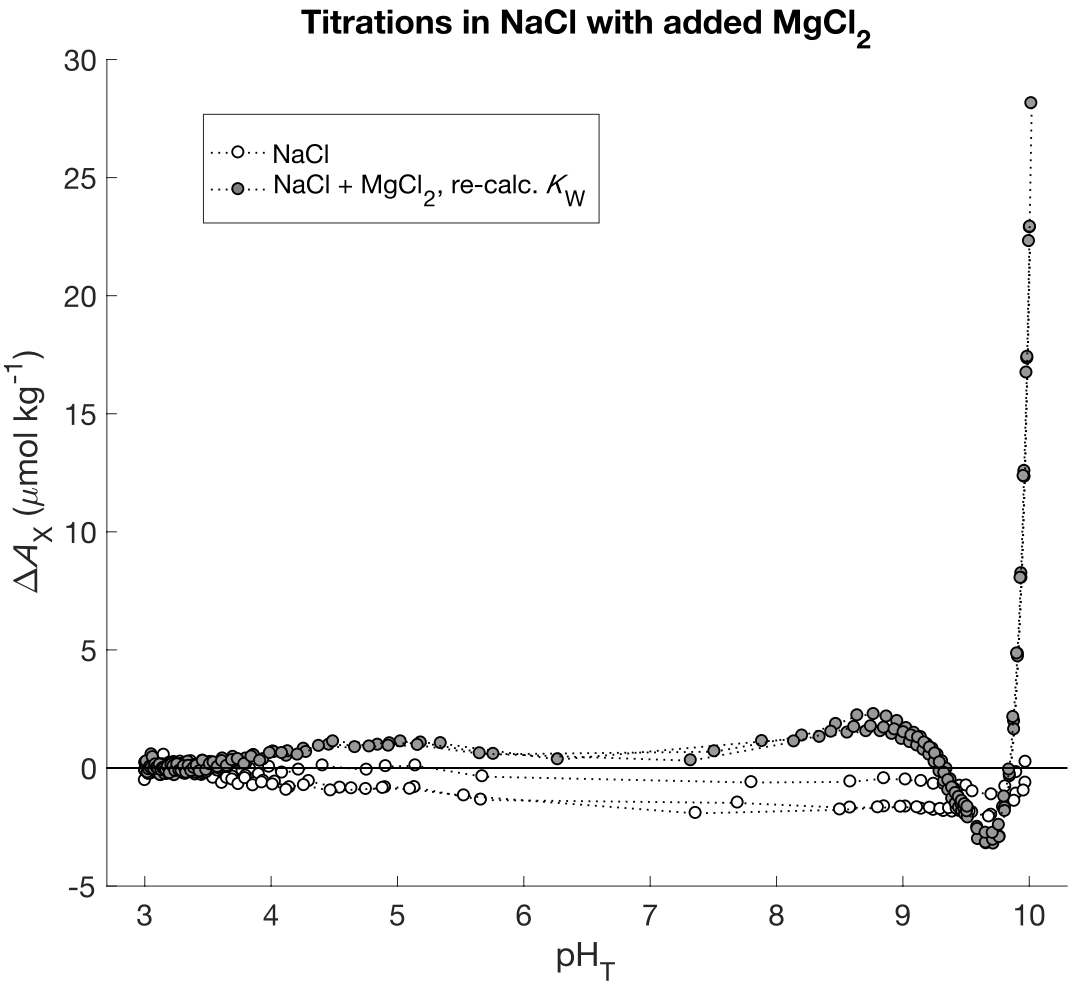

Figure 4-3 The effect of $MgCl_2$ on the titration of NaCl, including the ΔA_X curve when K_W was re-calculated in the presence of magnesium, yelding a pK_W of 13.504 ± 0.002.

The key points from these initial sets of titrations in "simple salt" solutions are a) the alkali error is unlikely to be relevant as the effects of an uncertainty in K_W will be apparent at a much lower pH_T and b) error from the precipitation of $Mg(OH)_2$ will likely show in the titration curve, possibly earlier than pH_T of 9.4. These results confirm the modelling efforts and uncertainty assessments performed in the previous chapter, and sets an upper practical pH_T limit of 9.4, but noting a chance of decreased data quality as early as pH_T 9 due to uncertainty in K_W.

4.1.3 Repeatability of the titration system

The titration method described in the previous chapter should have a repeatability of 2.3 μmol kg^{-1} at pH_T of 8 due to random errors in titrant mass and E, in addition to an accuracy of 3.4 μmol kg^{-1} from the addition of systematic errors.

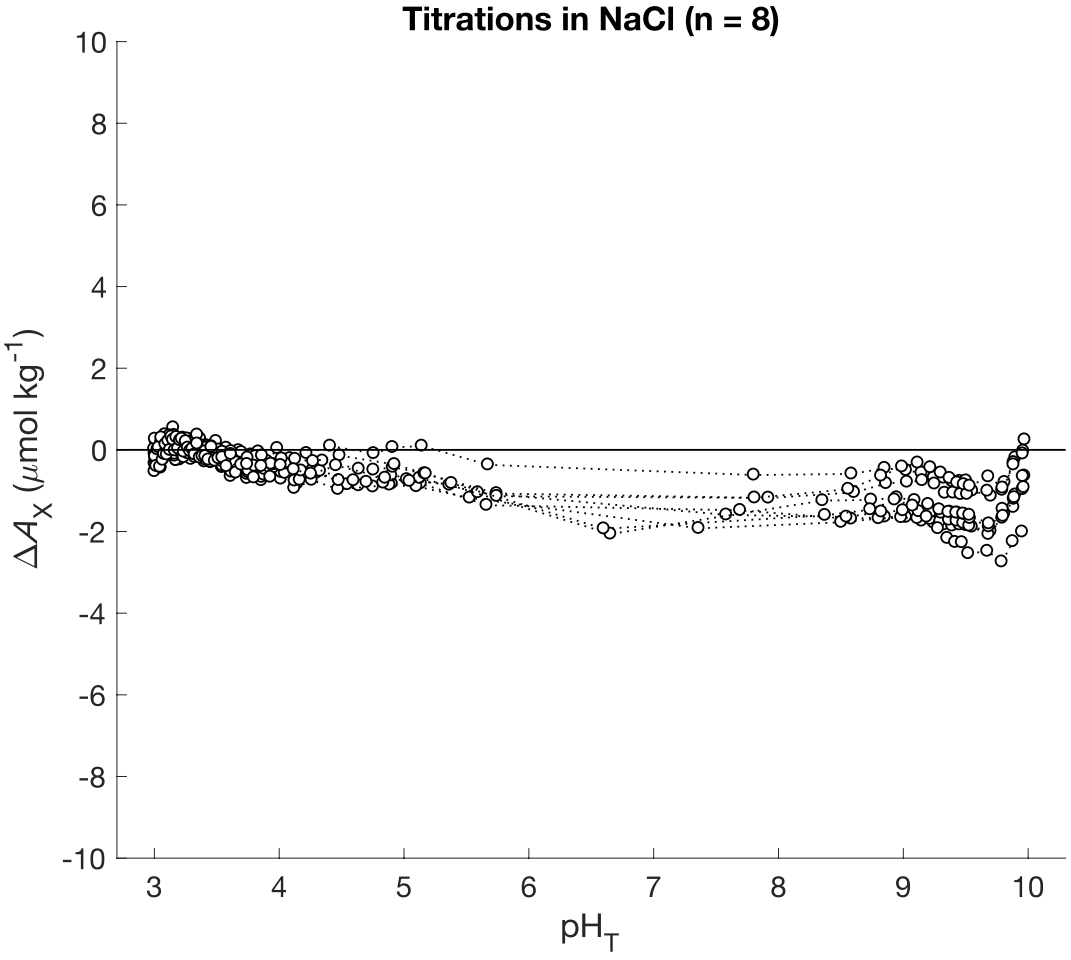

Figure 4-4 The ΔA_X curves for octuplicate titrations in the NaCl solution in one single day, using $C_{T,degas}$ = 3.5 μmol kg^{-1} and without re-calculating K_W.

To test that the method holds up to these specifications, eight titrations were performed in the 0.7 mol kg^{-1} NaCl solution (the triplicates shown above are amongst these replicates), together with six titrations in seawater that was expected to have little to no A_X. For the NaCl solution,

expected to have zero unidentified alkalinity components, Figure 4-4 shows that the titration curves below pH_T ~9.4 are within 2 μmol kg^{-1} of one another, showing that the repeatability of the system within one day is as good as, or better than expected.

The seawater used for these initial analyses was collected from the Scripps seawater system near the SIO pier, which coarsely filters water sampled near the end of the pier and delivers it to an accessible spigot. Five gallons were collected in a clean plastic jug, and this was filtered into another plastic jug through 0.45 μM polycarbonate filters. The filtered seawater sat in the plastic jug for over a month with the cap loosely on before being analyzed, and its salinity measured 33.63 using a densimeter (method described in section 4.3.2). A total of six titrations were made over the course of a day, and the resulting ΔA_X curves are shown in Figure 4-5 which also includes the overall uncertainty calculated in Chapter 3 (shown in Figure 3-11 as the positive uncertainty only) and accounts for the silicate in the sample at the time of the measurement (Si_T). As is evident, the six titrations fall well within the estimated error envelope, and until a pH_T of approx. 8.5 the ΔA_X ranges from 0–2 μmol kg^{-1}. At the higher pH_T values, errors associated with pK_W (estimated at 0.01) dominate the error curve in Figure 4-5.

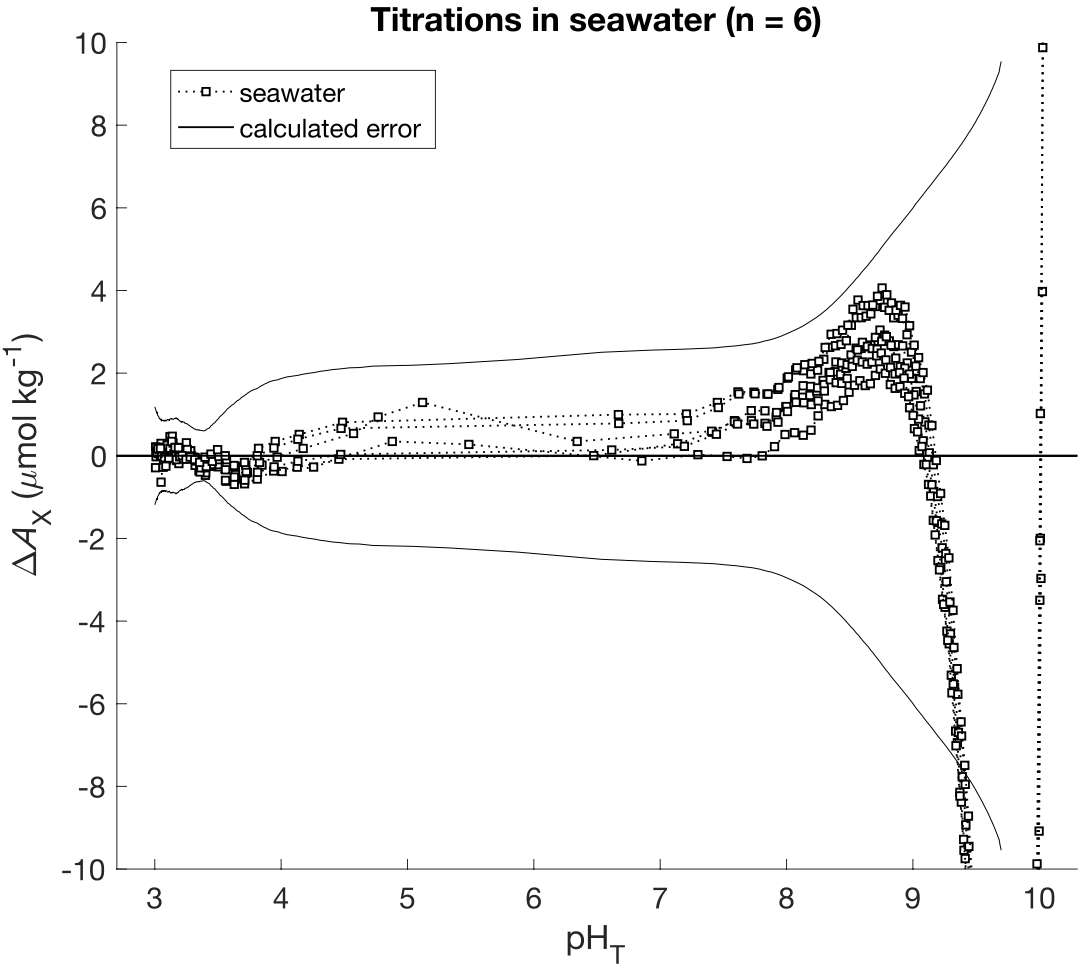

Figure 4-5 The ΔA_X curves for sextuplicate titrations in the low-nutrient seawater sample in one single day, showing the error calculated in section 3.5.

From pH_T 8.5–9 there is a distinct increase in ΔA_X, after which it drops rapidly about –35 μmol kg^{-1} (outside the range of the plot), before it starts to increase again just before pH_T 10. There are three likely explanations for these phenomena, and chances are that neither one of them alone can fully explain the ΔA_X curve behavior. First, as was just discussed the formation of $Mg(OH)_2$ precipitate is likely to remove hydroxides from solution and produce the drop in apparent A_X. Figure 4-6 shows the titration of the NaCl solution with added $MgCl_2$ overlaid the

seawater solutions, showing that while they don't fully agree in magnitude, the likely effect of precipitation of $Mg(OH)_2$ starts to appear just before pH_T 9.5 and the points of inflection in either curve agree.

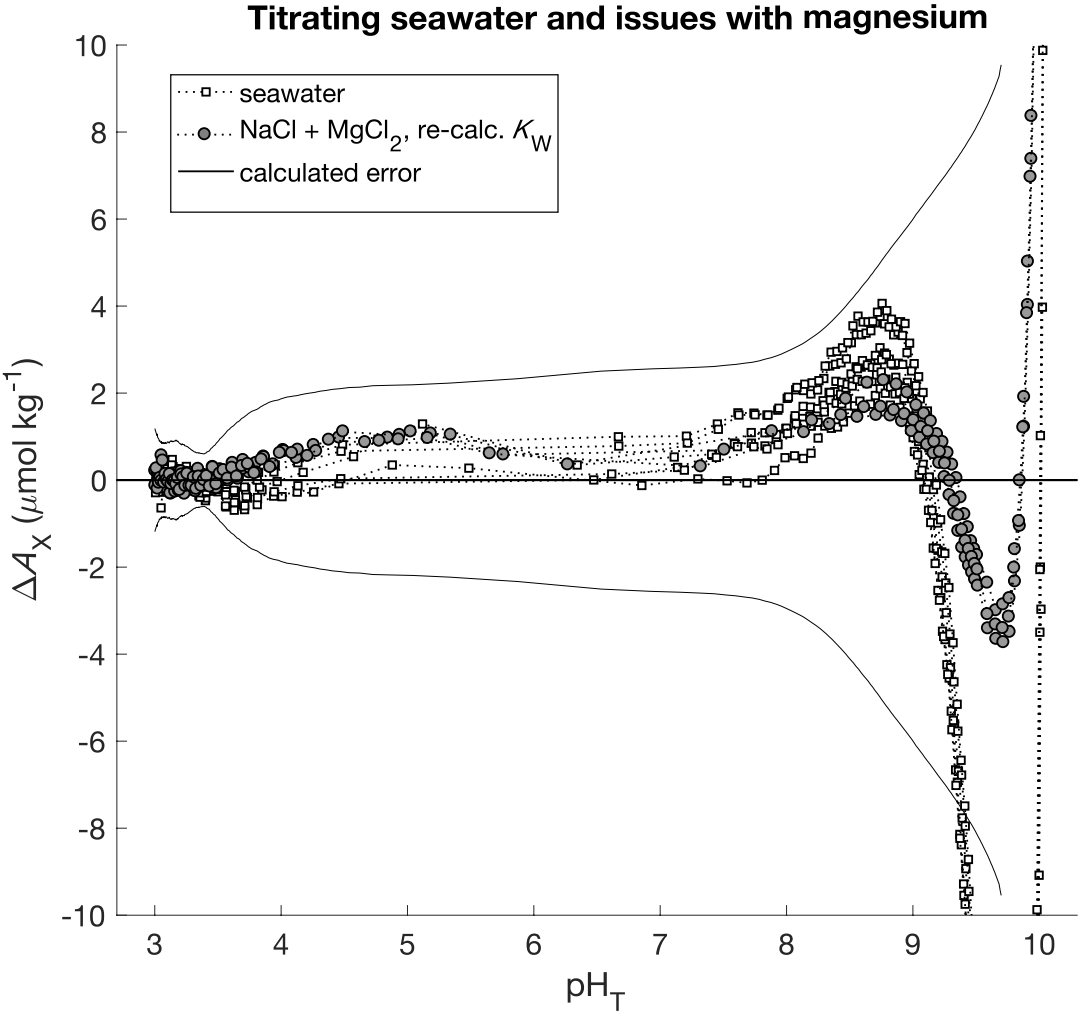

Figure 4-6 The titration of the seawater solution (n = 6) overlaid the titration of a NaCl solution with added $MgCl_2$ at a level similar to that in the seawater solution.

Next is the issue with the sensitivity of the A_X curve to errors in K_W, and the black squares in Figure 4-7 shows the effect of estimating K_W in the seawater solution using Eq. 4-4,

resulting in a pK_W of 13.175 ± 0.6 which is about 0.3 units lower than the value from Millero (1995) used in the rest of the work for seawater solutions.

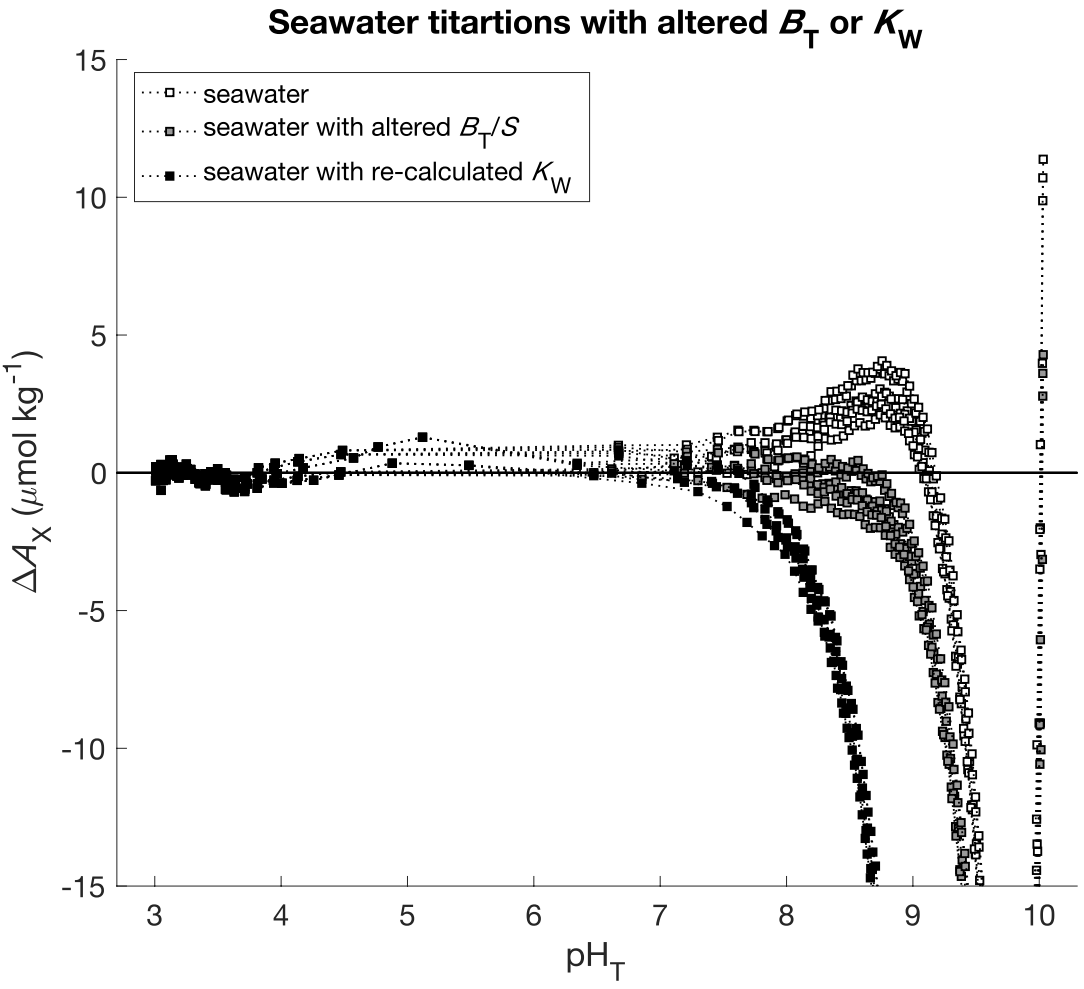

Figure 4-7 The titration of the seawater and a comparison to altering B_T/S and re-calculating K_W form the titration data.

Thirdly, and as has been mentioned earlier there is some uncertainty associated with estimating B_T from salinity. The titration data was originally processed using the B_T/S ratio from Uppström (1974), although modelling efforts by Fong and Dickson (2019) suggested that a B_T/S ratio somewhere between the two ratios by Uppström and Lee et al. might be more appropriate. The grey squares in Figure 4-7 shows the effect of using the average of these two B_T/S ratios.

These three sources of uncertainty raise questions about the data collected after a pH_T of ~9, if not a little earlier. Future research should involve a more thorough assessment of the relevant equilibrium constants in this higher pH_T range. Further, for any subsequent processing of seawater titrations in this chapter, the altered B_T/S ratio was used.

So far it is clear that the titration system can collect high-precision data in the pH_T range 3–9, and in these events where the sample acid-base chemistry has been characterized to the best of our abilities, "no A_X" appears as no A_X to within the uncertainty of the method. At least that is the hypothesis – next I shall examine adding a known amount of two different simple organic bases to both the NaCl and the seawater solution.

4.2 What does "a known amount of A_X" look like?

Two acid-base systems with well separated K_A values were chosen to represent "A_X" and were added to the NaCl and seawater solutions. These bases were potassium hydrogen phthalate (KHP) and TRIS. The pK_A of KHP has been reported as approx. 4.8 in deionized water, and is likely to increase in a salt background due to decreased activity of the hydrogen ion from interactions with salt anions. The pK_A of TRIS is 8.25 in synthetic seawater at the titration temperature of 20 °C (DelValls and Dickson 1998) and somewhat lower in 0.7 mol kg^{-1} NaCl solutions, 8.22 as measured by Millero et al. (1987) at 25 °C and thus likely to increase slightly at lower temperatures. Two separate 1 kg stock solutions of KHP and TRIS were prepared to 0.02 mol kg^{-1} in Pyrex screwcap bottles, and each base was added to the NaCl and seawater solutions to reach a total amount content of 5–10 μmol kg^{-1}. A total of six unique solutions were prepared, including a single base or a mixture, where the total amount contents of each base are shown in Table 4-1.

Table 4-1 Solutions prepared with "A_X"

Sample	$[KHP]_T$	$[TRIS]_T$
NaCl + KHP	10.3 μmol kg^{-1}	0
NaCl + TRIS	0	6.3 μmol kg^{-1}
NaCl + KHP + TRIS	10.3 μmol kg^{-1}	8.0 μmol kg^{-1}
SW + KHP	10.4 μmol kg^{-1}	0
SW + TRIS	0	5.9 μmol kg^{-1}
SW + KHP + TRIS	5.5 μmol kg^{-1}	5.9 μmol kg^{-1}

The resulting titration curves for 0.7 mol kg^{-1} NaCl solutions with added A_X are shown in Figure 4-8, and the ΔA_X curves clearly show that a well-defined base has been added to the "pure" NaCl solution. Additionally, one can see that one base had a lower pK_A (KHP) than the other (TRIS). The titration curves containing a mixture of the bases show two inflection points that correspond to the inflection points found in the single base curves. The same was true for the seawater solutions, as can be seen in Figure 4-9.

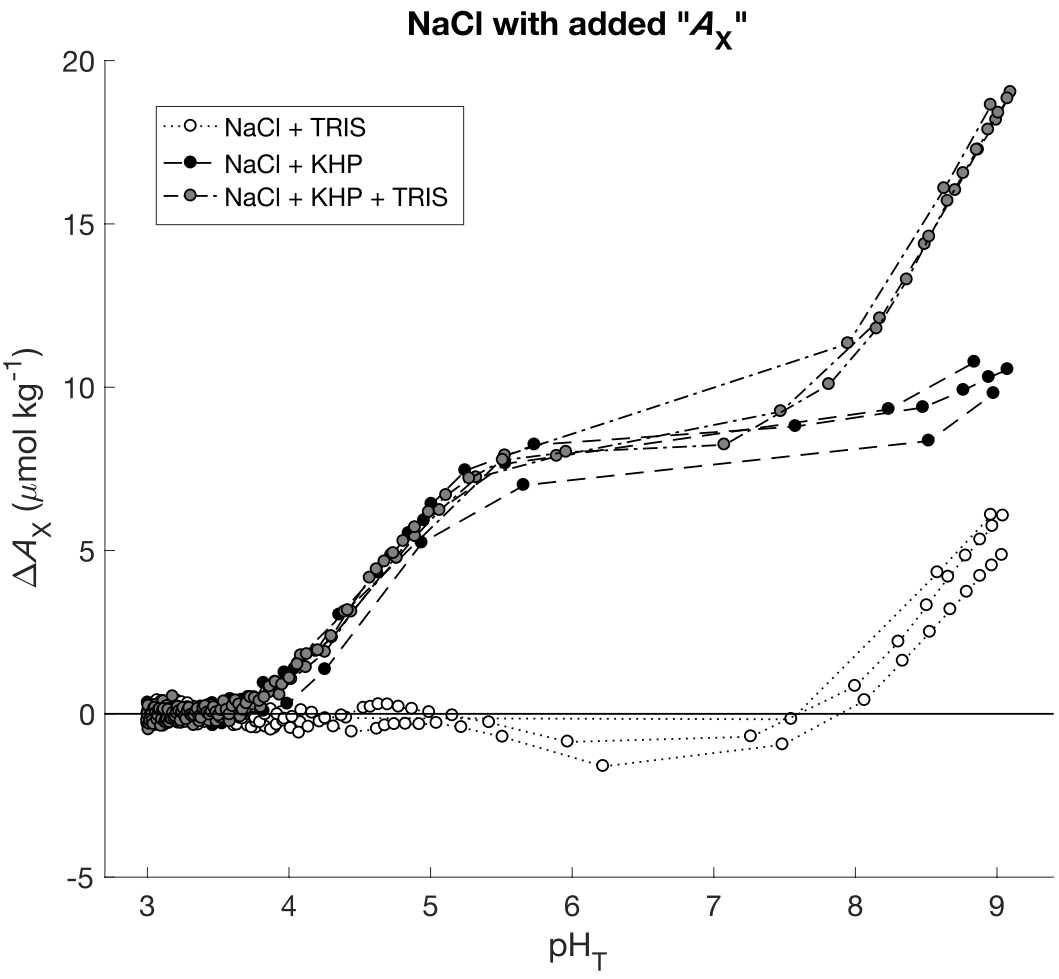

Figure 4-8 Measured ΔA_X in the NaCl solution with added A_X in the form of either KHP, TRIS, or a mixture (n = 3 for each).

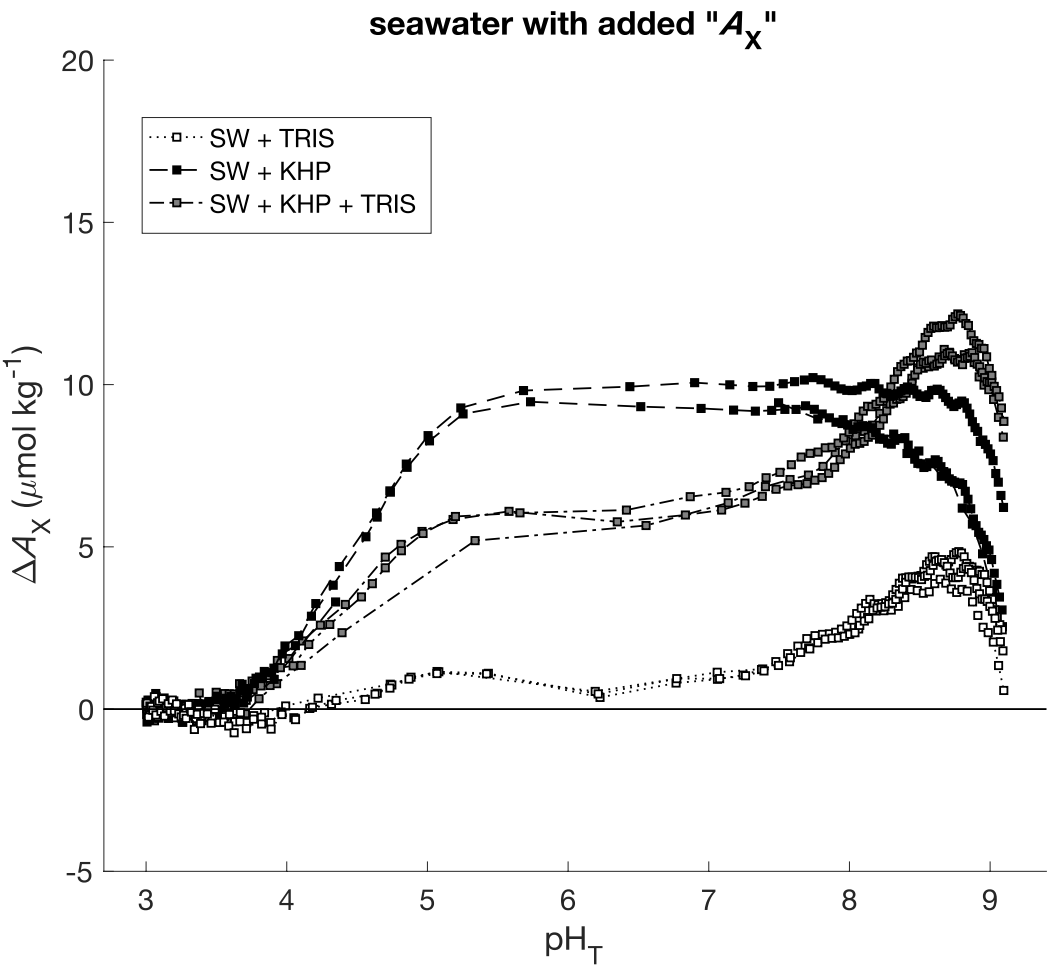

Figure 4-9 Measured ΔA_X in the seawater solution with added A_X in the form of either KHP, TRIS, or a mixture (n = 3 for each).

However, the actual A_X of the solution will not be the total amount of base added, but rather the amount content of the base species at a given pH_T. For simplicity, a pH_T of 8 is used as the "initial pH_T" of either solution, and the A_X of the sample caused by the addition of KHP and TRIS can be calculated according to Eq. 4-5 using the total amount contents listed in Table 4-1.

$$A_X = \frac{[KHP]_T}{1+[H_T^+] / K_{KHP}} + \frac{[TRIS]_T}{1+[H_T^+] / K_{TRIS}}$$

Eq. 4-5

A_X of the sample at $pH_T = 8$ was calculated by linearly interpolating the ΔA_X curve using Eq. 3-18. Table 4-2 shows that there is excellent agreement between the measured and calculated A_X of these simple solutions, where the disagreement is 1.5 μmol kg^{-1} or better!

Table 4-2 A_X in the prepared solutions of 0.7 mol kg^{-1} NaCl and *S* ~33.6 seawater

Sample	Calculated A_X at $pH_T = 8$	Measured A_X at $pH_T = 8$
NaCl + KHP	10.3 μmol kg^{-1}	9.7 ± 1.7 μmol kg^{-1}
NaCl + TRIS	2.4 μmol kg^{-1}	2.0 ± 2.6 μmol kg^{-1}
NaCl + KHP + TRIS	13.4 μmol kg^{-1}	14.6 ± 2.7 μmol kg^{-1}
SW + KHP	10.4 μmol kg^{-1}	8.9 ± 1.0 μmol kg^{-1}
SW + TRIS	2.3 μmol kg^{-1}	2.9 ± 0.1 μmol kg^{-1}
SW + KHP + TRIS	7.7 μmol kg^{-1}	8.6 ± 0.5 μmol kg^{-1}

What Chapter 4 has shown us so far is that the titration system used here can unambiguously identify if there are unidentified acid-base components, the method has a better repeatability than expected, and can estimate A_X at a given pH_T value to within the uncertainty limit of 3.4 μmol kg^{-1}. Of course, the titration method will only be an unambiguous measurement of A_X if all identified alkalinity components have been appropriately accounted for, and all mechanical aspects are within the uncertainty limits previously discussed (for example, that the automated burettes and voltage measuring system are of the quality used here).

In the event that the above-statements are true, the titration system will be able to measure A_X successfully in real seawater samples. A small set of examples will be shown in the next section.

4.3 A_X in real seawater samples

A set of samples were collected as part of a research cruise facilitated by SIO and involved samples from five different stations near Santa Barbara. In this was included samples from three different depths, and one station was in the hypoxic Santa Barbara Basin. In addition to these, two CRMs were also titrated to compare the A_X from this titration method to those measured by Sharp and Byrne (2021).

4.3.1 Sample collection

In February 2018, as part of a SIO student run cruise (SR1802) seawater samples were collected at five stations along the coast north of Santa Barbara, CA (Figure 4-10): three depths at each station, including bottom (just above the bottom boundary layer), depth of chlorophyll max, and surface. These were collected in greased ground joint 500 mL Pyrex bottles according to best practices: rinsed three times with the sample before filling, leaving ~1 % headspace (Dickson et al. 2007). The sample was mixed with saturated $HgCl_2$ to reach a concentration of 0.05 % Hg^{2+} to halt biological activity. Samples were stored in dark boxes at ~20 °C until analysis, which amounted to a storage time of about three years.

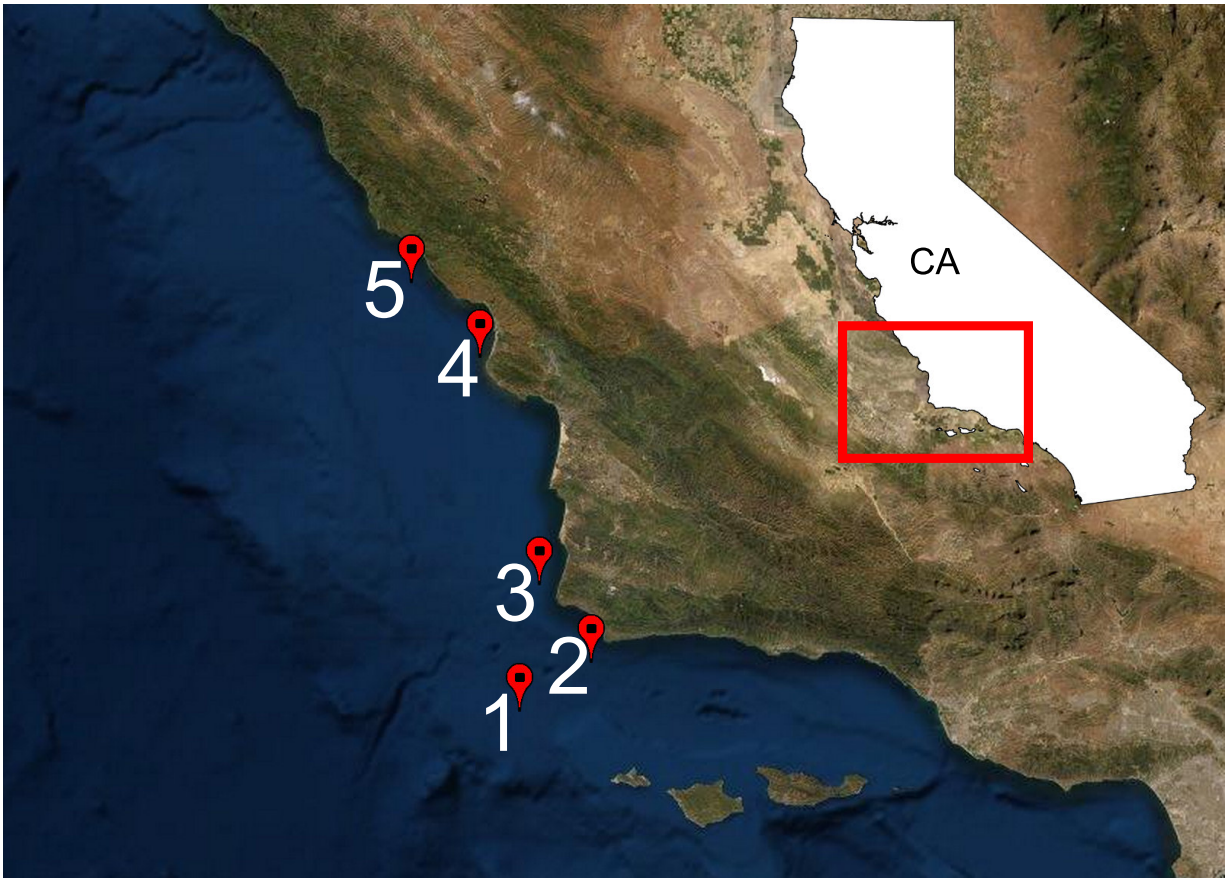

Figure 4-10 Locations for sample collection during SR1802, along the CA coast north of Santa Barbara. Numbers next to sample locations indicate station number.

4.3.2 Methods: A_X and other measurements

All samples were analyzed for A_X according to the method described in the previous chapter. In addition to this, silicate samples were collected at the time of A_X measurement and analyzed as previously described. Phosphate, nitrite, and ammonia were measured for all samples by ODF within a few weeks of sample collection. Dissolved oxygen was measured as part of the sensor package on the research vessel, and S was inferred from density measured using a Mettler Toledo DE45 Delta Range densitometer using the density-to-S equation described in the thermodynamic equation of seawater (IOC 2010).

4.3.3 Results from the coastal cruise

Unidentified protolytes appeared to be present in nearly every sample collected off the middle of the California coast, but there was not a wide range of variability in the ΔA_X curves, shown in Figure 4-11 through Figure 4-15. The mean A_X calculated for all the samples was 4.5 μmol kg^{-1} with a standard deviation of 2.5 μmol kg^{-1}, which makes them in agreement with previously published estimates of A_X for open-ocean waters including Fong and Dickson (2019) who suggested a value of A_X of 4.3 μmol kg^{-1} in the central North Pacific, and somewhat lower than the value of 8 μmol kg^{-1} suggested by Millero et al. (2002).

The main feature observed at nearly all stations and depths is a near zero or low ΔA_X from pH_T 3–6, after which the unidentified component(s) become apparent. This is unlikely to be an artefact of the measurement method since the waters from the surface and chlorophyll max at station 1 had zero ΔA_X until a pH_T of ~8 (Figure 4-11). Visually, this unidentified component that seem to be present in all samples, save two, appears to have a pK_A of approx. 6.5. Here it should be noted that hydrogen sulfide in seawater has a pK_A of ~6.5 (Millero et al. 1988). Because total sulfide was not measured one cannot discount that some or all of this A_X was composed of hydrogen sulfide, especially considering the fact that these water masses are all in or near an oxygen minimum zone (Sigman et al. 2003). On the other hand, the two samples without evidence of a protolyte with such characteristics had the lowest oxygen amount contents out of any unique samples (Figure 4-11).

Table 4-3 Measured A_X at the initial pH_T of the sample at each station and depth, corresponding oxygen amount content ($[O_2]$) for each unique sample at the time of sample collection, and Si_T measured at the time of A_X analysis.

Station-depth	A_X (μmol kg^{-1})	$[O_2]$ (μmol kg^{-1})	Si_T (μmol kg^{-1})
St 1–surface	2.3	249	31
St 1–Chl max	0.7	98	52
St 1–bottom	1.0	15	90
St 2–surface	5.9	247	49
St 2–Chl max	4.5	240	31
St 2–bottom	3.9	200	36
St 3–surface	3.4	256	39
St 3–Chl max	6.3	256	39
St 3–bottom	2.4	115	33
St 4–surface	7.3	240	43
St 4–Chl max	4.5	236	33
St 4–bottom	4.8	184	202
St 5–surface	4.8	252	29
St 5–Chl max	4.6	249	31
St 5–bottom	10.5	207	31

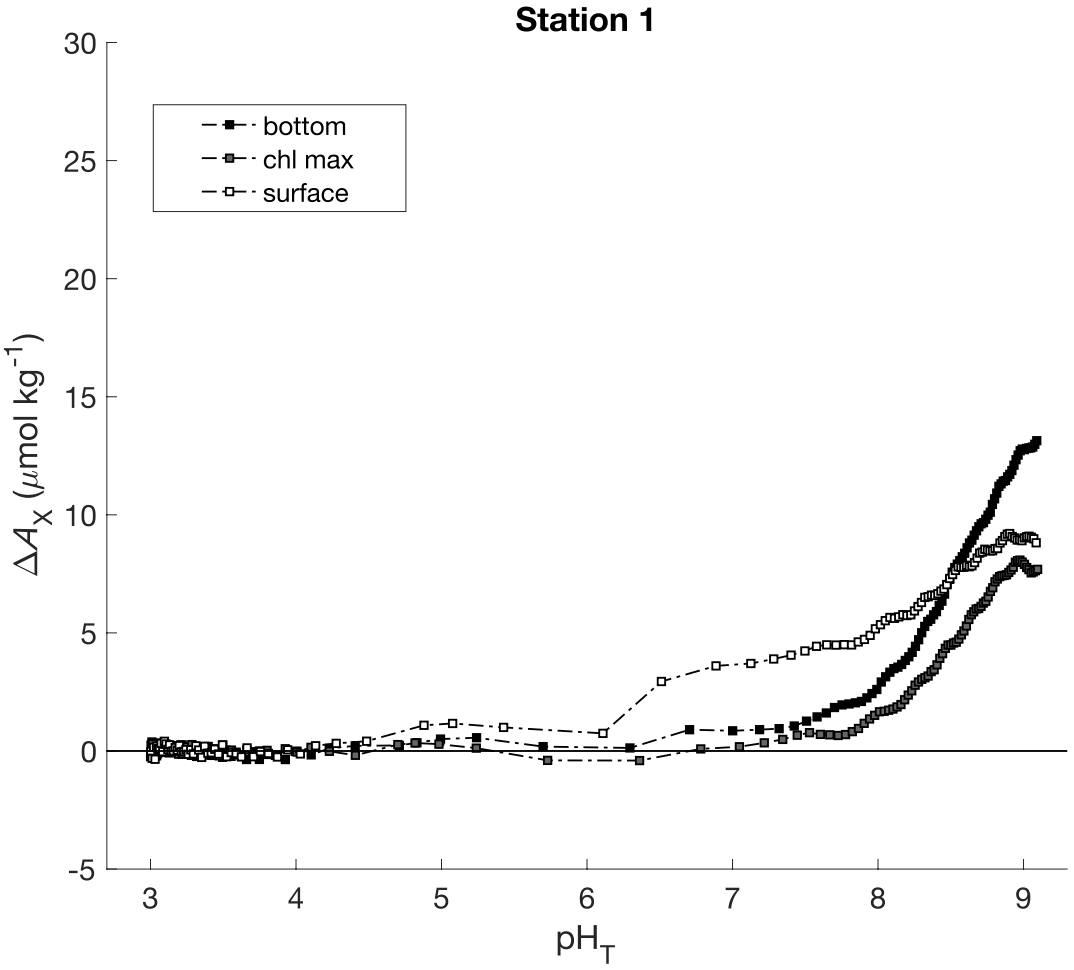

Figure 4-11 ΔA_X curves for station 1 during cruise SR1802, showing the A_X curve for the samples collected at the surface, chlorophyll max (Chl-max) and the bottom boundary layer.

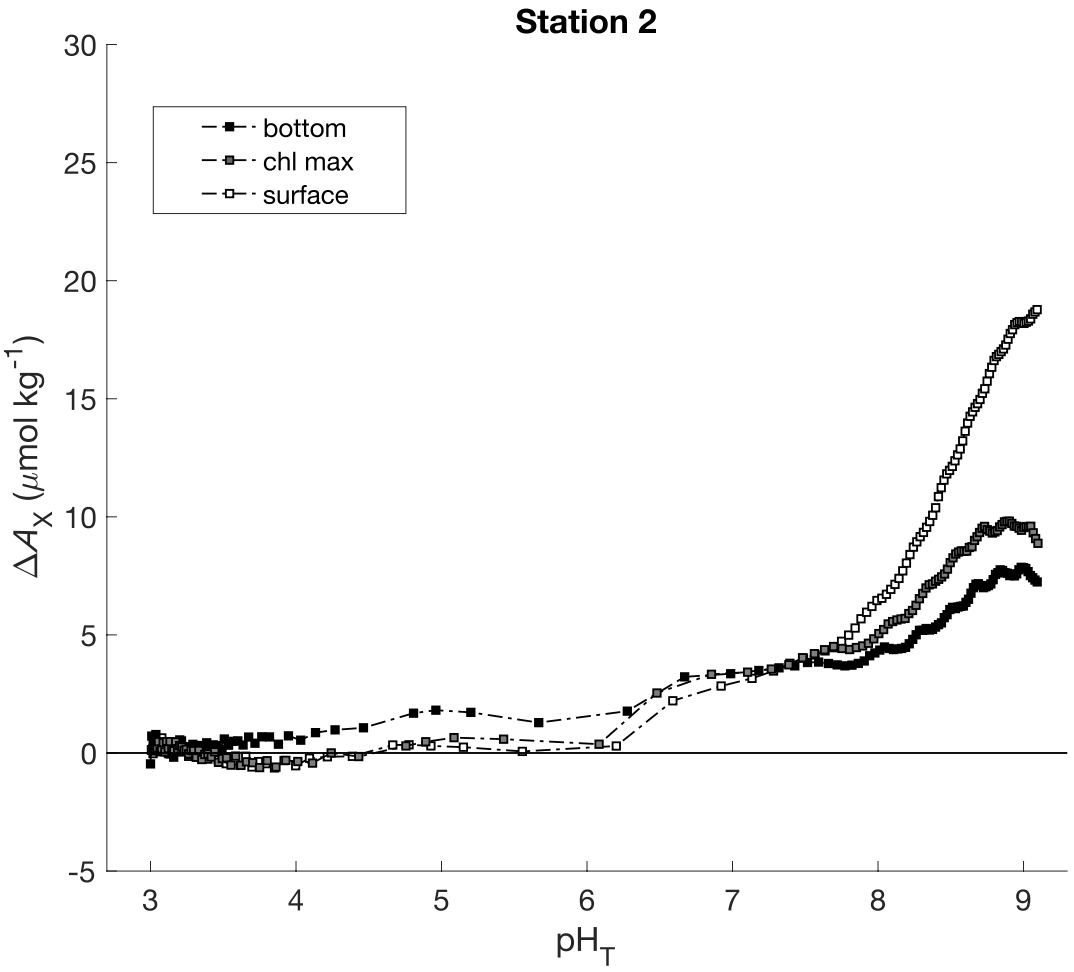

Figure 4-12 ΔA_X curves for station 2 during cruise SR1802, showing the A_X curve for the samples collected at the surface, chlorophyll max (Chl-max) and the bottom boundary layer.

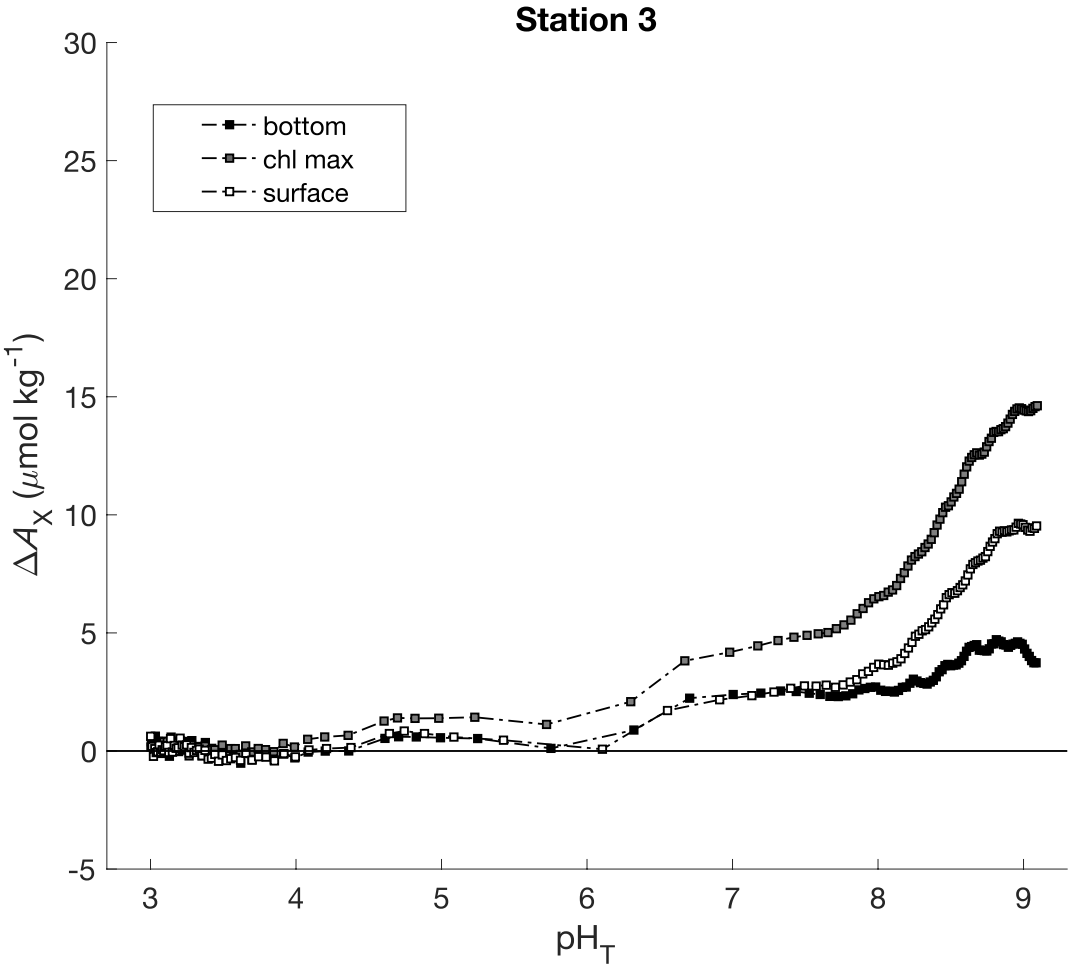

Figure 4-13 ΔA_X curves for station 3 during cruise SR1802, showing the A_X curve for the samples collected at the surface, chlorophyll max (Chl-max) and the bottom boundary layer.

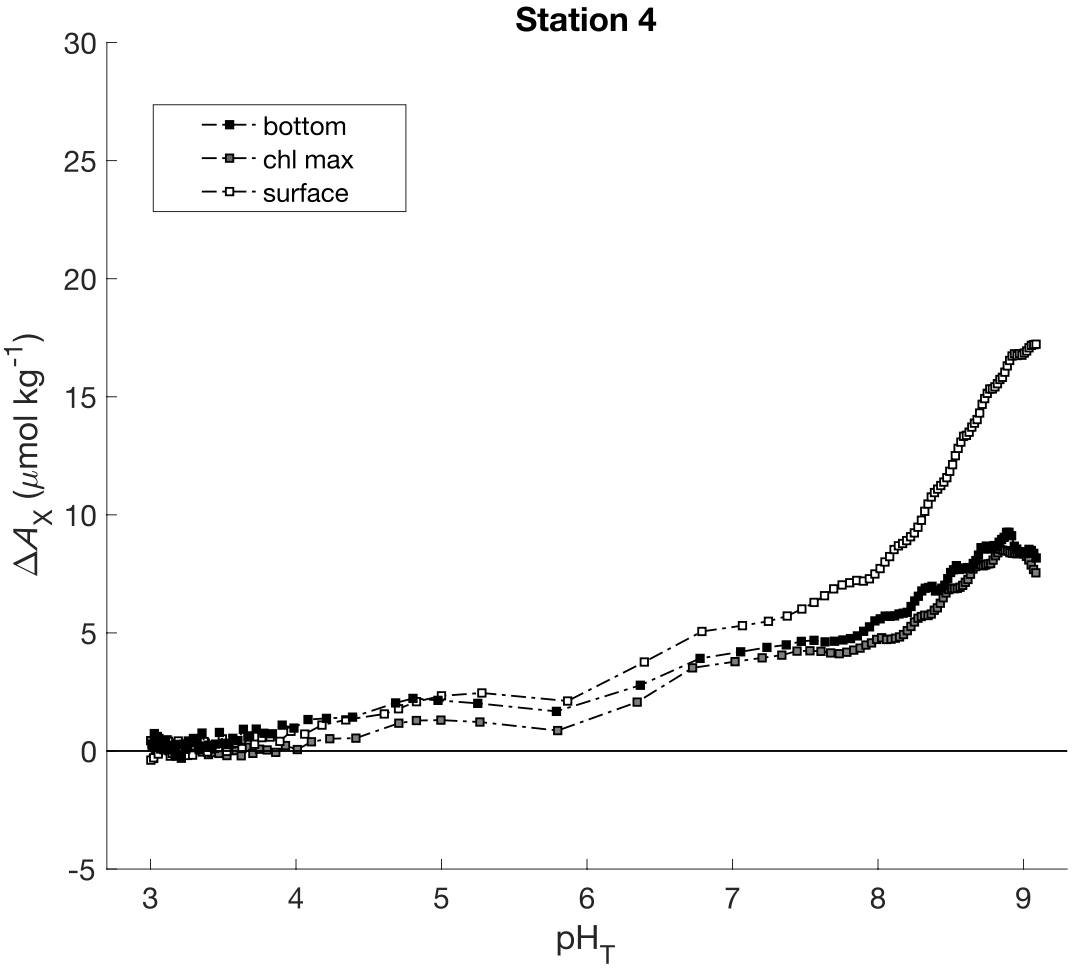

Figure 4-14 ΔA_X curves for station 4 during cruise SR1802, showing the A_X curve for the samples collected at the surface, chlorophyll max (Chl-max) and the bottom boundary layer.

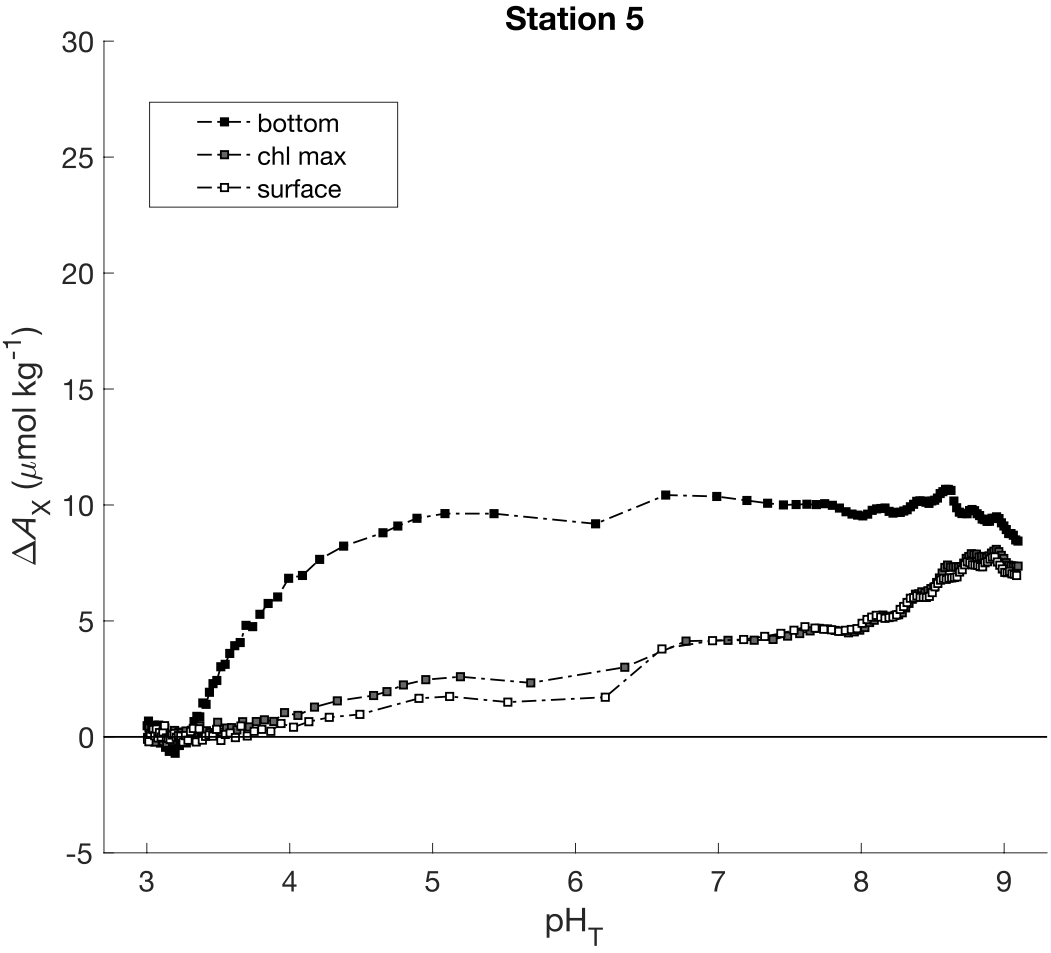

Figure 4-15 ΔA_X curves for station 5 during cruise SR1802, showing the A_X curve for the samples collected at the surface, chlorophyll max (Chl-max) and the bottom boundary layer.

Further, all samples showed a rapid increase in ΔA_X after pH_T 8. This is somewhat in agreement with the observations for the low-nutrient seawater analyzed in the previous sections (see, e.g., Figure 4-5), although a few samples in have an even more dramatic increase towards the higher pH_T values, including the surface seawaters at station 2 (Figure 4-12) and 4 (Figure 4-14). One sample that stands out is the bottom water sample from station 5 (Figure 4-15), where there appears to be an unidentified protolyte with a pK_A of near 4 (in addition to the

omnipresent unidentified component of pK_A of 6.5). Many smaller carboxylic acids have a pK_A around 4 (Reusch 2020) and it is not unlikely that this is evidence for an organic acid in this particular sample.

4.3.4 Results in the CRMs

Sharp and Byrne (2021) published measurements of A_X in two batches of reference materials that was also accessible to me from our laboratory, namely CRM-176 and CRM-183. To them this was part of measuring K_B spectrophotometrically and the while the method was not as rigorously tested for A_X measurements as the method presented in this dissertation, it is currently the only two samples available to compare between laboratories. They calculated an A_X in CRM-176 of 10 or 2.5 μmol kg^{-1}, and in CRM-183 7.5 or 0 μmol kg^{-1} using the B_T/S by Uppström (1974) or Lee et al. (2010), respectively. To that end, using the average of the two values will be appropriate for comparison to the measurements made herein, meaning an A_X of CRM-176 of 6.2 μmol kg^{-1} and for CRM-183 an A_X of 3.8 μmol kg^{-1}.

The A_X measured in the only sample of batch 176 that was available was a staggering 157 μmol kg^{-1}, and sadly only two measurements were made possible because of the quantity available. The concurrently measured A_T was approximately 150 μmol kg^{-1} higher than the certified value in both duplicates (2374 vs 2224 μmol kg^{-1}), suggesting that a chemical alteration had occurred in the sample after bottling. Seeing as both measurements from the same bottle showed the near identical ΔA_X curves (Figure 4-16), it is likely that an unaccounted for protolyte was present. One possible explanation could be contamination of borate, as the pK_A suggested by the titration curve, ~8.5, is very close to the pK_B of 8.66 at the salinity and measurement temperatures of these CRMs. To explain the titration curve however, a B_T of more

than 1,300 μmol kg^{-1} would be needed. Such a large amount of borate is unlikely to originate in the marine environment, and would be better explained by contamination that occurred during bottling. The soap used in our laboratory for cleaning bottles used for CRMs does not contain borax, and although it does contain a low level of other organic acids their reported pK_As are not obvious in the titration curve (IPC 2020). Further, the Si_T measured in this particular bottle was outside the normal measurement range, at ~330 μmol kg^{-1}, which suggests that some glass had dissolved over time and contaminated the sample (Si_T at the time of bottling was 1.7 μmol kg^{-1}). For batch 183 the measured A_X was significantly lower than for batch 176, at 23.5 μmol kg^{-1} (and with a similar increase in A_T relative to the certified value) and also with a lower amount of silicate, with a Si_T of 163 μmol kg^{-1}. The two batches were bottled nearly a year apart, CRM-176 in May of 2018 and CRM-183 in March of 2019. The samples collected along the CA coast had similarly been sitting in storage for over three years at the time of analysis. Both CRM bottles did show signs of an unidentified protolyte with a pK_A of ~4.5 although at a very low level of approx. 2.5 μmol kg^{-1} which is just at the limit of detection of this method but unlikely to be a product of random error.

Clearly, the measurements made by Sharp and Byrne (2021) and those made here do not agree very well, except for the fact that both methods indicate there are unidentified (or, unaccounted for) protolytes present in both batches of CRM. Further, one of the bottles analyzed (CRM 183-0808) in this laboratory had originally been opened some years prior, and thus it seems possible that some physical or biological process could have occurred that either produced an unidentified protolyte or that catalyzed the dissolution of the glass bottle in which it

was stored. Any conclusive remark on the subject is not possible, and would likely necessitate a range of measurements outside the realm of marine inorganic CO_2 chemistry.

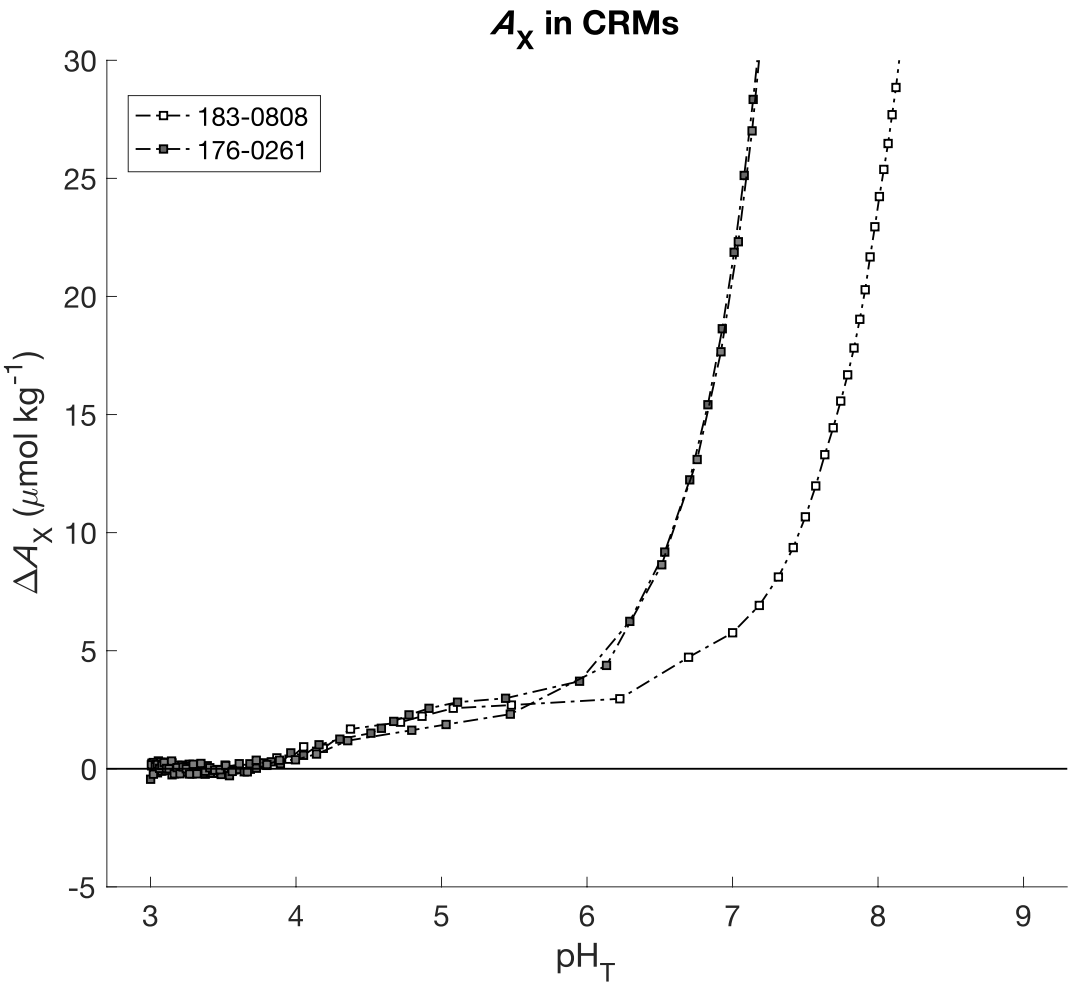

Figure 4-16 ΔA_X measured in two different batches of CRMs: 183, bottle 0808 (n = 1) and 176, bottle 0261 (n = 2).

4.4 Does the A_X titration method work?

In theory the titration method described in Chapter 3 and used in this chapter of the dissertation should able to measure the presence of unidentified protolytes, i.e., A_X, at amount contents of 3.4 μmol kg^{-1} or greater. The measurements made in the well-characterized NaCl

solution the ΔA_X curves showed a near perfectly zero-line for A_X until a pH_T of at least 10, showing that no bias is added during the titration process outside of what is accounted for in the uncertainty assessment presented in Chapter 3. These samples in concurrence with the low-complexity seawater samples, with and without added organic bases, shows that the titration method works better than expected, with standard deviation of replicates being on the order of 2.6 μmol kg^{-1} or better and measured A_X values within 1.5 μmol kg^{-1} of the calculated A_X. It should be noted that these data far exceed the hope I had of this system when the project was started over five years ago!

Now, when looking at the measurements made in the coastal samples and CRMs the performance of the titration method looks more questionable. However, at this point it is necessary to remember the previous paragraph in which the system performed nearly perfectly when the titrated solutions had spent only a limited time in storage. It is also necessary to highlight the fact that all samples collected at the student cruise, and the CRM samples, had been stored in glass bottles for over three years. Additionally, the various samples had been stored in glass bottles which likely had a range of care and cleaning histories. For example, the CRM bottles are recycled and cleaned more frequently than the bottles used to collect the samples during the cruise. Storage time and container handling history are therefore two likely culprits for contamination, and likely in the form of dissolved silicate and borate.

Moving ahead, then, it is imperative to answer the following questions before proceeding with careful sample collection for A_X measurements: a) what storage bottles are appropriate for A_X samples and b) how and for how long are they best preserved? Another side to this work will be to refine the mathematics and equilibrium modelling efforts to be able to calculate K_X values

for the unidentified protolytes. While this work was started and is in theory not too difficult, this problem proved harder to accomplish using real titration data that has some low level of noise.

For now, this work is concluded by echoing that it is possible to unambiguously measure A_X in a seawater sample using the titration method described in this dissertation. Or more precisely, **the A_X titration method will measure any protolyte not accounted for at amount contents above 3.4 μmol kg^{-1} (or perhaps even a little better), and whether such protolytes are unidentified or not cannot be determined by the titration method alone although it can provide hints at the pK_A(s) involved.**

4.5 Acknowledgements

The author would like to thank Wiley Wolfe and Todd Martz for training on and use of their C_T measurement system. The author would further like to acknowledge the crew and student participants of the student research cruise SR1802, and especially its organizers for allowing me to participate, including Angel Ruacho, Sara Rivera, Alyssa Finlay, Lauren Manck, Kiefer Forsch, Kayleen Fulton, Margot White, and Matthew A. Pendegraft. Lastly, the author would like to acknowledge all the work carried out by Canyon Breyer on boron measurements that ultimately did not make it into the dissertation, but that will be key moving forward with research on A_X.

REFERENCES

Armstrong, F. A. J., C. R. Stearns, and J. D. H. Strickland. 1967. The measurement of upwelling and subsequent biological processes by means of the Technicon Autoanalyzer(R) and associated equipment. Deep Sea Research **14:** 381-389.

Arrhenius, S. 1889. IV. Electrolytic dissociation versus hydration. The London, Edinburgh, and Dublin Philosophical Magazine and Journal of Science **28:** 30-38.

Arrhenius, S., and E. S. Holden. 1897. On the influence of carbonic acid in the air upon the temperature of the Earth. Publications of the Astronomical Society of the Pacific **9:** 14-24.

Bates, N. and others 2014. A Time-Series View of Changing Ocean Chemistry Due to Ocean Uptake of Anthropogenic CO_2 and Ocean Acidification. Oceanography **27:** 126-141.

Bates, R. G. 1961. Amine buffers for pH control. Annals of the New York Academy of Sciences **92:** 341-356.

Bates, R. G., and H. B. Hetzer. 1961. Dissociation Constant of the Protonated Acid Form of 2-Amino-2-(Hydroxymethyl)-1,3-Propanediol [Tris-Hydroxymethyl-Aminomethane] and Related Thermodynamic Quantities from 0 to 50°. The Journal of Physical Chemistry **65:** 667-671.

Bergman, T. 1784. Physical and chemical essays. J. Murray.

Bockmon, E. E., and A. G. Dickson. 2015. An inter-laboratory comparison assessing the quality of seawater carbon dioxide measurements. Marine Chemistry **171:** 36-43.

Bradshaw, A. L., and P. G. Brewer. 1988a. High precision measurements of alkalinity and total carbon dioxide in seawater by potentiometric titration. 1. Presence of unknown protolyte(s)? Marine Chemistry **23:** 69-86.

---. 1988b. High precision measurements of alkalinity and total carbon dioxide in seawater by potentiometric titration. 2. Measurements on standard solutions. Marine Chemistry **24**.

Bradshaw, A. L., P. G. Brewer, D. K. Shafer, and R. T. Williams. 1981. Measurements of total carbon dioxide and alkalinity by potentiometric titration in the GEOSECS program. Earth and Planetary Science Letters **55:** 99-115.

Bresnahan, P. J., T. R. Martz, Y. Takeshita, K. S. Johnson, and M. LaShomb. 2014. Best practices for autonomous measurement of seawater pH with the Honeywell Durafet. Methods in Oceanography **9:** 44-60.

Brewer, P. G., A. L. Bradshaw, and R. T. Williams. 1986. Measurements of Total Carbon Dioxide and Alkalinity in the North Atlantic Ocean in 1981, p. 348-370. *In* J. R. Trabalka and D. E. Reichle [eds.], The Changing Carbon Cycle: A Global Analysis. Springer New York.

Buch, K. 1933. On boric acid in the sea and its influence on the carbonic acid equilibrium. ICES Journal of Marine Science **8:** 309-325.

Buck, R. P. and others 2002. Measurement of pH. Definition, standards, and procedures (IUPAC Recommendations 2002). Pure and Applied Chemistry **74:** 2169-2200.

Butler, R. A., A. K. Covington, and M. Whitfield. 1985. The determination of pH in estuarine waters. II: Practical considerations. Oceanologica acta **8:** 433-439.

Cai, W.-J., Y. Wang, and R. E. Hodson. 1997. Acid-base properties of dissolved organic matter in the estuarine waters of Georgia, USA. Geochimica et Cosmochimica Acta **62:** 473-483.

Carter, B. R., J. A. Radich, H. L. Doyle, and A. G. Dickson. 2013. An automated system for spectrophotometric seawater pH measurements. Limnology and Oceanography: Methods **11:** 16-27.

Ciavatta, L. 1963. POTENTIOMETRIC PURITY CONTROL OF SALTS MEDIA FOR EQUILIBRIUM STUDIES-WITH AN APPENDIX ON ANALYSIS OF DILUTE SOLUTIONS OF STRONG ACIDS. ARKIV FÖR KEMI **20:** 417-&.

DelValls, T. A., and A. G. Dickson. 1998. The pH of buffers based on 2-amino-2-hydroxymethyl-1,3-propanediol ('tris') in synthetic sea water. Deep-Sea Research I **45:** 1541-1554.

Dickson, A., R. Wanninkhof, R. Feely, and J. Swift. 2018. Bottle and CTD data from cruise 320620180309. *In* CCHDO [ed.].

Dickson, A. G. 1981. An exact definition of total alkalinity and a procedure for the estimation of alkalinity and total inorganic carbon from titration data. Deep-Sea Research **28A:** 609-623.

---. 1990. Thermodynamics of the dissociation of boric acid in synthetic seawater from 273.15 to 318.15 K. Deep-Sea Research **37:** 755-766.

---. 1992. The development of the alkalinity concept in marine chemistry. Marine Chemistry **40:** 49-63.

---. 1993. pH buffers for sea water media based on the total hydrogen ion concentration scale. Deep-Sea Research I **40:** 107-118.

Dickson, A. G. 2010. The carbon dioxide system in seawater: equilibrium chemistry and measurements. Guide to best practices for ocean acidification research and data reporting **1:** 17-40.

Dickson, A. G., J. D. Afghan, and G. C. Anderson. 2003. Reference materials for oceanic CO_2 analysis: a method for the certification of total alkalinity. Marine Chemistry **80:** 185-197.

Dickson, A. G. and others 2016. Metrological challenges for measurements of key climatological observables. Part 3: seawater pH. Metrologia **53:** R26-R39.

Dickson, A. G., and J. P. Riley. 1978. The effect of analytical error on the evaluation of the components of the aquatic carbon-dioxide system. Marine Chemistry **6:** 77-85.

---. 1979. The estimation of acid dissociation constants in seawater media from potentiometric titrations with strong base. Marine Chemistry **7:** 89-99.

Dickson, A. G., C. L. Sabine, and J. R. Christian [eds.]. 2007. Guide to best practices for ocean CO_2 measurements.

Dittmar, W. 1880. Report on researches into the composition of ocean-water collected by HMS Challenger during the years 1873-76.

Easley, R. A., and R. H. Byrne. 2012. Spectrophotometric calibration of pH electrodes in seawater using purified m-cresol purple. Environmental Science & Technology **46:** 5018-5024.

Edmond, J. M. 1970. High precision determination of titration alkalinity and total carbon dioxide content of sea water by potentiometric titration. Deep Sea Research and Oceanographic Abstracts **17:** 737-750.

Fairhall, A. W. 1973. Accumulation of fossil CO2 in the atmosphere and in the sea. Nature **245:** 20-23.

Fong, M. B., and A. G. Dickson. 2019. Insights from GO-SHIP hydrography data into the thermodynamic consistency of CO2 system measurements in seawater. Marine Chemistry **211:** 52-63.

Gallego-Urrea, J. A., and D. R. Turner. 2017. Determination of pH in estuarine and brackish waters: Pitzer parameters for Tris buffers and dissociation constants for m -cresol purple at 298.15 K. Marine Chemistry.

Göbel, F. 1842. Resultate der Zerlegung des Wassers vom Schwarzen, Asowschen und Kaspischen Meere. Annalen der Physik und Chemie **131:** 187-188.

Gran, G. 1952. Determination of the equivalence point in potentiometric titrations. Part II. The Analyst **77:** 661.

Gran, G., H. Dahlenborg, S. Laurell, and M. Rottenberg. 1950. Determination of the Equivalent Point in Potentiometric Titrations. Acta Chemica Scandinavica **4:** 559-577.

Haider, D. C. 2004. Electrodes in Potentiometry. Teachware, Metrohm Ltd.

Hansson, I. 1973a. The determination of dissociation constants of carbonic acid in synthetic sea water in the salinity range of 20–40‰ and temperature range of 5–30◦ C. Acta Chemica Scandanavia **27:** 931-944.

---. 1973b. A new set of pH-scales and standard buffers for sea water. Deep Sea Research and Oceanographic Abstracts **20:** 479-491.

Harned, H. S., and W. J. Hamer. 1933. The ionization constant of water and the dissociation of water in potassium chloride solutions from electromotive forces of cells without liquid junction1. Journal of the American Chemical Society **55:** 2194-2206.

Harned, H. S., and G. E. Mannweiler. 1935. The thermodynamics of ionized water in sodium chloride solutions. Journal of the American Chemical Society **57:** 1873-1876.

Hernández-Ayón, J. M., A. Zirino, A. G. Dickson, C.-V. T-, and E. Valenzuela-Espinoza. 2007. Estimating the contribution of organic bases from microalgae to the titration alkalinity in coastal seawaters. Limnology and Oceanography: Methods **5:** 225-232.

Hofmann, G. E. and others 2011. High-frequency dynamics of ocean pH: a multi-ecosystem comparison. PLoS One **6:** e28983.

Humphreys, M. P., A. G. Dickson, D. R. Turner, and S. L. Clegg. 2020. Modelling Chemical Speciation in Seawater pH Buffers, Standard Seawater and Other Natural Waters: Applications and Uncertainties. Ocean Sciences Meeting 2020. AGU.

Hunt, C. W., R. H. Byrne, X. Liu, and J. Salisbury. 2020. Organic Alkalinity Distributions and Characteristics in Two Gulf of Maine Estuaries. Ocean Science Meeting. AGU.

IOC, I. O. C. 2010. The international thermodynamic equation of seawater – 2010: Calculation and use of thermodynamic properties. UNESCO (English).

IPC. 2020. Micro 90 (R) Concentratred Cleaning Solution Safety Data Sheet.

Isard, J. O. 1967. The dependence of glass-electrode properties on composition. Glass Electrodes for Hydrogen and Other Cations**:** 88.

Johnson, K. M., K. D. Wills, D. B. Butler, W. K. Johnson, and C. S. Wong. 1993. Coulometric total carbon dioxide analysis for marine studies: maximizing the performance of an automated gas extraction system and coulometric detector. Marine Chemistry **44:** 167-187.

Johnston, J. 1916. THE DETERMINATION OF CARBONIC ACID, COMBINED AND FREE, IN SOLUTION, PARTICULARLY IN NATURAL WATERS. Journal of the American Chemical Society **38:** 947-975.

Keeling, C. D., R. B. Bacastow, A. E. Bainbridge, C. A. J. Ekdahl, P. R. Guenther, and L. E. Waterman. 1976. Atmospheric carbon dioxide variations in Mauna Loa Observatory, Hawaii. Tellus **XXVII:** 538-551.

Knap, A. and others 1993. Bermuda Atlantic Time-series Study Methods Manual (Version 3).

Ko, Y. H., K. Lee, K. H. Eom, and I.-S. Han. 2016. Organic alkalinity produced by phytoplankton and its effect on the computation of ocean carbon parameters. Limnology and Oceanography **61:** 1462-1471.

Koch, W. F., D. L. Biggs, and H. Diehl. 1975. Tris(hydroxymethyl)aminomethane—a primary standard? Talanta **22:** 637-640.

Krogh, A. 1904. On the Tension of Carbonic Acid in natural Waters and especially in the Sea. "Meddelelser om Grønland". Vol. XXVI. Copenhagen.

Kuliński, K., B. Schneider, K. Hammer, U. Machulik, and D. Schulz-Bull. 2014. The influence of dissolved organic matter on the acid–base system of the Baltic Sea. Journal of Marine Systems **132:** 106-115.

Kuliński, K., B. Szymczycha, K. Koziorowska, K. Hammer, and B. Schneider. 2018. Anomaly of total boron concentration in the brackish waters of the Baltic Sea and its consequence for the CO 2 system calculations. Marine Chemistry.

Lee, K., T.-W. Kim, R. H. Byrne, F. J. Millero, R. A. Feely, and Y.-M. Liu. 2010. The universal ratio of boron to chlorinity for the North Pacific and North Atlantic oceans. Geochimica et Cosmochimica Acta **74:** 1801-1811.

Lichtenberg, F. D. v. 1811. Chemische Untersuchung des Ostsee-Wassers. J. Chem. Phys **2:** 252-257.

Liu, X., M. C. Patsavas, and R. H. Byrne. 2011. Purification and characterization of meta-cresol purple for spectrophotometric seawater pH measurements. Environmental Science and Technology **45:** 4862-4868.

Lueker, T. J., A. G. Dickson, and C. D. Keeling. 2000. Ocean pCO_2 calculated from dissolved inorganic carbon, alkalinity, and equations for K1 and K2: validation based on laboratory measurements of CO_2 in gas and seawater at equilibrium. Marine Chemistry **70:** 105-119.

Marsigli, L. F. 1725. Histoire physique de la mer. Aux depens de la comp.

Martz, T. R., J. G. Connery, and K. S. Johnson. 2010. Testing the Honeywell Durafet for seawater pH applications. Limnology and Oceanography: Methods **8:** 172-184.

McClendon, J. F. 1917. The standardization of a new colorimetric method for the determination of the hydrogen ion concentration, CO2 tension, and CO2 and O2 content of sea water, of animal heat, and of CO2 of the air, with a summary of similar data on bicarbonate solutions in general. Journal of Biological Chemistry **30:** 265-288.

McClendon, J. F., C. C. Gault, and S. Mulholland. 1917. The hydrogen-ion concentration, CO2 tension, and CO2 content of sea-water. Carnegie Institution.

Millero, F., and J. Swift. 2018. Bottle and CTD data from cruise 33HQ20150809. *In* CCHDO [ed.].

Millero, F. J. 1974. The Physical Chemistry of Seawater. Annual Review of Earth and Planetary Sciences **2:** 101-150.

Millero, F. J. 1995. Thermodynamics of the carbon dioxide system in the oceans. Geochimica et Cosmochimica Acta **59:** 661-677.

Millero, F. J., J. P. Hershey, and M. Fernandez. 1987. The pK∗ of TRISH+ in Na-K-Mg-Ca-Cl-SO4 brines—pH scales. Geochimica et Cosmochimica Acta **51:** 707-711.

Millero, F. J. and others 2002. Dissociation constants for carbonic acid determined from field measurements. Deep Sea Research Part I: Oceanographic Research Papers **49:** 1705-1723.

Millero, F. J., T. Plese, and M. Fernandez. 1988. The dissociation of hydrogen sulfide in seawater1. Limnology and Oceanography **33:** 269-274.

Moberg, E. G., and M. W. Harding. 1933. The Boron Content of Sea Water. Science **77:** 510-510.

Morris, A. W., and J. P. Riley. 1966. The bromide/chlorinity and sulphate/chlorinity ratio in sea water. Deep Sea Research and Oceanographic Abstracts **13:** 699-705.

Muller, F. L., and B. Bleie. 2008. Estimating the organic acid contribution to coastal seawater alkalinity by potentiometric titrations in a closed cell. Anal Chim Acta **619:** 183-191.

Müller, J. D. and others 2018. Metrology for pH Measurements in Brackish Waters—Part 1: Extending Electrochemical pH_T Measurements of TRIS Buffers to Salinities 5–20. Frontiers in Marine Science **5:** Article 176.

Müller, J. D., and G. Rehder. 2018. Metrology of pH Measurements in Brackish Waters—Part 2: Experimental Characterization of Purified meta-Cresol Purple for Spectrophotometric pH_T Measurements. Frontiers in Marine Science **5:** Article 177.

Murray, J. 1818. XI. An Analysis of Sea-Water; with Observations on the Analysis of Salt-Brines. Earth and Environmental Science Transactions of The Royal Society of Edinburgh **8:** 209-244.

Narvekar, P., and M. Zingde. 1992. Influence of pollution of boron chlorinity ratio. Society of Biosciences, Muzaffarnagar, India.

Nemzer, B. V., and A. G. Dickson. 2005. The stability and reproducibility of Tris buffers in synthetic seawater. Marine Chemistry **96:** 237-242.

Newton, J. A., R. A. Feely, E. B. Jewett, P. Williamson, and J. Mathis. 2015. Global Ocean Acidification Observing Network: Requirements and governance plan, p. 57.

Olsen, A. and others 2016. The Global Ocean Data Analysis Project version 2 (GLODAPv2) – an internally consistent data product for the world ocean. Earth System Science Data **8:** 297-323.

Orr, J. C. and others 2005. Anthropogenic ocean acidification over the twenty-first century and its impact on calcifying organisms. Nature **437:** 681-686.

Patsavas, M. C., R. H. Byrne, R. Wanninkhof, R. A. Feely, and W.-J. Cai. 2015. Internal consistency of marine carbonate system measurements and assessments of aragonite saturation state: Insights from two U.S. coastal cruises. Marine Chemistry **176:** 9-20.

Paulsen, M.-L. and others 2017. Temporal Changes in Seawater Carbonate Chemistry and Carbon Export from a Southern California Estuary. Estuaries and Coasts **41:** 1050-1068.

Pawlowicz, R. 2015. The Absolute Salinity of seawater diluted by riverwater. Deep Sea Research Part I: Oceanographic Research Papers **101:** 71-79.

Perez, F. F., and F. Fraga. 1987. Association constant of fluoride and hydrogen ions in seawater. Marine Chemistry **21:** 161-168.

Pratt, K. W. 2014. Measurement of pH_T values of Tris buffers in artificial seawater at varying mole ratios of Tris:Tris·HCl. Marine Chemistry **162:** 89-95.

Ramette, R. W., C. H. Culberson, and R. G. Bates. 1977. Acid-base properties of tris (hydroxymethyl) aminomethane (Tris) buffers in sea water from 5 to 40. degree. C. Analytical Chemistry **49:** 867-870.

Reusch, W. 2020. Acidity of Carboxylic Acids.

Revelle, R., and H. E. Suess. 1957. Carbon dioxide exchange between atmosphere and ocean and the question of an increase of atmospheric CO2 during the past decades. Tellus **9:** 18-27.

Riley, J. P. 1965. The occurrence of anomalously high fluoride concentrations in the North Atlantic. Deep Sea Research and Oceanographic Abstracts **12:** 219-220.

Rossotti, F. J. C., H. S. Rossotti, and R. J. Whewell. 1971. The use of electronic computing techniques in the calculation of stability constants. Journal of Inorganic and Nuclear Chemistry **33:** 2051-2065.

Schoepf, V. and others 2017. Coral calcification under environmental change: a direct comparison of the alkalinity anomaly and buoyant weight techniques. Coral Reefs **36:** 13-25.

Schoonover, R. M., and F. E. Jones. 2002. Air buoyancy correction in high-accuracy weighing on analytical balances. Analytical Chemistry **53:** 900-902.

Sharp, J. D., and R. H. Byrne. 2021. Excess alkalinity in carbonate system reference materials. Marine Chemistry **233:** 103965.

Shirodkar, P., and V. Sankaranarayanan. 1984. Boron in seawater of Wadge Bank region in the Indian Ocean.

Sigman, D. M. and others 2003. Distinguishing between water column and sedimentary denitrification in the Santa Barbara Basin using the stable isotopes of nitrate. Geochemistry, Geophysics, Geosystems **4**.

Sipos, P., P. May, and G. Hefter. 2000. Carbonate removal from concentrated hydroxide solutions. Analyst **125:** 955-958.

Song, S. and others 2020. An important biogeochemical link between organic and inorganic carbon cycling: Effects of organic alkalinity on carbonate chemistry in coastal waters influenced by intertidal salt marshes. Geochimica et Cosmochimica Acta **275:** 123-139.

Sørensen, S. P. L. 1909. Enzyme studies II. The measurement and importance of the hydrogen ion concentration in enzyme reactions. Comptes rendus des travaux du laboratoire Carlsberg **8**.

Takahashi, T. and others 2014. Climatological distributions of pH, pCO_2, total CO_2, alkalinity, and $CaCO_3$ saturation in the global surface ocean, and temporal changes at selected locations. Marine Chemistry **164:** 95-125.

Takahashi, T. and others 1970. A carbonate chemistry profile at the 1969 Geosecs Intercalibration Station in the eastern Pacific Ocean. Journal of Geophysical Research (1896-1977) **75:** 7648-7666.

Tanaka, Y., T. Miyajima, A. Watanabe, K. Nadaoka, T. Yamamoto, and H. Ogawa. 2011. Distribution of dissolved organic carbon and nitrogen in a coral reef. Coral Reefs **30:** 533-541.

Thompson, T. G., and R. U. Bonnar. 1931. The buffer capacity of sea water. Industrial & Engineering Chemistry Analytical Edition **3:** 393-395.

Tornøe, H. 1880. The Norwegian North-Atlantic Expeditions 1876-1878. Volume 1. Chemistry.

Tyner, T., and J. Francis. 2017. ACS Reagent Chemicals.

Uppström, L. R. 1974. The boron/chlorinity ratio of deep-sea water from the Pacific Ocean. Deep-Sea Research **21:** 161-162.

Vogel, A. I. 1961. Text-book of quantitative inorganic analysis including elementary instrumental analysis.

von Bibra, E. 1851. Untersuchung von Seewasser des stillen Meeres und des atlantischen Oceans. Annalen der Chemie und Pharmacie **77:** 90-102.

Waters, J. F., and F. J. Millero. 2013. The free proton concentration scale for seawater pH. Marine Chemistry **149:** 8-22.

Wunsch, C. 2006. Towards the World Ocean Circulation Experiment and a bit of aftermath, p. 181-201. Physical Oceanography. Springer.

Yang, B., R. H. Byrne, and M. Lindemuth. 2015. Contributions of organic alkalinity to total alkalinity in coastal waters: A spectrophotometric approach. Marine Chemistry **176:** 199-207.

Zimen, K. E., and F. K. Altenhein. 1973. The future burden of industrial CO2 on the atmosphere and the oceans. Zeitschrift für Naturforschung A **28:** 1747-1752.